



Norwegian University of
Science and Technology

Energy Integration Opportunities in Zero Emission LNG Re-Gasification

Katrine Willa Hjertnes

Product Design and Manufacturing

Submission date: June 2011

Supervisor: Truls Gundersen, EPT

Co-supervisor: Åse Slagtern, Aker Solutions

Norwegian University of Science and Technology
Department of Energy and Process Engineering

EPT-M-2011-Nr 32

MASTER THESIS

for

Stud.techn. Katrine Willa Hjertnes
Spring 2011

Energy Integration Opportunities in Zero Emission LNG Re-Gasification

Energiintegrasjonsmuligheter ved re-gasifisering av LNG uten utslipp

Background

Aker Solutions offers global engineering and construction services, technology products and integrated solutions for the oil and gas industries. The company is heavily involved in finding solutions for utilizing natural gas where traditional pipeline cannot be applied for technical and/or practical reasons. Thus, Aker Solutions have been involved in development of several solutions for offshore gas processing such as offshore LNG, HLG (Heavy Liquefied Gas), Methanol, GTL (Gas To Liquids), and gas hydrates. Presently no such offshore installations have been built. Currently a main focus in Aker Solutions lies on Aker Solutions GBS (Gravity Based Structures) solutions for LNG production and LNG re-gasification. Aker Solutions recently delivered a GBS re-gasification terminal that is installed outside Italy. The GBS is placed on the seabed at about 20 m water depth. This means that offloading of LNG to and from a GBS is a proven technology.

Offshore LNG re-gasification terminals are considered several places in the world. Outside California LNG re-gasification projects have been stopped due to environmental restrictions. Based on this fact and the unique position Aker Solutions has on GBS products, Aker Solutions has developed a concept called "Zero emission LNG re-gasification".

Motivation

Traditional re-gasification of LNG uses sea water or heat from combustion of natural gas as heat source. This leads to either discharge of cold chlorinated sea water or emissions of flue gas with CO₂. Aker Solutions has developed a process for re-gasification of LNG, where oxy-combustion of natural gas is used to produce steam which is used as heat source for the re-gasification while at the same time producing power for the facility. CO₂ from the combustion is treated and sent to injection. The motivation behind this Master thesis (that follows a last year student project from the fall 2010) is the expectation that several opportunities exist for process integration between re-gasification, oxygen production and CO₂ injection. The cooling available in the re-gasification process will be attempted used in an optimal way to provide low temperature cooling to the air separation unit and the CO₂ compression and purification unit.

Objective

The main objective of this Master thesis is to evaluate such process integration opportunities based on data provided from process simulations using HYSYS. The Air Separation Unit (ASU) should be treated as a black box, however, with a specified need for low temperature cooling, i.e. load (duty) and level (temperature) is specified.

The following issues should be considered in the Master thesis:

1. Evaluate the heat integration solutions between the LNG re-gasification, the power plant and the CO₂ purification and compression unit. This includes a study of the proposed fluids (amounts and temperatures) used for indirect heat exchange. Minimizing total heat transfer area is the main motivation for this study.
2. Quantify opportunities for heat integration between the ASU and the LNG re-gasification process, where details about the ASU is omitted, and the ASU simply acts as a heat source (cooling sink) with a pre-specified cooling requirement (load(s) and temperature(s)). Two different cases for oxygen purities should be used for the oxy-fuel unit, based on possible step changes in ASU design and seen in relation to the performance of cryogenic separation of CO₂ and N₂.
3. Based on results from the previous two points, recommendations should be given for the best overall process integration solutions for the entire concept including the four distinct elements: (a) LNG re-gasification, (b) Power plant, (c) Air Separation Unit, and (d) CO₂ Purification and compression Unit (CPU).
4. If time allows, preliminary work on the use of membranes in air separation from the last year project mentioned above should be continued with main emphasis on the purity issue, since there exists an important trade-off between the efforts made in the ASU and the corresponding load on the CPU.

-- ” --

Within 14 days of receiving the written text on the Master thesis, the candidate shall submit a research plan for his project to the department.

When the thesis is evaluated, emphasis is put on processing of the results, and that they are presented in tabular and/or graphic form in a clear manner, and that they are analyzed carefully.

The thesis should be formulated as a research report with summary both in English and Norwegian, conclusion, literature references, table of contents etc. During the preparation of the text, the candidate should make an effort to produce a well-structured and easily readable report. In order to ease the evaluation of the thesis, it is important that the cross-references are correct. In the making of the report, strong emphasis should be placed on both a thorough discussion of the results and an orderly presentation.

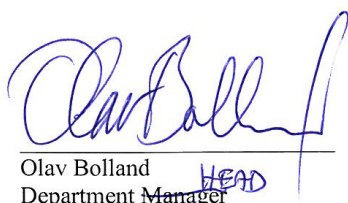
The candidate is requested to initiate and keep close contact with his/her academic supervisor(s) throughout the working period. The candidate must follow the rules and regulations of NTNU as well as passive directions given by the Department of Energy and Process Engineering.

Pursuant to “Regulations concerning the supplementary provisions to the technology study program/Master of Science” at NTNU §20, the Department reserves the permission to utilize all the results and data for teaching and research purposes as well as in future publications.

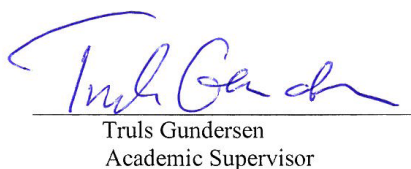
One – 1 complete original of the thesis shall be submitted to the authority that handed out the set subject. (A short summary including the author’s name and the title of the thesis should also be submitted, for use as reference in journals (max. 1 page with double spacing)).

Two – 2 – copies of the thesis shall be submitted to the Department. Upon request, additional copies shall be submitted directly to research advisors/companies. A CD-ROM (Word format or corresponding) containing the thesis, and including the short summary, must also be submitted to the Department of Energy and Process Engineering

Department of Energy and Process Engineering, 31 January 2011



Olav Bolland
Department Manager



Truls Gundersen
Academic Supervisor

Industrial Contacts:

Manager Åse Slagtern, LNG/Gas Solutions & Renewables, Aker Solutions,
Phone: +47 67 59 57 46, Mobile: +47 930 59 481, e-mail: aase.slagtern@akersolutions.com

Senior Engineer Hans Kristian Rusten, LNG/Gas Solutions & Renewables, Aker Solutions,
Phone: +47 67 52 74 18, Mobile: +47 917 17 903,
e-mail: hans.kristian.rusten@akersolutions.com

Preface

This master thesis is written by Katrine Willa Hjertnes at NTNU, Department of Energy and Process Engineering, and is an extension of the project work from fall 2010. The thesis is provided by Aker Solutions, Norway.

Firstly I would like to thank Aker Solutions for an interesting and challenging project. I will also express my gratitude to my supervisors Truls Gundersen and Hans Kristian Rusten for support with material, answering questions and giving great guidance throughout the project. In addition I would like to thank my fellow student Mia Skrataas for proofreading, and PhD student Fu Chao for technical advises regarding the air separation unit.

Special thanks are addressed to my co-habitants; Marthe Aalvik, Ruth Helene Kyte and Adele M. Slotsvik. Finally, I would like to thank my wonderful family; Hilde M. Hjertnes, Ketil Nesse and Petter Hjertnes for their patience, support and love through five years of studies. I could not have done this without you.

June 27th 2011, Trondheim



Katrine Willa Hjertnes

Summary

Due to the increasing demand for LNG, more environmental friendly regasification solutions are of interest. Aker Solutions has developed a concept for zero emission regasification of LNG, where the regasification train is heat integrated with an oxy-fuel power and steam plant. The oxy-fuel combustor burns part of the send-out gas in an oxygen enriched environment. The flue gas produced is CO₂ rich, making CO₂ capture feasible. 95mol% pure oxygen is produced by cryogenic distillation in an ASU. Today, oxy-fuel combustion is not economical feasible, mainly due to the significant power demand in the ASU and the CO₂ Compression and Purification Unit (CPU). This thesis investigates opportunities of reducing the power consumption in the plant. Pinch analysis is used to evaluate the heat integration in the Aker Solutions' concept. Simulation models are created in Aspen Hysys to investigate possibilities of integrating the ASU with the power and steam plant, and to find the impact of changing the oxygen purity. Three different oxygen purities (90, 95 and 97mol %) were tested. In addition the use of membranes to separate air is discussed.

The heat integration was evaluated in terms of sequence of the pair matches, and placement of Heat Transfer Fluids (HTFs). The sequence of the streams was found acceptable. However, changing the HTF in LNG heater 2 and 3 from MEG/Water to Methanol could be beneficial. The freezing point of Methanol is lower than that of MEG/Water; hence the HTF can be shifted to a lower temperature. Because LNG has a higher h-value than the hot streams, ΔT between the LNG and the HTF should be lower than that of the hot fluid and the HTF.

If the oxygen purity was set to 90mol%, the load of the CO₂ CPU and the condenser duty of the N₂/CO₂ distillation were increased by 10% and 65% respectively. If the purity was increased to 97mol% the opposite results were obtained. Although increasing the purity leads to savings in the CO₂ CPU, this unit only accounts for a small part of the overall power consumption compared to the ASU, hence the impact on the ASU is of greater concern. For the ASU, decreasing the purity would lead to some energy savings. However, the required equipment size of the unit would increase. If the purity is increased, the separation of Argon is required in the distillation column, thus a significant increase in energy of separation is experienced. In addition the capital expenses of the ASU are increased, due to implementation of a supplementary distillation column. Based on the previous facts, it was recommended to keep the oxygen purity at 95mol%.

If integrating the ASU, cryogenic LNG should be used to cool the air upstream and downstream the air compressor. Results from Hysys showed that this would lead to 18 % reduction in external utility consumptions. In addition the compressor work of the ASU would be decrease by 14%, and the yield of the LP turbine would increase with 2MW.

Today, membranes are not capable of producing large quantities of oxygen. However, there exist some membranes with great potential. The most promising membranes are found to be MIECs with a perovskite structure, especially Ba_{0.5}Sr_{0.5}Co_{0.8}Fe_{0.2}O_{3- δ} . At 800°C the oxygen flux of these membranes are found to be approximately $1.56 \cdot 10^{-6}$ mol/scm², and the oxygen

purity obtained is above 99mol%. The thickness of one of these membrane were found to be 1.8mm, hence more than $1 \cdot 10^9$ membranes are required to produce enough oxygen for the oxy-combustion plant. Although these membranes have a great potential, they need to be further evolved before implemented to oxy-fuel power plants.

Sammendrag

Grunnet en økende etterspørsel etter LNG, har interessen for å finne mer miljøvennlige regasifiseringsteknologier økt. AKSO har utviklet et konsept der LNG regasifiseres med svært lave utslipp. Regasifiseringsenheten er varmeintegret med et kraft- og dampanlegg, der deler av den produserte naturgassen brennes i et oksygen rikt miljø. Dette fører til en CO₂-rik eksosgass, og muliggjør CO₂ fangst. Kryogenisk luftseparasjon er brukt til å produsere 95mol % ren oksygen. AKSO sitt konsept er ikke en konkurransedyktig teknologi idag. Hovedgrunnen er at både luftseparasjonen og CO₂ fangsten har et høyt kraftforbruk. Denne masteroppgaven ser på muligheter for å senke kraftforbruket ved å evaluere varmeintegrasjonen i anlegget. I tillegg vil muligheter for varmeintegrasjon av luftseparasjonsenheten bli vurdert, og innvirkningen av å øke eller senke oksygenrenheten. Implementering av membraner for luftseparasjon er også diskutert. Aspen Hysys er brukt som simuleringsverktøy i denne masteroppgaven.

Varmeintegrasjonen i anlegget er vurdert på følgende vilkår; rekkefølge av strømmer som varmeveksles, og plassering av mellomliggende medier. Rekkefølgen på strømmene som varmeveksles ble funnet akseptabel. I LNG varmeveksler 2-3 viste undersøkelser at det kan være gunstig å bruke Metanol isteden for MEG/Vann, som mellomliggende mediet. Dette er grunnet det lave frysepunktet til Metanol, som fører til at det mellomliggende mediet kan plasseres nærmere den kalde strømmen.

Systemet ble testet for to forskjellige oksygenrenheter; 90 mol % og 97 mol %. Resultatene viser at kompressor arbeidet, nedstrøms brenneren, vil øke noe (10 %) hvis renheten ble senket. Derimot vil kjølebehovet i N₂/CO₂ destillasjonskolonnen øke betydelig; 65 %. Hvis oksygen renheten derimot økes til 97mol % vil det motsatte skje, kjølebehovet synker med 65 %, og kompressorarbeidet med 10 %. Selv om økning av oksygenrenheten fører til reduksjon i kraftbehovet for CO₂ renseanlegget, vil denne reduksjonen være liten sett i forhold til økning av kraftbehovet i luftseparasjonsenheten. For luftseparasjonsenheten vil separasjonsenergien i destillasjonskolonnen minke med noen få prosent når oksygenrenheten senkes. Derimot vil størrelsen på produksjonsutstyret øke betydelig. Hvis oksygenrenheten derimot økes vil økningen i separasjonsenergi være signifikant. Dette er fordi argon da må separeres fra oksygenet. I tillegg vil kapitalkostnadene øke da implementeringen av en ekstra kolonne er nødvendig. Det er derfor anbefalt å ikke endre oksygenrenheten i systemet.

Luftseparasjonsenheten ble varmeintegret med LNG regasifiseringsenheten ved å varmeveksle LNG mot luft før og etter luftkompressoren. Dette førte til 18 % reduksjon i dampforbruk. I tillegg ble kompressorarbeidet i luftseparasjonsenheten redusert med 14 %, og 2 MW mer kraft ble produsert i lavtrykksturbinen.

Idag finnes det ingen membraner som kan produserer store kvantum oksygen, men det finnes noen membraner med stort potensial; ion - elektron ledende membraner. En av de mest lovende membranene er Ba_{0,5}Sr_{0,5}Co_{0,8}Fe_{0,2}O_{3-δ}. Oksygen fluksen gjennom disse membranene

er $1.56 \cdot 10^{-6}$ mol/scm² ved 800 °C, og de kan produsere oksygen med 99 mol % renhet. Disse membranene er 1.8 mm tykk, og det kreves derfor over $1 \cdot 10^9$ membraner for å produsere nok oksygen til kraftverket. Selv om membranene har stort potensial må de videreutvikles før de kan tas i bruk i store kraftanlegg.

Acronyms and abbreviations

°C	Degree of centigrade
AKSO	Aker Solutions
AL	Air Liquids
ASME	American Society of Mechanical Engineering
ASU	Air Separation Unit
BFW	Boiler Feed Water
CAPEX	Capital Expenses
CCS	Carbon Capture and Storage
CO ₂ CPU	CO ₂ Compression and Purification Unit
CW	Cooling Water
DEG	Di Ethylene Glycol
EIA	Energy Information Administration
HRSG	Heat Recovery and Steam Generator
HTF	Heat Transfer Fluid
HP	High Pressure
HX	Heat Exchanger
IGCC	Integrated Gasification Combined Cycle
ITM	Ionic Transport Membrane
kPa	Kilo Pascal
kW	Kilo Watt
LNG	Liquefied Natural Gas
LP	Low Pressure
MEG	Mono Ethylene Glycol
MIEC	Mixed Ionic-Electronic conducting Membrane

MP	Medium Pressure
MW	Mega Watt
NG	Natural Gas
NGCC	Natural Gas Combined Cycle
OPEX	Operating Expenses
ORV	Open Rack Vaporizer
PC	Pulverized Coal
ppm	Parts per million
SCV	Submerged Combustion Vaporizer
SRK	Soave-Redlich-Kwong
TEG	Tri Ethylene Glycol
WEG	Water Ethylene Glycol

Nomenclature

A	Speed of sound	[m/s]
A	Area	[m ²]
AF	Air-Fuel ratio	[kg Air/kg Fuel]
C _p	Heat capacity at constant pressure	[kg/kgK]
C _v	Heat capacity at constant volume	[kg/kgK]
D _{ij}	Mass diffusivity	[m ² /s]
F	Faradays constant	[C/mol]
F	Feed	[kmol/h]
H	Specific enthalpy	[kJ/kg]
H	Film heat transfer coefficient	[W/m ² K]
K	Isentropic index	[-]
L	Length	[m]
L	Liquid	[kmol/h]
M	Molecular weight	[kg/kmol]
M	Mass	[kg]
ṁ	Mass flow	[kg/s]
N	Charge	[C]
N	Polytropic index	[-]
N	Amount of moles	[mole]
P	Pressure	[kPa]
PM	Permeability	[m ³ (STP)/m ² bar h]
Q	Heat flow	[kW]
R	Ideal gas constant	[kJ/kmolK]
R _f	Thermal resistance	[K/W]

S	Solubility	$[\text{m}^3 \text{ solute(STP)}/\text{m}^3 \text{ solid atm}]$
T	Temperature	[K] [C]
U	Overall heat transfer coefficient	$[\text{W}/\text{m}^2\text{K}]$
V	Volume	$[\text{m}^3]$
V	Vapor	$[\text{kmol}/\text{h}]$
V	Specific volume	$[\text{m}^3/\text{kg}]$
W	Work	[kW]
X	Molar fraction in liquid phase	[mol%]
Y	Molar fraction in vapor phase	[mol%]
Z	Compressibility factor	[-]

Chemical symbols

Ba	Barium
CH ₄	Methane
C ₂ H ₆	Ethane
C ₃ H ₈	Propane
CO	Carbon monoxide
Co	Cobalt
CO ₂	Carbon dioxide
Fe	Iron
Gd	Gadolinium
H ₂ O	Water
N ₂	Nitrogen
NO _x	Nitrogen oxides
O ₂	Oxygen
O ₃	Ozone

Sr Strontium

Zn Sink

Greek letters

A	Relative volatility	[-]
Δ	Mean difference	[-]
Σ	Ionic conductivity	[S/m]
H	Efficiency	[-]

Subscript

C	Cold stream
H	Hot stream
I	Component i of a gas
J	Component j of a gas
`	Denotes the state of the gas at the feed side
``	Denotes the state of the gas at the permeate side

Table of Contents

Preface.....	I
Summary	III
Sammendrag.....	V
Acronyms and abbreviations	VII
Nomenclature	IX
Table of Contents	XIII
List of figures	XVII
List of tables	XVIII
1 Introduction	1
1.1 Background.....	2
1.2 Thesis structure and limitations	2
2 Introduction to Aker Solutions regasification concept.....	5
2.1 Regasification unit.....	5
2.2 Oxy – fuel steam and power system.....	6
2.3 Air separation unit	7
2.4 CO ₂ compression and purification unit	7
2.5 Overall plant performance	8
3 CO ₂ Capture and storage	9
3.1 CO ₂ capture by oxy-fuel combustion	9
3.2 CO ₂ Compression and purification.....	10
3.2.1 Fundamentals of compression.....	10
3.2.2 CO ₂ CPU design.....	11
3.3 Available oxy-fuel configurations	13
3.3.1 Oxy-fuel NGCC	14
3.3.2 Oxy-fuel burner	14

4	Air separation technology	17
4.1	Distillation	17
4.2	Cryogenic air separation unit.....	18
5	Possibilities of power reduction	21
5.1	Integration between an ASU and an oxy-fuel power cycle.....	21
5.2	Impact of changing the oxygen purity.....	22
5.2.1	Impact on the ASU.....	22
5.2.2	Impact on the CO ₂ CPU	23
6	Membranes used for air separation	25
6.1	Introduction	25
6.2	Inorganic membranes for air separation	25
6.2.1	Transportation mechanism of inorganic membranes	26
6.2.2	Structure of MIECs	27
6.2.3	Performance of MIECs.....	28
6.3	Implementation of membranes in oxy-fuel systems.....	30
6.3.1	ITMs used for oxygen production today	30
6.3.2	MIECs integrated with an oxy-fuel plant.....	30
7	Fundamentals of heat integration	33
7.1	Composite and grand composite curves	33
7.2	Steam generation	35
7.3	Intermediate Heat Carriers.....	36
7.4	Heat transfer coefficient	37
7.5	Area targeting	39
8	Simulation model and methodology	41
8.1	Simulation software.....	41
8.2	Fluid packages	41

8.2.1	Distillation column in Hysys.....	41
8.3	Process design and methodology.....	42
8.3.1	Specifications of the LNG stream	43
8.3.2	Specifications of the steam cycle	44
8.3.3	Specifications of the reactor	45
8.3.4	Specifications of the CO ₂ recovery process	45
8.4	Results and discussion	47
8.4.1	LNG stream	47
8.4.2	Steam cycle	48
8.4.3	CO ₂ CPU	49
8.4.4	Power and heat balance	52
9	Evaluation of existing heat integration in the system	53
9.1	Methodology.....	53
9.2	Data extraction.....	53
9.2.1	Steam cycle	53
9.2.2	LNG and flue gas streams	55
9.3	Results and discussion	57
9.3.1	Composite curves for the system	57
9.3.2	Sequence of the streams	57
9.4	Placement of HTFs	61
9.4.1	Placement of HTF in LNG HX 1	62
9.4.2	Placement of HTF in LNG HX 2 and LNG HX3	63
10	Different oxygen purities	65
10.1	Case studies.....	65
10.2	Result and discussion.....	66
10.2.1	Flue gas composition.....	66

10.2.2	Compressor work of the CO ₂ CPU and the ASU.....	67
10.2.3	Energy of separation in the CO ₂ CPU and the ASU	69
11	Possibilities of integrating the ASU	71
11.1	Methodology	71
11.1.1	Simulation models.....	72
11.2	Results and discussion	73
12	Proposed system.....	75
12.1	Chosen parameters and assumptions	75
12.1.1	Selected oxygen purity	75
12.1.2	Selected heat integration scheme	75
12.2	Proposed system configuration	75
12.3	Possibility of using ITMs for oxygen production	77
12.4	Possible configuration of the system	77
12.5	Impact on the CO ₂ CPU	78
13	Conclusion and further work.....	79
13.1	Conclusion	79
13.2	Further work.....	79
	List of References.....	81
	Appendices	85
	Appendix A	i
	Appendix B	v
	Appendix C	vi

List of figures

Figure 1 Heat integration between power cycle and LNG regasification unit.....	6
Figure 2 Simple schematic of the oxy-fuel steam and power system	7
Figure 3 Multistage compression with intercooling [18]	12
Figure 4 Specific power of CPU as a function of CO ₂ in flue gas [19]	13
Figure 5 oxy-fuel combined cycle with steam generation [13].....	14
Figure 6 Equilibrium stage for distillation	17
Figure 7 Cryogenic distillation of air	19
Figure 8 Power requirement of a cryogenic ASU [19]	22
Figure 9 Specific work of CPU as a function of CO ₂ in flue gas [19]	24
Figure 10 Transportation in a typical Membrane [32]	25
Figure 11 Different membrane concept: a) mixed conducting membrane,.....	26
Figure 12 Ideal Perovskite [40]	28
Figure 13 Factors influencing the MIEC[39]	28
Figure 14 Mass flux as a function of temperature[39]	29
Figure 15 ITM oxycombustion plant[46]	31
Figure 16 Typical composite curve [49]	33
Figure 17 Typical grand composite curve	35
Figure 18 T-Q diagram, for heat transfer in steam generation[10]	36
Figure 19 Simulation model of steam boiler	44
Figure 20 T-H profile of LNG HX 4.....	48
Figure 21 Power and steam cycle.....	49
Figure 22 CO ₂ separation and compression	51
Figure 23 Stream extraction of water cycle	54
Figure 24 T-H diagram steam boiler	55
Figure 25 Steam data of the flue gas	56

Figure 26 CC for the base case.....	57
Figure 27 T-Q Diagram for the different streams in the system	58
Figure 28 Different boiler scheme	59
Figure 29 T – Q Diagram omitting H4 and C2	60
Figure 30 GCC for the base case.....	61
Figure 31 Placement of HTF in LNG HX 1	62
Figure 32 MEG/Water cycle	63
Figure 33 Left: WEG/Water as HTF Right: Methanol as HTF.....	64
Figure 34 Compressor work of CO ₂ CPU	67
Figure 35 Condenser duty for different oxygen purities	69
Figure 37 Shifted CC.....	71
Figure 38 Integrated ASU	72
Figure 39 Conventional ASU.....	73
Figure 40 Left: CC of base case. Right: CC when integrating the ASU.....	74
Figure 41 Integration of the ASU.....	75
Figure 42 T-Q Diagram system with integrated ASU.....	76

List of tables

Table 1 Power requirement of the different process systems.....	8
Table 2 Influence on ASU by changing the oxygen purity [2]	23
Table 3 Performance of the cryogenic CO ₂ recovery process [2].....	24
Table 4 Oxygen permeation flux data for perovskite single-phase membranes [42-44]	30
Table 5 Properties of Methanol and WEG/water[8, 52]	37
Table 6 Typical h-values for gas at different pressure [55]	38
Table 7 Fuel composition.....	43
Table 8 Duties of LNG heat exchangers	43

Table 9 Specifications of steam cycle	45
Table 10 Specifications of flue gas stream.....	46
Table 11 Specification of CO ₂ CPU.....	46
Table 12 Exit temperatures of LNG HXs.....	47
Table 13 Output parameters for steam cycle.....	49
Table 14 Reaction balance for the oxy-burner	50
Table 15 Flue gas composition.....	50
Table 16 Output parameters for the CO ₂ CPU	51
Table 17 Power requirements for different process systems.....	52
Table 18 Stream data for water cycle.....	55
Table 19 Stream data of flue gas streams.....	56
Table 20 Chosen h-values for the hot streams in the system	62
Table 21 Molar fraction of CO ₂ in flue gas for different oxygen purities	66
Table 22 Specific compressor work in CO ₂ CPU	69
Table 23 Composition of the air prior to the purification	72
Table 24 Properties of HXs prior and after the air compressor	73
Table 25 Impact on the CO ₂ CPU	78

1 Introduction

Global warming is one of the main challenges the world will face in the years to come. Carbon dioxide (CO₂) makes the largest anthropogenic contribution to global warming, where fossil fuels like oil, gas and coal accounts for approximately 75 % of the anthropogenic CO₂ emissions. The emissions of greenhouse gases can be reduced by use of alternative energy sources, like renewable energy. However, renewable energy is not yet reliably to produce sufficient power to meet the increasing energy demand. In addition, no renewable energy sources are economical feasible to produce large quantities of energy. Thus combustion of fossil fuels is likely to meet the immediate demand. To reduce emissions from fossil fuel power plants, improving the overall efficiency can, to a certain point contribute to reduce CO₂ emissions. But to sufficiently decrease the CO₂ emissions it will be essential to develop technology to capture and store the CO₂ generated [1-3].

One of the fossil fuel sources that are relevant for CO₂ capture is Natural Gas (NG). NG is a growing energy source worldwide; according to Energy Information Administration (EIA) the world's natural gas consumption will increase with 44 % from 2007 to 2035 [4]. Compared to Oil and Coal, NG is a more environmental friendly fuel. It emits less greenhouse gases, and has higher relative fuel efficiency for a given amount of energy. The CO₂ produced from oil and coal is approximately 1.4 – 1.75 times higher than for NG. Thus, the increased consumption of NG could lead to decreased CO₂ emission if produced, and processed in a more environmental friendly manner.

NG can be transported as compressed gas through pipelines or as Liquefied Natural Gas (LNG), where the latter transportation technology is more convenient when the gas is to be transferred over large distances. This is due to costs, safety and technical issues. When NG is liquefied its volume is reduced, hence the specific energy content increases, making the transportation economically feasible. NG is liquefied at approximately -160 °C, and is classified as a cryogenic liquid¹. The LNG is transported to regasification terminals where it is stored and vaporized before distributed to end users. As the production rate of LNG is likely to increase in the years to come, several new regasification terminals are required. The heat source for regasification of LNG is today either a burner system where a part of the NG produced is utilized to produce heat to vaporize the LNG, or sea water. Both systems induce local and global emissions to the atmosphere or the sea. To make NG production more environmental friendly, Aker Solutions (AKSO) has developed a regasification technology which offers minimal emissions. The objective is to limit external utility consumption by heat integrating the LNG regasification unit with a power and steam plant. The CO₂ from the power facility will be captured by using oxy-fuel combustion technology. Thus the system will manage to vaporize LNG without significant environmental impact [4, 5].

¹ Cryogenic liquid: Below -150°C

1.1 Background

The motivation for the zero emission regasification plant is the increased demand for natural gas worldwide, and the regulations that require minimum emissions and effluent discharge to the environment from such plants. Today the most common technology for vaporizing LNG is Open Rack Vaporizers (ORVs), which uses ambient sea water as the heat source. The heat exchanger consists of vertical aluminum panels, where sea water is fed at the top, flowing downwards on the outside of the panels, while the LNG flows on the tube side. The disadvantages of the system is that a considerable amount of water is required, resulting in discharge of vast amounts of cold water to the sea. This induces a local temperature drop, which harms marine life. The system is climate sensitive, and is therefore not an adequate solution if the ambient sea water temperature tends to drop below 8 degrees during winter. In addition the water is treated with chlorinate resulting in emissions to the sea [6].

In addition to the ORVs, Submerged Combustion Vaporizers (SCVs) are broadly used. In a SCV the LNG is routed through tubes, submerged in a water bath. The water is heated by flue gas from a burner combusting part of the send-out gas. The combustion products are discharged to the atmosphere, causing both local and global emissions. The CO₂ emissions from a SCV system is approximately 310 000 tons/year for a NG production rate of 42.5 Sm³/day. This is equivalent to 850 tons CO₂/day [7].

If new regasification units are to apply either the ORV or SCV technology this will result in significant emissions. Research in new low-emission regasification technology is therefore important to limit emissions from such plants.

1.2 Thesis structure and limitations

The main objective of this thesis is to look at opportunities of reducing the overall power consumption of the regasification plant. As of today, the technology is not able to compete economically with conventional regasification technologies. This is mainly due to the cryogenic Air Separation Unit (ASU) and the CO₂ capture, which contributes to large efficiency penalties and high costs.

This thesis evaluates the heat integration solution proposed by AKSO to minimize the total heat transfer area in the plant. Simulation models of the regasification terminal are made in Aspen Hysys, and all data used to evaluate the system are extracted from these models. The simulation model is made by the author and is based on utility flow diagrams of the plant. As the author had no knowledge of Aspen Hysys, the simulation models could possibly be simplified more than those used in this thesis.

The heat integration in the system is evaluated in terms of sequence of the stream matches, the temperature profile for the intermediate heat carriers used and the use of steam. In addition to evaluate the heat integration in the system, opportunities of integrating a cryogenic ASU are discussed. As the cryogenic ASU includes complicated unit operators, a complete simulation model of the ASU is not constructed. Since the main air compressor accounts for most of the

power consumption in the ASU, only the compressor is simulated to quantify opportunities of reducing the power consumption by using the ASU as a heat sink for the regasification unit. Three different oxygen-purities are tested for the oxy-fuel burner to examine the impact on the ASU and the CO₂ Compression and Purification Unit (CPU). This part of the thesis is limited by the reactor in the simulation model, which for simplicity, is simulated with complete combustion.

The first chapter of this thesis describes the regasification concept planned by AKSO to give the reader an understanding of the basis of the concept before the different technologies are further described. In accordance with AKSO, all information regarding economics and all utility flow diagrams are left out, including specifications found in these diagrams.

Chapter 3-7 presents theory regarding oxy-fuel combustion, ASU technology, heat integration and membrane technology. This theory forms the basis for the simulation cases. For the ASU only a brief introduction to distillation is given, as this is a broad subject and only an understanding of the fundamentals is required for the discussion of the simulation model. In Section 3.3 the fundamental of an oxy-fuel NGCC is described. The regasification plant planned by AKSO is based on a steam cycle with a simple oxy-fuel burner. However, a basic understanding of an oxy-fuel NGCC is required as most literature regarding NG fired oxy-combustion, is based on NGCCs. In Chapter 7 an introduction to intermediate heat transfer fluids is given. Though this heat transfer method is broadly used, the available theory is limited. In Chapter 6 the fundamentals of membranes used for air separation is presented. This subject is broad, and only membranes capable of producing high purity oxygen will be discussed.

The description of the simulation models, and results from these models are discussed in five different chapters. All the different chapters include methodology and results. It is chosen to discuss the results throughout these chapters, instead of gathering all results in the end. This is due to the fact that the results gained for the different simulation models are connected to each other. The structure of these chapters is as follows:

Chapter 8: Describe which specifications and assumptions are applied in Aspen Hysys, when creating the main simulation model. The last part of Chapter 8 discusses the results gained in the main simulation model. It is chosen to have this discussion prior to the evaluation of the system, as all data used in the evaluation is extracted from this chapter.

Chapter 9: Describes the methodology used to evaluate the heat integration in the system. The results are given in the last part of the chapter. All data used to evaluate the system are extracted from Chapter 8.

Chapter 10: Discuss the impact of changing the oxygen purity in the plant. Three different oxygen purities are tested; 90, 95 and 97mol%.

Chapter 11: Based on results from Chapter 8-10, the possibility of integrating an ASU is discussed.

Chapter 12: Based on the previous chapter a proposed process solution is presented in this chapter. In addition the possibility of using membranes for air separation is discussed. This is limited to information extracted from literature, as it is not possible to simulate a membrane in Aspen Hysys.

2 Introduction to Aker Solutions regasification concept

AKSO has developed a concept called; “*Zero emission power production for LNG regasification*”. The objective of this concept is to develop a system that vaporizes and heats LNG without CO₂ emissions. In addition, the system is planned to be self contained with power to make the system employable to off-shore sites. The system contains an LNG regasification train, an oxy-fuel boiler system with power and steam generation and a CO₂ purification and compression unit.

The following sections will explain the fundamentals of AKSO’s regasification system. Details regarding the system configuration are collected from Aker Solutions Base Case report [8].

2.1 Regasification unit

The regasification unit is the main unit of the facility; all other units provide power and heat to the regasification train. According to the calculation from Aker Solutions’ study report, 736 kJ/kg LNG is required to vaporize and heat the LNG from -161 °C to the required sales gas temperature [8].

The cold LNG feed is pumped to 80 bar before entering the vaporization and heating section, consisting of five Heat Exchangers (HXs). The first two HXs are heat integrated with the CO₂ CPU and heat the LNG to -151 °C by cooling CO₂ rich flue gas to -40 °C. The third heat exchanger is integrated with the oxy-fuel burner, and is heating the LNG to -131 °C, by condensing flue gas from the combustion. In the fourth heat exchanger LNG is vaporized by steam condensate. And finally, Low Pressure (LP) steam is used in the last heat exchanger to heat the gas to 8.7 °C. The first three heat exchangers use an intermediate Heat Transfer Fluid (HTF); either Methanol or a mixture of Mono-Ethylene-Glycol (MEG) and water. Figure 1 gives a simplified schematic of the proposed heat integration in the system.

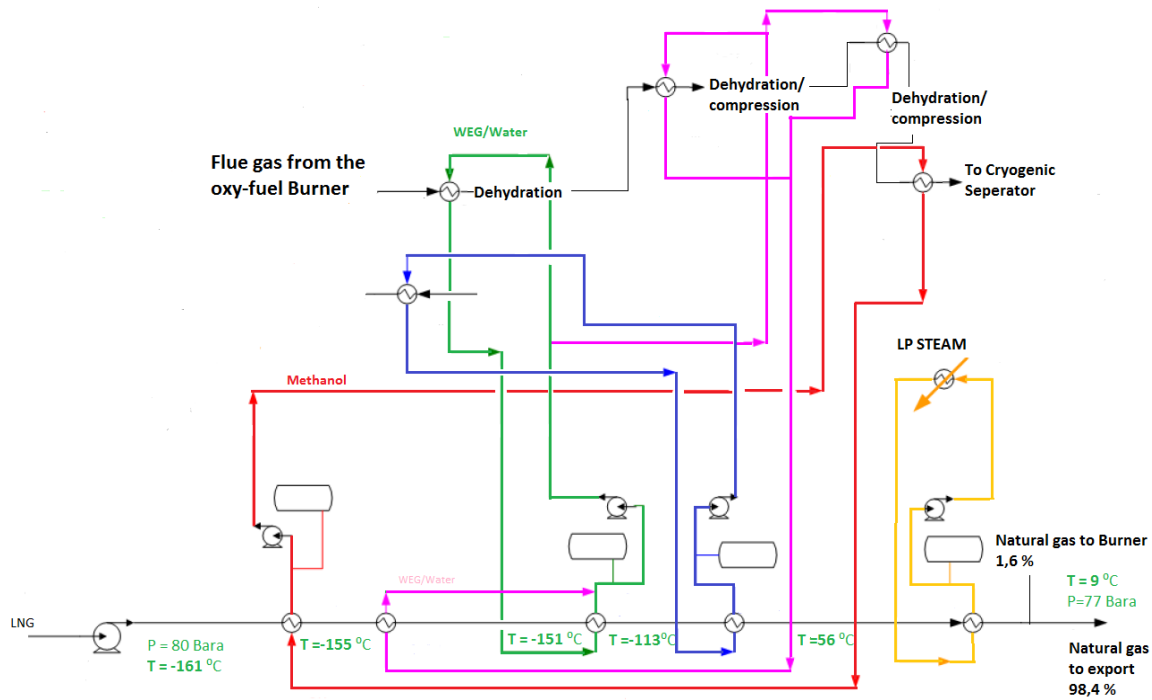


Figure 1 Heat integration between power cycle and LNG regasification unit

2.2 Oxy – fuel steam and power system

The oxy-fuel steam and power system provides heat and power to the facility, and consists of an oxy-fuel burner, a steam boiler, a Low Pressure (LP) and a Medium Pressure (MP) steam turbine. For oxy-fuel boilers, almost all literature refers to Pulverized Coal (PC) fired oxy-fuel systems. AKSO has developed a similar NG fired oxy-fuel system. The fundamentals of oxy-fuel combustion are discussed in Chapter 3.

Approximately 1.5 % of the send-out gas is sent to the oxy-fuel burner where it burns in an oxygen rich environment. To control the flame temperature, a considerable amount of the CO₂-rich flue gas is recycled to the burner. The recycle rate is controlled to limit the flame temperature to 1450°C. The flue gas from the oxy-burner is cooled by preheating Boiler Feed Water (BFW), generate steam and superheat the MP steam before it is further processed in the CO₂ CPU. Figure 2 shows a simplified schematic of the oxy-fuel burner and steam boiler.

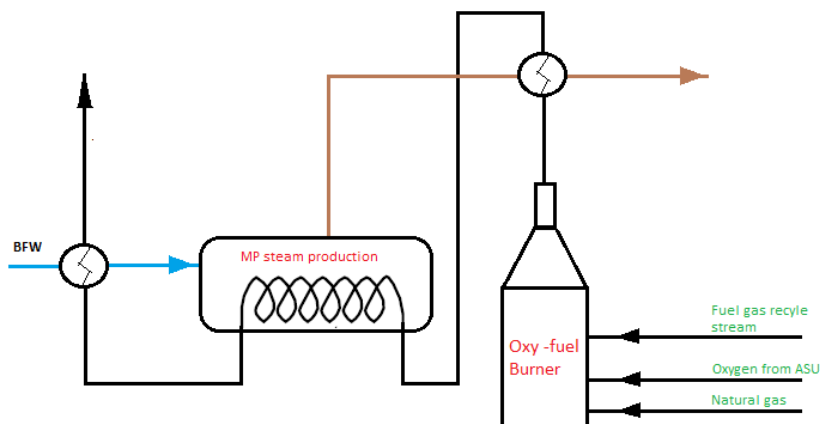


Figure 2 Simple schematic of the oxy-fuel steam and power system

The superheated MP steam from the boiler is routed through a two stage turbine where it is expanded to produce the required electrical energy; approximately 34 MW. The power demand in the facility equals the production rate; hence no power is exported. A portion of steam leaving the MP turbine is drawn-off and used to heat NG, oxygen and fuel prior to the burner. The oxy-fuel plant is planned to operate at 100% of design capacity. The turndown requirement is assumed to be 40%.

2.3 Air separation unit

Oxygen is separated from ambient air by cryogenic distillation in an ASU. The ASU provides 95mol% pure oxygen, and produces 1181 tons/day at full capacity. In AKSO's base case, the ASU is not heat integrated with the power plant, thus it accounts for a significant part of the overall power consumption. AKSO's calculations show that 33% of the power produced is required to run the ASU.

The ASU in AKSO's concept is based on Linde's dual reboiler configuration (further explained in Section 4.2). The air is compressed to approximately 4.4 bar in three stages with intercooling. Cooling Water (CW) is used as the external cold utility. The air is then filtered and dried by a molecular sieve, before cooled to -192°C in the main heat exchanger. Air is then separated to N_2 and O_2 by cryogenic distillation. To produce 1181 tons of oxygen per day, 7000 kmol ambient air/h, is required. When the oxy-fuel plant is turned down the excess oxygen produced is stored in buffer tanks.

2.4 CO_2 compression and purification unit

The flue gas from the oxy-fuel burner is routed to the CO_2 CPU where it is cooled to 20°C by heating LNG. The flue gas is then sent to a scrubber where the bulk of water is removed. Approximately 87.9 % of the CO_2 rich flue gas is recycled to the oxy-fuel burner to maintain the flame temperature, while the remaining flue gas is compressed and further cooled and dehydrated. The cooled CO_2 gas is sent to a cryogenic distillation column where a CO_2 liquid stream is recovered at the bottom, while a nitrogen and oxygen rich gas leaves the vessel as

distillate. The CO₂ is further compressed and heated before exported or stored in underground storage.

2.5 Overall plant performance

At full capacity, the flow of LNG feed is estimated to 25 MillionSm³/day. 1.5% of the sales-gas is burnt in the oxy-fuel burner. The production rate of CO₂ is estimated to be about 796 tons/day. With a CO₂ recovery rate of 92%, the CO₂ emissions will be approximately 65 tons/day. This equals 7.6% of the CO₂ emissions from a SCV. It is important to notice that the CO₂ emission from the system is dependent on the application of the distillate from the N₂/CO₂ separation. If the gas is vented, the emission will be as stated above.

The system requires a CW recirculation system for cooling air prior to the cold box in the ASU; this is the only cold utility requirement in the plant. When running at full capacity, the heat required to vaporize the LNG is calculated to 157.7MW. Most of the heat (123 MW) is provided by either steam or steam condensate produced in the plant.

The overall power consumption by the different units in the plant is given in Table 1. The numbers are extracted from simulation models created in Aspen Plus.

Table 1 Power requirement of the different process systems

Process system	Duty [MW]
ASU	11.3
LNG pumps	4.3
Flue gas fan	4.2
Flue gas recycle fan	1.5
CO₂ compressors and pumps	3.1
BFW pump	0.5
CO₂ heater (air fan)	2.3
20 % margin for others	6.8
SUM	34

3 CO₂ Capture and storage

One way of reducing CO₂ emissions is to develop CO₂ capture plants for fossil-fired power generation. Carbon Capture and Storage (CCS) is intended to be installed at large point sources of emission, including NG fired power plants. There exists three main CO₂ capture technologies currently being investigated; post-combustion CO₂ capture, pre-combustion CO₂ capture and oxy-fuel combustion CO₂ capture. The latter technology will be referred to as oxy-combustion in the following. In post combustion, CO₂ is separated from the flue gas by absorption or another separation technology. In pre-combustion, the fuel is converted to syngas (H₂ and CO), which is shifted to H₂ and CO₂ by the presence of steam. CO₂ can then be captured prior to the combustion. Oxy-combustion is combustion of fuel in an oxygen rich environment, which results in a CO₂-rich flue gas, making it easier to separate the CO₂. None of these CCS technologies are economically feasible today. Some of the main challenges researchers encounter when trying to find solutions for CO₂ capture, are economics, the time CO₂ can be stored, the means of transporting the CO₂ and technological issues [9, 10].

This thesis will focus on oxy-fuel combustion, and in the following a description of the technology will be given and two different oxy-combustion configurations will be presented. Technological issues regarding oxy-fuel combustion will be discussed.

3.1 CO₂ capture by oxy-fuel combustion

In conventional air combustion the nitrogen content is approximately 79 mol% and dilutes the CO₂ concentration in the flue gas, making CO₂ capture complicated and expensive. In oxy-combustion the combustion takes place in an oxygen rich environment, i.e. the molar fraction of oxygen are typically between 90 – 97mol%. Because of the high oxygen purity, the flue gas becomes enriched in CO₂, making CO₂ capture less complicated. The water is condensed to get the CO₂ for depositing, and CO₂ is separated from the flue gas.

Though the flue gas mainly consists of CO₂ and water, other impurities will be present. In a complete stoichiometric combustion, the fuel reacts with the exact amount of oxygen required to oxidize all the carbon in the fuel to CO₂, and the hydrogen to H₂O. For a real combustion however, the flue gas will consist of other substances like CO, NO_x and O₂. CO is produced both in lean and rich combustion, where the first is combustion where the Air Fuel -ratio (AF) is below that of stoichiometric combustion and the latter is combustion where the AF is higher than that of stoichiometric combustion. In lean combustion CO is formed as a result of the dissociation of CO₂, and because of the lack of oxygen. The NO_x and N₂O amount formed in combustion stem from the nitrogen in the air used for the combustion. The NO_x formation is dependent on temperature, time and oxygen availability. In oxy-combustion the NO_x formation is lower compared to conventional combustion due to the low N₂ concentration in the furnace. For lignite fired oxy-combustion the NO_x emissions has been reported to be 50 % lower than for conventional air fired combustion [11, 12].

Oxy-combustion differs from conventional combustion in several ways; in conventional air supported combustion, nitrogen has a minor chemical effect, but a large thermodynamic impact as it absorbs heat during the combustion. Thus, the flame temperature in oxy-combustion will exceed that of conventional air combustion. The flame temperature reaches 3500 °C, which can cause complications in the burner. To reduce the combustion temperature either part of the CO₂ rich flue gas has to be recycled or water injected. In addition to increased flame temperature, the flue gas volume is reduced and the density of the flue gas is increased due to the high molecular weight of CO₂ which exceeds that of N₂ [1, 13].

The main reasons why CCS is not yet commercially available is the cost and risks of CCS which overweigh the commercial benefits. In addition, the regulatory framework for CO₂ storage is not sufficiently defined, and the power consumption for an oxy-fuel system is significantly higher than for a conventional plant, mainly due to extra units operators [5, 14].

3.2 CO₂ Compression and purification

Implementing CCS to oxy-fuel configurations results in significant auxiliary power load. The compressor work in the ASU and the CO₂ CPU are the main causes of the increased power consumption. Therefore reducing the CO₂ compression work is an important parameter in commercializing oxy-fuel combustion. In the following the fundamentals of compression will be presented and the design parameters of the CO₂ CPU discussed.

3.2.1 Fundamentals of compression

For a reversible compressor neglecting changes in potential and kinetic energy, compression work can be expressed as [15]:

$$\left(\frac{\dot{W}}{\dot{m}}\right)_{\text{int}}^{\text{rev}} = -\int_1^2 v dp \quad (3.1)$$

Where \dot{m} [kg/s] is the mass flow rate, \dot{W} [kW] is the compressor work and v [m³/kg] is the specific volume. If integrating Eq.(3.1) for a polytropic compression (i.e. a real compression) the specific work can be expressed as [16]:

$$\dot{W} = Z_1 \cdot \frac{n}{n-1} RT_1 \left[\left(\frac{P_2}{P_1}\right)^{\frac{n}{n-1}} - 1 \right] \quad (3.2)$$

Where Z is the compressibility factor, n is the polytropic index, T_1 is the compressor inlet temperature, P_1 [kPa] is the inlet pressure and P_2 is the outlet pressure. R [kJ/kgK] is the gas constant, expressed as the ratio between the universal gas constant R_o (8.314 kJ/kmolK) and the molecular weight M [kg/kmol]

As can be seen from Eq.(3.2), the inlet temperature T_1 plays an important role for the magnitude of the compression work. The temperature ratio in a compressor can be expressed in terms of the pressure:

$$\frac{T_2}{T_1} = \left(\frac{p_2}{p_1} \right)^{\frac{n-1}{n}} \quad (3.3)$$

Where n can be calculated from:

$$n = \frac{\eta_p}{\eta_p - \frac{k-1}{k}} \quad (3.4)$$

Where η_p is the polytropic efficiency for the compressor, and k is the isentropic index, which is given by the ratio of heat capacity at constant pressure (C_p) and heat capacity at constant volume (C_v).

From Eqs.(3.2) and (3.3), it can be seen that a low inlet temperature will decrease the compressor work, if the pressure ratio is fixed. From Eqs.(3.2) and (3.4), it can be seen that for a constant polytropic efficiency a high k -value results in lower power consumption for the same pressure ratio. The compressor work is also affected by the molecular weight of the gas, as \dot{W} is a function of the gas constant. A high molecular weight will result in a lower R -value, hence the specific work will decrease.

3.2.2 CO₂ CPU design

The objective of the CO₂ CPU is to compress the flue gas and condense most of the water, before the CO₂ is purified and pumped to the required product pressure. The combination of compression, condensation and pumping reduces the overall power consumption. In most CO₂ CPU configurations, the flue gas is compressed in several stages with intercooling. By dividing the compression in a number of stages the net work required by each compressor is reduced. The gas is cooled and water removed between each compression step. Water needs to be removed in several stages because the solubility of water in CO₂ decreases with pressure. The effect of multistage compression with intercooling for an isentropic compressor can be seen in the pressure-enthalpy diagram (Figure 3) [8, 17].

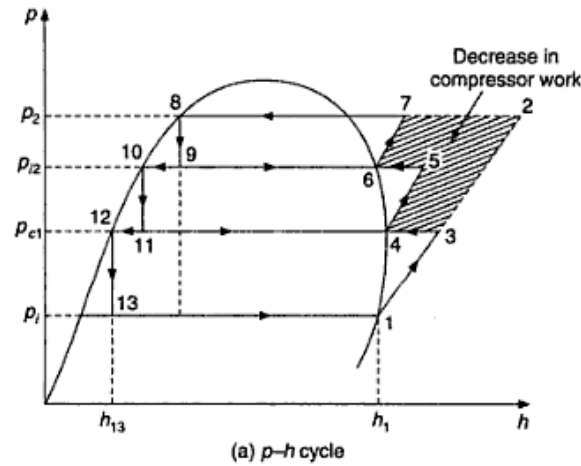


Figure 3 Multistage compression with intercooling [18]

For a one stage compressor with pressure ratio p_2/p_1 the total enthalpy increase is h_2-h_1 . If the gas is compressed in three stages, and cooled near its saturation line between each stage, the compression work will decrease as can be seen from the graph above. The total enthalpy increase can then be expressed as $(h_7-h_6) + (h_5-h_4) + (h_3-h_1)$.

There exist different CO₂ CPU configurations. The choice of configuration is dependent on the fuel used (NG or PC), desired CO₂ recovery rate, product specifications and the trade-off between Capital expenses (CAPEX) and operating expenses (OPEX). There exist three main CO₂ CPU schemes. If a 100 % CO₂ recovery rate is required the CO₂ CPU can be designed with *no purification*, meaning that the flue gas is only compressed and cooled with no separation of N₂/CO₂. Another solution is *partial condensation in a cold box*. In this scheme the flue gas is compressed and dehydrated before cooled to a very low temperature to condensate most of the CO₂. This scheme has a 90% CO₂ recovery rate. An extension of this configuration is a scheme with *cryogenic distillation*, where the flue gas is purified by distillation after the cold box. This results in a purer product stream; it can exceed 99 % depending on the scheme. If using cryogenic distillation, the separation should take place between the triple point (5.1795 bar and -56.6 °C) and the critical point (73.773 and 31.03 °C) of CO₂, meaning that the partial pressure of CO₂ should exceed 5.1795 to experience a phase change [10, 19]. Figure 4 shows the specific power of the CO₂ CPU for the different configurations as a function of the CO₂ content in the flue gas.

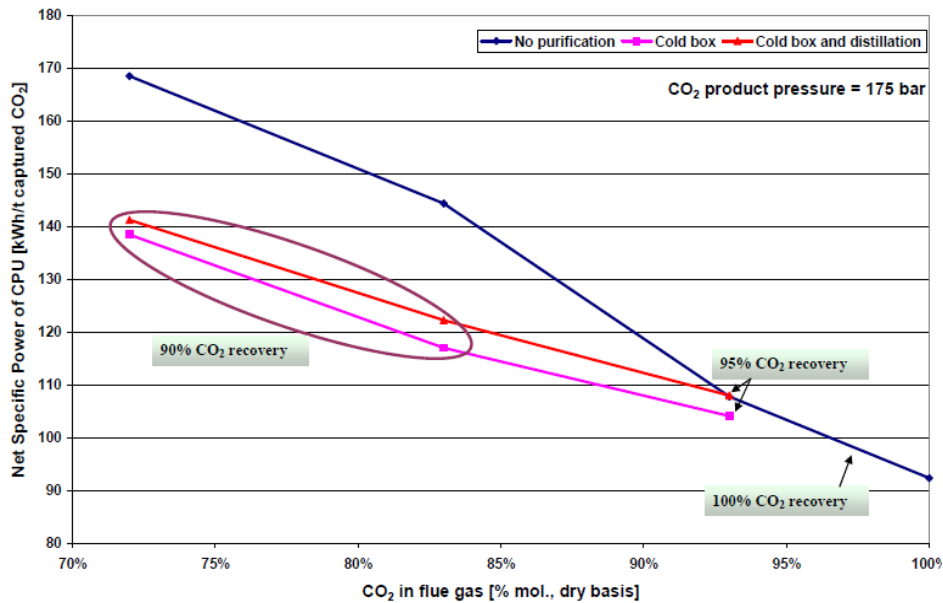


Figure 4 Specific power of CPU as a function of CO₂ in flue gas [19]

From Figure 4 it can be seen that the power requirement increases with decreasing CO₂ content in the flue gas, for all the different schemes. At the interception between the red and the blue graph, the different schemes require nearly the same amount of energy, though the recovery rate differs. For low CO₂ content in the flue gas (less than 90%), it can be seen that the cold box configuration with or without distillation is less energy demanding than the no purification scheme. It is important to notice that this graph is drawn based on pulverized coal as fuel and a CO₂ product pressure of 175 bar [19].

The power consumption in the CO₂ CPU is also dependent on the CO₂ application. The CO₂ can either be stored in underground storage, or used for enhanced oil and gas recovery, as it is proven more efficient than steam, for such applications. If geologically stored, a high CO₂ density is required and the CO₂ needs to be compressed above the critical point. The specific volume is more than 500 times smaller at supercritical conditions, than for CO₂ in a gas phase at atmospheric pressure. The same requirements apply to pipeline transportation, as a high density decreases the required diameter. The water specification is also dependent on the CO₂ application. For AKSO's system the water specification is set to 50 ppm, resembles specification for pipeline transportation. Independent of the CO₂ application the water content should be limited to prevent freeze-out if using a cold box scheme [8, 17, 20].

3.3 Available oxy-fuel configurations

Most ongoing and planned pilot projects on oxy-combustion schemes are PC fired. Those systems tested for NG are typically either based on a Brayton cycle, a Rankine cycle or a combination of these two. In this thesis two different configurations will be presented; an oxy-fuel NGCC and an oxy-fuel burner (steam cycle) scheme. AKSO's system is based on the latter and technological issues regarding this technology will be described.

3.3.1 Oxy-fuel NGCC

A conventional NGCC consist of a gas turbine, with air as the working fluid, combined with a steam cycle. Figure 5 shows a semi closed oxy-fuel combined cycle. The working fluid in the cycle is diluted CO₂, which is used to limit the flame temperature. The flue gas is sent through a heat recovery steam generator (HRSG), generating steam that is utilized in a two stage turbine. Water is removed from the flue gas, and CO₂ is captured. Because diluted CO₂ is used as the working fluid, the gas turbine needs to be redesigned. When using diluted CO₂ an increased speed of sound is experienced (80% higher than for air), resulting in a lower mach number. The density is approximately 50% higher for CO₂, and the specific heat ratio is lower which results in a lower temperature change in an adiabatic compression or expansion. The optimal pressure ratio is higher for oxy-fuel NGCCs than for a conventional cycle. Typically 30-35, compared to 15-18 for a conventional gas turbine. A higher pressure ratio increases the required compressor work, hence the efficiency will decrease. The efficiency for a typical oxy-fuel combined cycle is approximately 45 – 47%, which is nearly 10 % less than for a conventional combined cycle [10, 13].

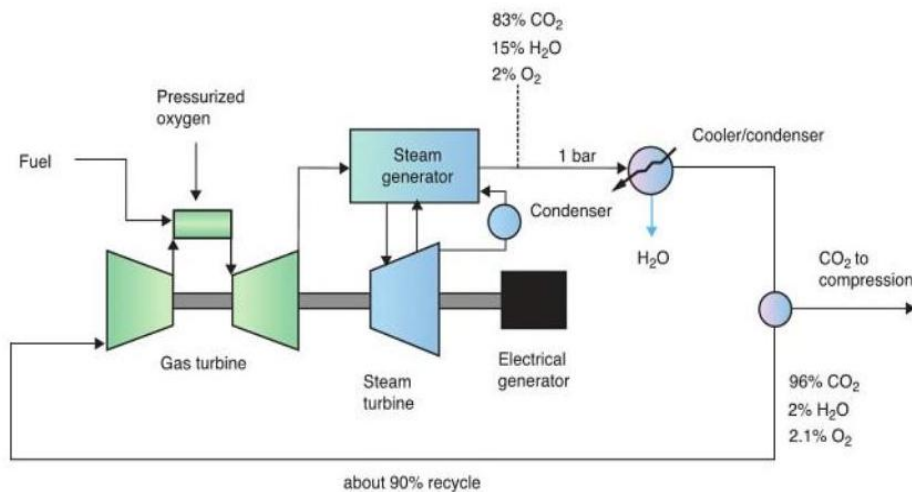


Figure 5 oxy-fuel combined cycle with steam generation [13]

3.3.2 Oxy-fuel burner

Retrofitting a conventional gas turbine to oxy-fuel combustion is complicated because the working fluid differs from that of a conventional gas turbine. Another configuration which can be used is an NG fired oxy-fuel burner with steam generation. NG is combusted in an oxygen rich environment producing a CO₂ rich flue gas. In most oxy-fuel boiler configurations, a part of the flue gas is recycled to the burner to limit the flame temperature. The remaining part of the flue gas is sent to the CO₂ purification unit where water is drained out, and the gas is compressed and purified as explained in Section 3.2.2.

Studies on PC fired oxy-burners indicate that conventional burners can be retrofitted to oxy-fuel, but there are several challenges to overcome before oxy-fuel boilers are feasible [21]. The next section will explain the most critical technological challenges.

Technical challenges for oxy-fuel burners

Increased heat transfer for oxy-fuel burners compared to air-combustion is expected. The main reason is the increased concentration of tri-atomic (molecules formed by three atoms) gases in the furnace. These molecules absorb and emit radiation, resulting in an improved radiative heat transfer. In addition, CO₂ and water has higher specific heat capacity than nitrogen, resulting in increased heat transfer in the convective heat transfer zone [22].

The change in flame characteristics is one challenge researchers need to overcome to be able to manufacture oxy-fuel boilers or retrofit existing boilers. But according to Bensakhria and Leturia [22], the flame characteristics for oxy-combustion can be adjusted to give the same conditions as for conventional combustion. Another challenge for oxy-fuel boilers is the recycle ratio. As opposed to conventional burners, which operate at a fixed excess air ratio and air composition, an oxy-fuel burner needs to be custom-made. The configuration of the burner is dependent on the recycle rate which differs with oxygen purity and fuel composition.

According to a study carried out by SINTEF Energy AS for AKSO, there are three suppliers with experience in natural gas oxy-fuel burners for CCS; Air Liquid, Clean Energy System and Jupiter Oxygen [5]. Jupiter Oxygen has tested an NG fired oxy-boiler, without recycling flue gas. As already mentioned, oxygen rich combustion leads to extremely high flame temperatures, mainly because of the increased heat transfer in the radiative zone. According to Jupiter Oxygen simulations, the radiant zone increases by 31 % for oxy-fuel combustion compared to conventional air combustion. As the heat flux from radiation is proportional to T^4 , the increased flame temperature result in a significant heat flux. Jupiter Oxygen has developed a boiler which tolerates these high temperatures by limiting the heat flux, thus no reflux is needed making it more economically feasible to retrofit existing steam boilers [23].

4 Air separation technology

There exists different air separation technologies; Adsorption, membrane and cryogenic distillation. In the following chapters, the two latter technologies will be described. Adsorption is not further discussed, as this technology is not economically feasible for oxygen production above 200 tons/day [13].

4.1 Distillation

The most complex unit operation in an ASU is the cold box where all the cryogenic equipments are located, including the main heat exchanger and the cryogenic distillation column. To understand the structure of an ASU a brief introduction to distillation is presented in this section.

In a single-stage separation of a homogenous mixture, the mixture is partly vaporized and the components are separated based on their difference in boiling point. A single separation stage can only achieve a limited separation, thus to increase the separation rate the components can be separated by distillation. A distillation column can be thought of as several single stage separators where the feed enters the column as liquid, vapor or a mixture. In the column, a part of the feed vaporizes and flows upwards, while the liquid flows downwards. The less volatile components will be transferred to the liquid phase, while the more volatile components are transferred to the vapor phase. The liquid leaving the bottom of the column is partly or totally vaporized in a reboiler and routed back to the column. The vapor leaving the top of the column is partly or fully condensed before routed back to the column as reflux, to increase the separation rate. An equilibrium stage for distillation is given in Figure 6. Eq.(4.1) expresses the material balance for component i in stage n [24].

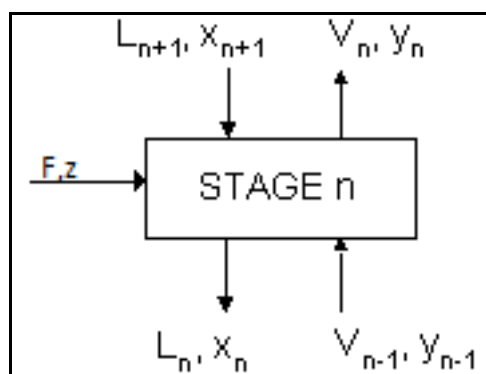


Figure 6 Equilibrium stage for distillation

$$F \cdot z + L_{n+1} x_{n+1} + V_{n-1} y_{n-1} = V_n y_n + L_n x_n \quad (4.1)$$

F is the feed, L is the flowrate of liquid and V is the flowrate of vapor. The rate of distillation is dependent on the K value and the relative volatility of the mixture. The K for component i is given in the equation below [25]:

$$K_i = \frac{y_i}{x_i} \quad (4.2)$$

Where y_i is the mole fraction of component i in the vapor phase, and x_i is the mole fraction of component i in the liquid phase. The K value is a measure of the tendency of component I to vaporize and is dependent on temperature, composition and pressure. For a binary mixture, the separation of components in a distillation is dependent on the ratio of the K value for component i and j, respectively. This ratio is called the relative volatility and is expressed by Eq.(4.3). If the relative volatility is high one component has a much greater volatility than the other, making the separation easier.

$$\alpha_{i,j} = \frac{K_i}{K_j} \quad (4.3)$$

There are several operating conditions affecting the distillation column; operating pressure, reflux ratio, condition of the feed, type of condenser and number of stages. There exists a trade-off between these operation conditions E.g. if the operating pressure is raised the separation becomes more difficult, but the condenser/reboiler duties are decreased. Therefore the accurate design of the column is of great importance [24].

4.2 Cryogenic air separation unit

An oxy-fuel steam and power plant requires an oxygen production greater than 1000 tons/day. Today, cryogenic distillation is the only available technology to produce large quantities of high purity oxygen. There exists several different ASU configurations; in the following the basics of cryogenic distillation with double column will be explained.

An ASU mainly consist of air compressors, a purification unit and a cold box, containing the main HX and the distillation column, both operating at cryogenic temperatures. Ambient air is fed to the air compression and purification unit where it is compressed to about 5 bar before it is purified. Ambient air typically contains 21% oxygen, 0.04 % CO₂, 1% H₂O, 0.9% Argon and 77.1 % N₂.The water and CO₂ content is limited to prevent freeze out in the cold box, as both components have a higher boiling points than both oxygen and nitrogen. The air is then routed to the cold box where it is cooled to or below its dew point before entering the rectification section, which consists of two integrated distillation columns. The columns are integrated by having a condenser-reboiler that furnish reflux for the bottom column and vapor for the upper one. Air enters the bottom of the HP column partially liquefied. In the HP column vapor, enriched in nitrogen, is rising to the HP condenser. The liquid nitrogen from the condenser is split into two different reflux streams for both the HP column and the LP

column. By condensing the nitrogen rich stream, heat is transferred to the LP upper column where high purity oxygen is vaporized. High purity oxygen is drawn off at the bottom of the LP column, while a nitrogen rich vapor stream leaves the top of the column. If separating argon, or other rare gases in the distillation column, additional columns need to be added to the system. Figure 7 shows a simplified schematic of the distillation [26].

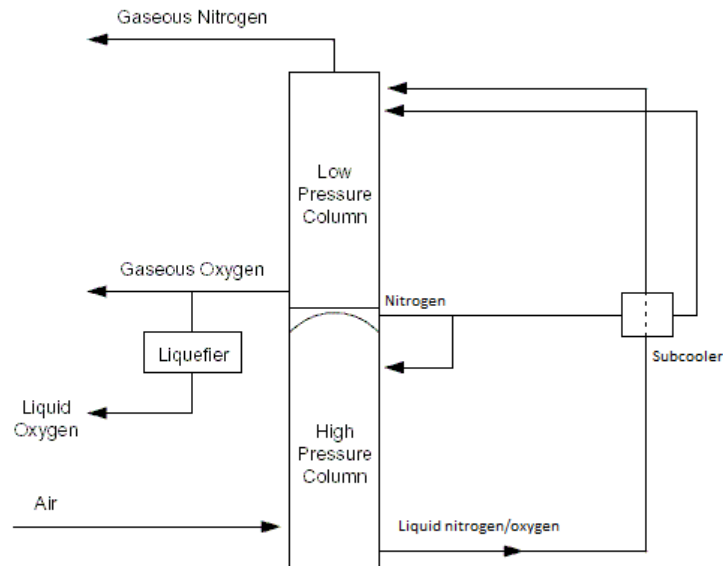


Figure 7 Cryogenic distillation of air

When applying an ASU to an oxy-combustion scheme the specification of the system differs in working pressure, purity and size compared to a conventional ASU. The oxygen purity is lower; typically 85 – 98 % compared to greater than 99.5% for a conventional ASU. The oxygen pressure is lower than for a conventional plant; for a PC fired oxy-fuel burner the oxygen pressure is typically between 1,5 – 2,0 bar, while for a oxy-fuel NGCC the pressure are between 30- 40 bar. Therefore ASUs needs to be specially design for their purpose. Cycles for low purity oxygen were developed in the 1990s, but these cycles were not adapted to low pressure oxygen product streams. In 2007 air liquids started a program for development of ASUs specified for oxy-combustion, i.e. low purity, low oxygen pressure and no nitrogen requirements. The power consumption of an oxy-fuel configured ASU has decreased as a result of this program. However, the power demand is still significantly higher than the theoretical energy requirements [19].

5 Possibilities of power reduction

If oxy-fuel combustion shall be commercialized, reduction in CAPEXs, OPEXs and power consumptions is required. One possibility is integrating the ASU with the power plant. This is an instinct subject, due to lack of research on the matter. Another possibility is to change the oxygen purity. Both the power consumption in the ASU and the CO₂ CPU is a function of the oxygen purity, therefore it is essential to investigate the subject to find the ideal purity for the plant. In the following these subjects will be discussed.

5.1 Integration between an ASU and an oxy-fuel power cycle

Integrating an ASU with an oxy-fuel combustion system is proven difficult, due to the rigid integration within the ASU cold box. Air is cooled to cryogenic temperatures by returning streams from the distillation train, i.e. the cold box is fully heat integrated [8].

For oxy-fuel NGCCs there exists some integration concepts. Compressed air can be drawn from the gas turbine's compressor, and fully or partially supply the feed requirements of the ASU. As the distillation pressure will be set by the extraction air pressure, a supplemental air compressor is necessary if the mass flow from the turbine is less than the required mass flow in the ASU. Another solution for an NGCC is to compress the byproduct nitrogen, and heat it against the extracted air from the gas turbine. This will lead to heat recovery, as the extracted air needs to be cooled before entering the ASU. By injecting nitrogen into the gas turbine the NO_x emission are reduced, as nitrogen reduces the flame temperature and thus the production of NO_x [27].

For oxy-fuel boilers, heat integration with an ASU includes heat transfer from the air compressors to the steam and power production unit. The surplus heat can be used to preheat BFW, preheat oxygen prior to the combustion, or it can be used to heat other cold streams in the plant. Because of the rigid integration in the cold box, thermal integration is limited to recover heat of compression.

AKSO has evaluated the possibility of integrating the ASU with the regasification unit. It was found complicated because turn-down of the ASU during off-peak demand, is difficult. This flexibility problem is the most prominent issue regarding the subject. According to Dubettier et al. [28], the air compressors can achieve a turn down of 75% and the cold box a turn down of 50% for a one train ASU configuration. If a further turn-down is required the excess oxygen can be stored in buffer tanks. Air Liquid (AL) has developed a new concept called AL Innovative Variable Energy where excess oxygen is stored as liquid during off-peak [19].

As already mentioned, integration between an ASU and an oxy-plant is not broadly investigated. However, AL has tested a lignite fired oxy-fuel boiler, integrated with a cryogenic ASU. The electric efficiency of the plant was increased by 1%, when heat integrating the air compressors with the oxy-combustion plant. Research was done on an ASU

with both 95 and 99%-volume oxygen purity. The high purity scheme only decreased the overall efficiency by 1 %. This is an important result as higher oxygen purity result in lower cost of the CO₂ CPU. This is further discussed in the following section [29].

5.2 Impact of changing the oxygen purity

The following sub-chapters will discuss the impact of changing the oxygen purity. As the literature on NG fired oxy-fuel boilers are limited, these chapters are based on literature regarding PC fired oxy-fuel boiler and oxy-fuel NGCCs.

5.2.1 Impact on the ASU

When increasing the oxygen purity the energy demand in the ASU increases. Figure 8 demonstrates the energy of separation in an ASU, as a function of the oxygen purity. Energy of separation [kWh/t] is defined as the power required producing 1 ton of gaseous oxygen at 1 atm.

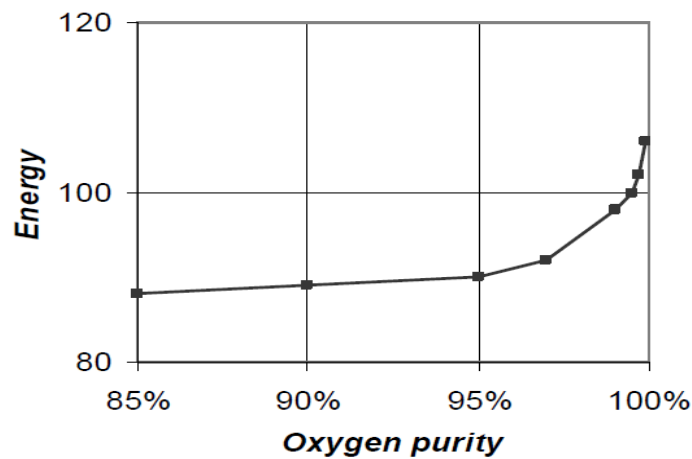


Figure 8 Power requirement of a cryogenic ASU [19]

The graph in Figure 8 is quite rectilinear below 95mol% purity. At 97mol% oxygen purity, the energy of separation increases sufficiently. This is because the separation changes from oxygen-nitrogen to oxygen-argon in the LP column. This leads to increased power demand, as well as increased CAPEX and OPEX.

The main energy-consuming component in an ASU is the air compressors. The power consumption in the air compressors is dependent on the air feed flow and the outlet pressure, hence it is dependent on the oxygen purity. According to a study carried out by Amann et al. [2] the HP column pressure needs to be increased with 30 %, if changing the purity from 85 mol% to 97 %. The study was carried out for a NGCC converted to oxy-fuel. The results from the study are given in Table 2.

Table 2 Influence on ASU by changing the oxygen purity [2]

O₂ purity [mol%]	85	90	95	97
O ₂ stream flow [tons/h]	271.7	255.7	241.4	236.8
ASU power [MW]	60.1	61.2	62.8	63.6
Specific consumption [kWh/tO ₂]	221.3	239.2	260.2	268.7
ASU penalty [%]	5.4	5.8	6.2	6.3

The results in Table 2 are from simulations performed in Aspen Plus. The oxygen stream flow is calculated with 5 mol% excess oxygen in the flue gas. The air feed to the ASU is specified to 279 kg/s. The ASU penalty corresponds to the difference in electric efficiency for the oxy-fuel system, and a conventional Integrated Gasification Combined Cycle (IGCC). The ASU power calculated is the electric power required in the air compressors [2].

From Table 2 it can be seen that the required oxygen flow decreased with oxygen purity. This is because less oxygen is required to maintain a near-complete combustion in the furnace. The compressor power of the ASU increases with increased oxygen purity. However, the increase is relatively small, because of the reduced flow rate. Though the change in compressor work is minor, the OPEX of the ASU will increase for increasing oxygen purity, due to the alternate separation operation. Though the power consumption decreases with decreasing oxygen purity, the required ASU equipment size will increase for oxygen purities below 95 mol%, due to the inferior pressure in the system. This results in increased capital costs [30].

5.2.2 Impact on the CO₂ CPU

As can be seen from Figure 8, oxygen purities above 95% are not favorable for the ASU. However, it has a positive impact on the CO₂ recovery process. With high oxygen purity the CO₂ concentration in the flue gas increases and the required molar flow of oxygen is reduced, resulting in a lower flow rate of flue gas in the CO₂ CPU. As a result, the compression work in the CO₂ CPU is reduced. In addition, the energy of separation in the distillation column is reduced, due to the increased CO₂ content in the flue gas. This can be seen from Figure 9, showing the specific work of a CO₂ CPU as a function of the CO₂ content in the flue gas, for different capture schemes (explained in Chapter 3).

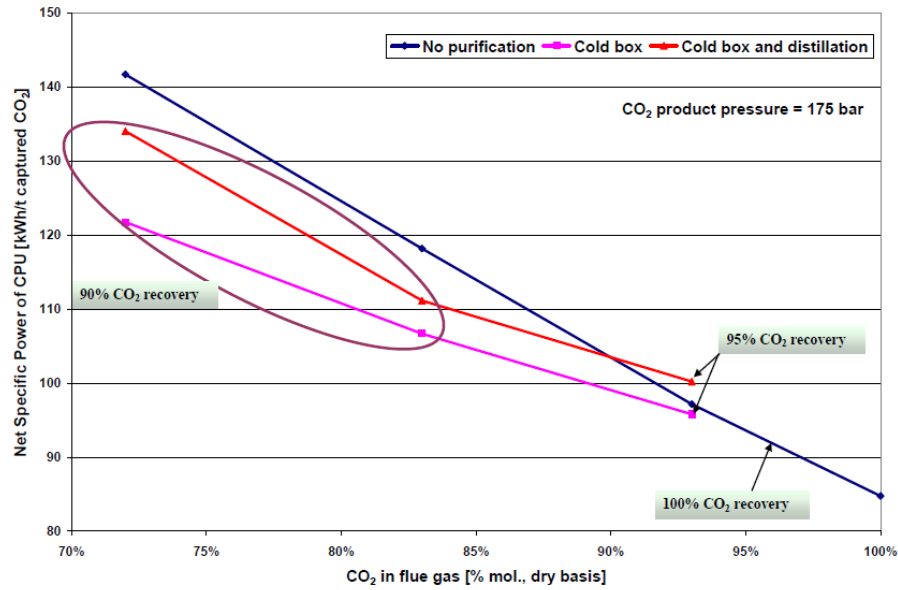


Figure 9 Specific work of CPU as a function of CO₂ in flue gas [19]

Amann et al. study also examines the impact on the CPU, when changing the oxygen purity. Oxygen purities between 85-97mol% have been tested for a CO₂ CPU is with cryogenic distillation. The result from the study is given in Table 3, and it shows that both the compressor work in the CO₂ CPU and the recovery process power are dependent on the oxygen purity. In addition the waste expansion power will depend on the flue gas flow, which changes with oxygen purity [2].

Table 3 Performance of the cryogenic CO₂ recovery process [2]

O ₂ purity [mol%]	Recovery rate [%]	Flue gas flow [kg/s]	CO ₂ compression [MW]	Recovery process power [MW]
85	75.0	58.0	4.0	19.1
97	75.0	48.3	3.4	15.2

6 Membranes used for air separation

As already mentioned the cryogenic ASU accounts for a significant amount of the overall power consumption in an oxy-fuel plant. The most promising alternative to cryogenic air separation is membrane technology, though this technology is not yet commercialized for large-scale oxygen. In the following sub chapters the fundamentals of membranes used for air separation is presented.

6.1 Introduction

A membrane acts as a barrier between two streams, and has the ability to transfer chemical components selectively. The chemical components transferred through the membrane are denoted permeate, while the remaining components exit on the retentate side of the membrane. Generally, the driving forces are the difference in concentration, i.e. the partial pressure difference on the feed and permeate side. Figure 10 indicates the separation of a mixture by membrane technology [31].

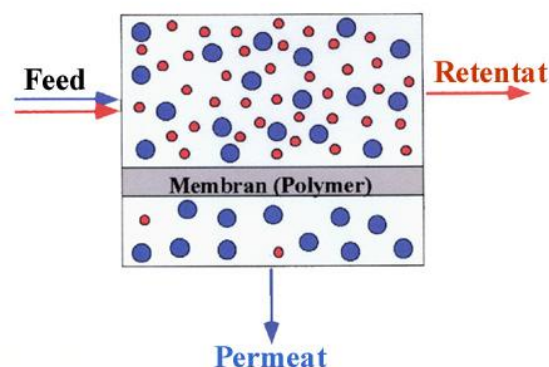


Figure 10 Transportation in a typical Membrane [32]

Selecting the right membrane for gas separation is challenging. The most important criteria are the required flux and selectivity for the given mixture. But in addition, costs, durability and operating conditions need to be accounted for. The fundamentals of membranes are complex. Thus this thesis will only give a brief overview of membranes suitable for oxygen production.

6.2 Inorganic membranes for air separation

There are several ways to classify membranes, but the most illustrative way is to classify them according to their structure, as the structure also determines the transport mechanism through the membrane. Membranes can be inorganic or organic, asymmetric, symmetric, porous or non porous. According to Burggraaf [33], the most promising membranes for high purity oxygen production are inorganic membranes, which can produce 99 mol% pure oxygen. Therefore only this type of membranes will be discussed in this thesis.

Inorganic membranes include symmetric/asymmetric single wall membranes, multilayer asymmetric membranes and membranes with modified structure. These membranes can either be dense or porous where the first denotes membranes made of solid layers of metal or mixed conducting oxides, and the latter membranes made of a porous wall/top layer. The most promising inorganic membranes for oxygen separation are ion transport membranes (ITMs). These membranes are made of solid inorganic ceramic materials, and produces oxygen by transferring oxygen ions (O^{2-}) through the membrane. The driving forces are either the difference in the partial pressure, or an electric voltage gradient. Membranes utilizing pressure difference as the driving force, are referred to as mixed conduction membranes or mixed ionic-electronic conducting membranes (MIECs), as they conduct both oxygen ions and electrons [33]. The two different membrane concepts are given in Figure 11.

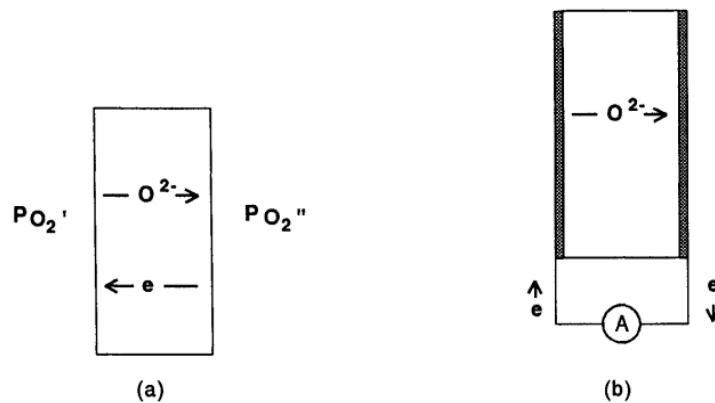


Figure 11 Different membrane concept: a) mixed conducting membrane, b) electrical driven membrane [34]

ITMs have the potential of producing several tons of oxygen and are seen as one of the most promising alternatives to cryogenic distillation, especially the MIECs since no electric circuit is required to enhance electronic transport [34, 35].

6.2.1 Transportation mechanism of inorganic membranes

The transport mechanism for inorganic membranes are either Knudsen diffusion, selective surface flow, molecular sieving or ionic transportation, where the latter is most common for dense inorganic membranes used for gas separation [31].

If assuming constant ionic conductivity, the flux of oxygen through a MIEC is given by the Wagner equation:

$$j_{O_2} = \frac{\sigma_i RT}{4Ln^2 F^2} \ln \left(\frac{P_{O_2}'}{P_{O_2}''} \right) \quad (6.1)$$

Where j is the oxygen flux through the membrane, R is the ideal gas constant, σ is the ionic conductivity, n is the charge and F is the Faraday's constant. P' is the partial pressure of oxygen in the air (feed side), and P'' is the partial pressure at the permeate side. As can be

seen from this formula, the flux is proportional to $\ln(p_1/p_2)$ rather than the pressure difference over the membrane [36].

Membranes are also characterized according to their permeability and selectivity. The permeability denote the quantity of the solute gas diffusing through the solid pr second pr area through a 1 m thick solid under a pressure of 1 atm. i.e. it denotes the amount of gas the membrane is able to selectivity transfer per second. The permeability is given by the product of solubility (S) and the diffusion (D) through the membrane (Eq.(6.2)). Where solubility denotes the pressure normalized amount of gas sorbed in the membrane under equilibrium conditions [10, 37].

$$P_M = D_{ij} \cdot S \quad (6.2)$$

The selectivity denotes the separation factor, and is expressed by the mole fraction or the partial pressure of the gas components in the feed(x) and permeate (y) respectively. A high selectivity provides a high purity. Eq.(6.3) denotes the selectivity (α) for a gas stream of two components(i,j) [10, 31].

$$\alpha_{i,j} = \frac{y_i / y_j}{x_i / x_j} \quad (6.3)$$

In MIECs an ionic current of oxygen is transferred through the membrane, while a simultaneous flux of electrodes is transferred in the opposite direction. Oxygen is transported from the high oxygen chemical potential side to the low potential side. Because oxygen is transported in ionic form instead of molecular diffusion, the selectivity can theoretically reach 100 %. These membranes are thermally activated and the operation temperature is typically between 700 °C and 1000 °C [34, 38].

6.2.2 Structure of MIECs

Finding the ideal membrane structure is challenging, and there exists several papers researching the composition and structure of MIECs [38, 39]. This thesis will only introduce the most promising materials in terms of oxygen flux and selectivity.

The most promising MIECs in terms of oxygen permeation, exhibit either a fluorite or perovskite structure. This report will focus on the latter, as they tend to have a higher flux. Perovskites have a cubic lattice, but it can be distorted into an orthorhombic structure which makes it stable at high temperatures. The ideal perovskite (Figure 12), has the chemical formula ABO_3 , where A, and B are metal ion with positive charge (cations) and O denotes oxygen molecules with negative charge (anions). A is typically barium, lanthanum or strontium, while B is typically cerium, cobalt or iron [38].

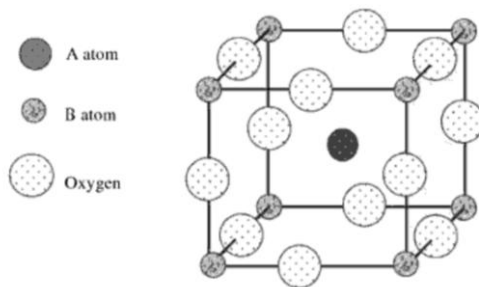


Figure 12 Ideal Perovskite [40]

If the perovskite had been ideal as in Figure 12, it would not be able to transport an ionic current. Some defects are required to enhance ionic transportation. Vacancies are a form of defects, and a high amount of vacancies gives a high oxygen permeation flux. There are many different strategies employed to enlarge the oxygen permeation properties. The most common strategy is doping the perovskite. Generally the ABO_3 is improved by doping the B-site with a more stable cation [34].

6.2.3 Performance of MIECs

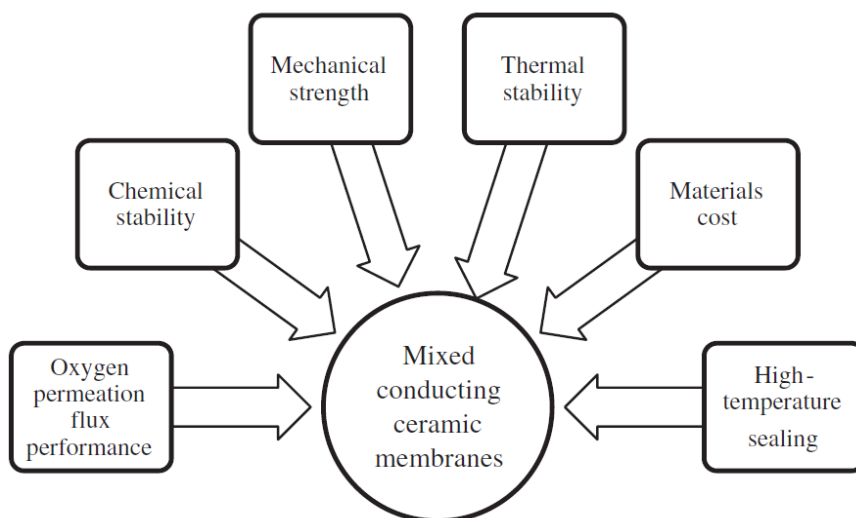


Figure 13 Factors influencing the MIEC[39]

Figure 13 shows different factors that influence the membrane selection. Firstly the membrane must possess high oxygen flux. The flux is influenced among others, by temperature, pressure, membrane thickness and structure. As can be seen from Figure 14 the temperature plays an essential role. The figure displays flux as a function of temperature and membrane thickness for a typical perovskite. At temperatures below 600 °C the flux is insignificant, but when exceeding 800 °C a sharp increase in oxygen flux is obtained. In addition the oxygen flux is inversely proportional to the membrane thickness, i.e. a thin membrane at high temperature will give the highest oxygen flux. As seen from Figure 14 this becomes more evident at high temperatures. However, the mechanical strength of thinner perovskite

membranes is poor, especially when exposed to high operational temperature and pressure. It is also important to notice that most mixed conducting membranes with high ionic conductivity (i.e. high flux) have low chemical stability [38, 39].

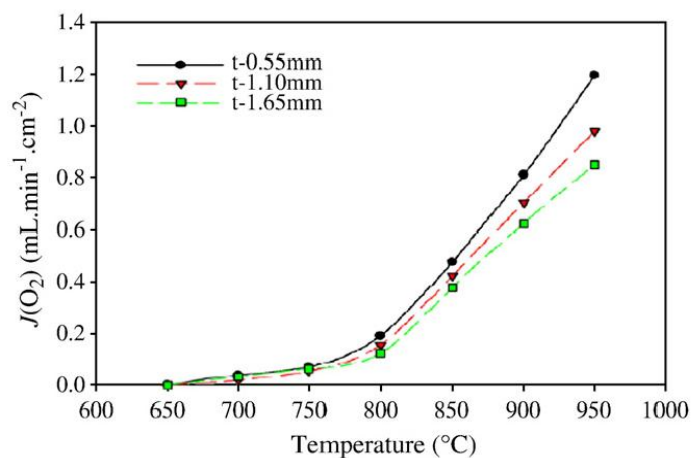


Figure 14 Mass flux as a function of temperature[39]

To compete with conventional air separation technology, the cost of membranes should be as low as possible. However they also need a high enough production rate to compete with conventional air separation technology. Hence, there exists a trade-off between energy cost and production rate. As an example the flux should be around 1ml (STP)/cm² from an economical point of view, while to be able to compete with current technology it should reach 3.5 ml (STP)/cm² [39].

The cost of the system is influenced by the method employed to induce a pressure difference over the membrane. This can be done in several ways; by compressing the feed, using a sweep gas or by creating a vacuum on the permeate side of the membrane. Each of these solutions has its advantages and disadvantages. If pressurized air is used, the required pressure is typically 20 bar. This leads to high energy and capital cost as well as inducing substantial stresses to the membrane. Using a vacuum on the permeate side will only give a limited pressure difference, and a lower flux. In addition, the oxygen needs to be re-compressed if a higher working pressure is needed. The best solution is a combination of using a sweep gas and air compression [41].

For the purpose of large-scale oxygen production the membrane should exhibit a perovskite structure with high flux. In addition, the membrane should be relatively thick to enhance the required durability. Some promising membrane structures are given in Table 4, where δ are the oxygen vacancies.

Table 4 Oxygen permeation flux data for perovskite single-phase membranes [42-44]

Membrane	Temperature[°C]	O ₂ Flux [mol/s·cm ²]	Thickness[mm]
Ba_{0.5}Sr_{0.5}Co_{0.8}Fe_{0.2}O_{3-δ}	850-900	1.563 10 ⁻⁶	1.8
Gd_{0.6}Sr_{0.4}CoO_{3-δ}	820	1.179 10 ⁻⁶	1.5
Ba_{0.5}Sr_{0.5}Zn_{0.2}Fe_{0.8}O_{3-δ}	800-975	2.604 10 ⁻⁶	1.45

6.3 Implementation of membranes in oxy-fuel systems

As the power consumption in an ASU is significant, AKSO is interested in finding another air separation technology suitable for their system. Even though MIECs are not yet commercial available, they are broadly investigated. In the following the implementation of ITMs (mainly MIECs) in oxy-fuel systems are discussed.

6.3.1 ITMs used for oxygen production today

One of the leading companies in ITM for air separation is *Air products*. They are currently producing equipment for a MIEC pilot project. A MIEC capable of producing 100tons O₂/day will be tested this year. According to Ted Foster, the director of advanced gas separation in *Air products*, the company will be able to fabricate enough ceramic membranes to produce 1000tpd in 2014 (See Appendix E). The company has developed both MIECs and electrically driven ITMs, but only the MIECs are capable of large-scale oxygen Production. The Company has, in cooperation with the US Department of Energy, successfully tested a prototype which produces 5tpd of oxygen. The MIEC is produced for CO₂ capture in coal plants, meaning that the integration of the component in a NG plant may differ. According to *Air products* the MIEC require 35 % less capital cost then the cryogenic air separation, and consumes 35 – 60 % less energy [45].

6.3.2 MIECs integrated with an oxy-fuel plant

The National Energy Technology Laboratory has tested MIECs integrated with a PC-fired oxy-fuel plant. When simulating the plant, the oxygen concentration was assumed to be 100%. The MIEC delivered oxygen to a 550 MW oxy-fuel plant. Figure 15 shows part of the block flow diagram of the “*ITM oxycombustion plant*” [46].

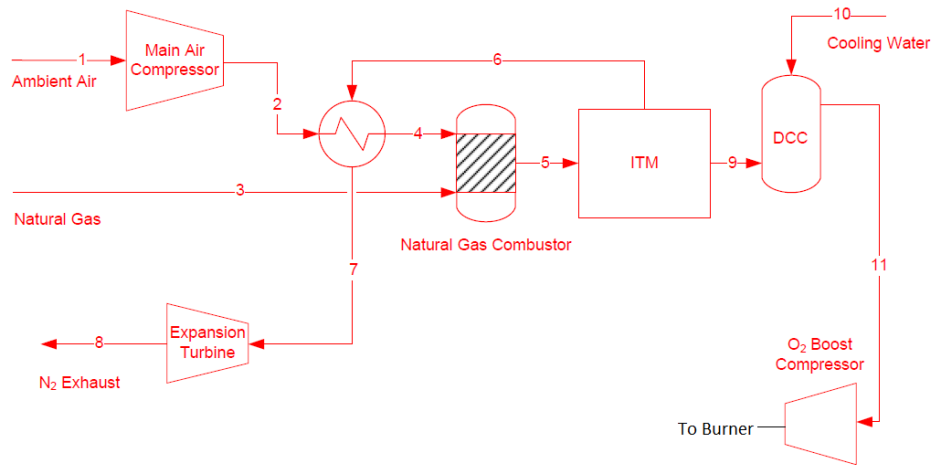


Figure 15 ITM oxycombustion plant[46]

Ambient air is fed to the main air compressor where it is compressed to 1.38 bar before heat exchanged by N_2 from the membrane. A NG fired burner is used to heat the air to $800^\circ C$. The oxygen produced is at 0.07 bar and $800^\circ C$, i.e. a vacuum is used to enhance a partial pressure difference over the membrane. The pure oxygen is then compressed and cooled upstream the PC-fired boiler [46].

The result from this test shows that 104 819 kmol/h of ambient air is required to produce enough oxygen, when the flowrate of PC is 43 476 kmol/h. It is then assumed that the ITM can produce 0.13 kmol/h oxygen from 1 kmol/h ambient air [46]. This assumption is based on prospective membrane technology. Today, there exist no systems which can produce the amount of oxygen required in an oxy-fuel system.

7 Fundamentals of heat integration

AKSO's oxy-fuel facility is based on heat integration between the different units in the system. The next sections will present the fundamentals of heat integration.

7.1 Composite and grand composite curves

Process integration is an approach to design and operation of industrial facilities, where the aim is to conserve process resources such as energy or material. In this thesis, the term **heat integration** will be used throughout the report, as only thermal energy is conserved in the system [47].

There are typically several hot streams that need to be cooled, and cold streams that need to be heated in a process or power plant. Without heat integration, each stream needs a cold or hot utility to reach its target temperature. This leads to large utility consumption and superfluous emissions. If the different processes are heat integrated, meaning that hot energy is transferred from a hot stream to a cold stream, less external utilities are required. This results in considerable energy savings. Accordingly, the main idea of heat integration is to utilize the available process heat before using external utilities [48].

The first key concept in heat integration is to identify available process streams and set an energy target. Based on collected stream data, an enthalpy-temperature diagram can be drawn for each stream. For a multi stream system all the hot curves can be plotted in an accumulated manner, forming a hot composite curve, while the same can be done for the cold streams forming a cold composite curve. The resulting diagram is called the Composite Curves (CC) and visualizes the available heat recovery in the system. An example of a CC is given in Figure 16.

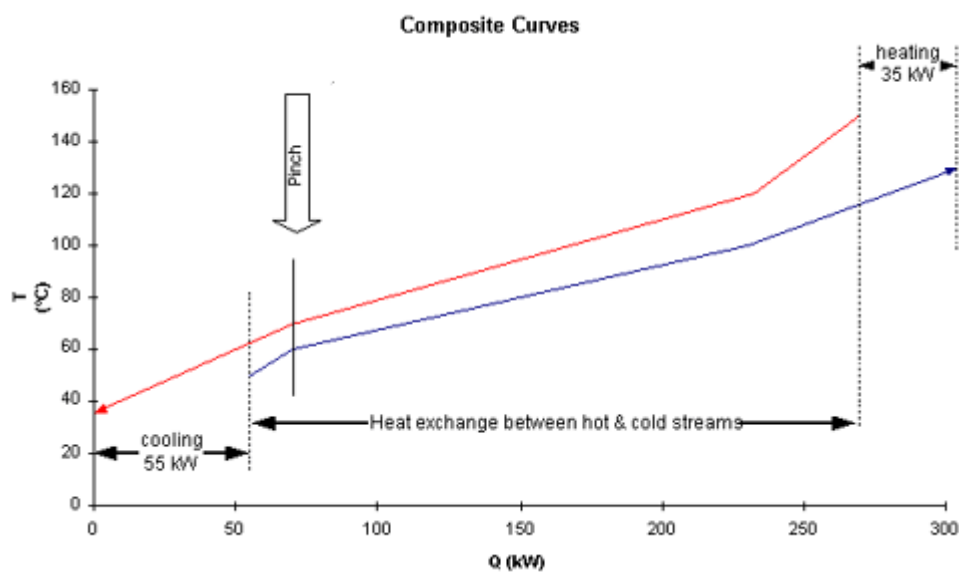


Figure 16 Typical composite curve [49]

The overlap of the composite curves represents the possible energy recovery in the system, i.e. the energy saved with heat integration. The point marked **pinch** denotes the pinch point in the system. This point indicates the closest temperature approach in the system, ΔT_{\min} , which is important as the external utilities requirements are dependent on ΔT_{\min} . A high value of ΔT_{\min} results in increased utility consumption. However, this is only true for a system with both hot and cold utility requirements. If the system has only one utility requirement, reducing the ΔT_{\min} would not lead to lower utility consumption. These types of systems are called threshold systems.

Assuming that the system operates at steady-state and no external work is done by the system, the energy balance for a stream undergoing a change from state 1 to state 2, can be expressed as in Eq. **Feil! Fant ikke referansekilden.** If we further neglect changes in potential and kinetic energy, assume constant C_p and assume the enthalpy to be only a function of temperature, neglecting the pressure dependence, the expression can be simplified to Eq.(7.2).

$$\frac{\dot{Q}}{\dot{m}} = (h_2 - h_1) + \left(\frac{V_2^2 - V_1^2}{2} \right) + (gz_2 - gz_1) \quad (7.1)$$

$$Q = mC_p (T_2 - T_1) = mC_p (T_t - T_s) \quad (7.2)$$

To visualize the required utility levels in a system, the Grand Composite Curve (GCC) is an important tool. The GCC plots shifted temperatures against net heat flow (Figure 17). The shifted temperatures represent common temperatures for hot and cold streams, and are found by reducing all hot stream temperatures by $\Delta T_{\min}/2$, and increasing all cold temperature with the same value. We can then plot a curve that gives us the net heat flow at various temperatures in the process, relative to the pinch point [50].

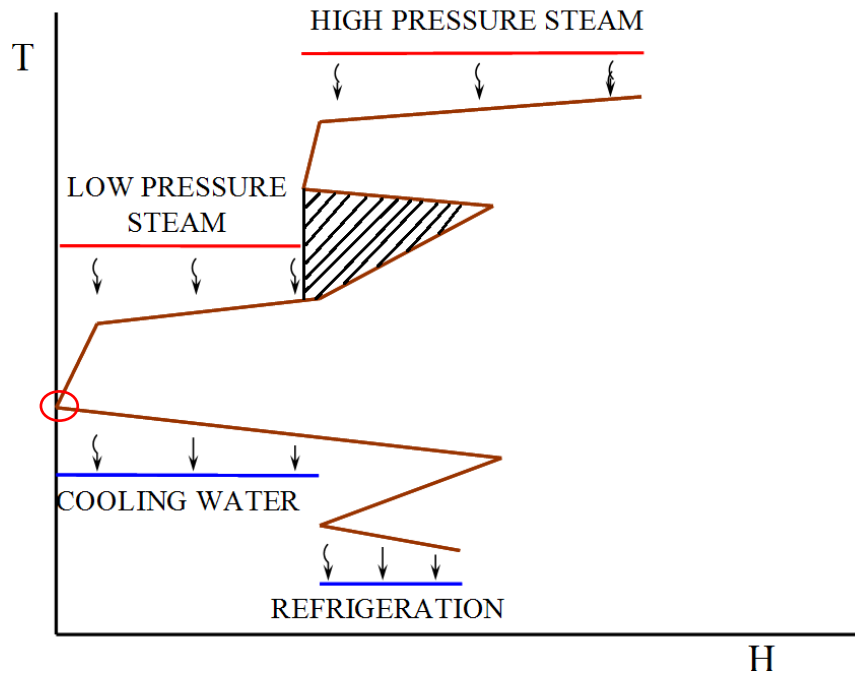


Figure 17 Typical grand composite curve

The red circle points out the pinch point. The shaded area of the curve denotes the area where heat can be exchanged between different temperature intervals. One of the “golden rules” in pinch analysis is that one should never use external heating below pinch, or use external cooling above pinch. Violating this rule will result in increased requirements of external utilities. However an external heat source should not only be placed above pinch, but also above the GCC. The curve is also used as a tool for selecting utilities, as it gives the required temperature level for the external utility [48].

7.2 Steam generation

The steam generation in AKSO’s system is an important unit in the facility. The excess energy in the flue gas is utilized to generate steam. In steam generation there exist three different heat transfer zones. If starting from the lowest temperature, the water is preheater in the economizer. The second zone is called the evaporator, where boiling at constant temperature occurs. The last zone is the superheater, where steam is superheated to a specified temperature [10]. A typical T-Q diagram for a HRSG is given in Figure 18.

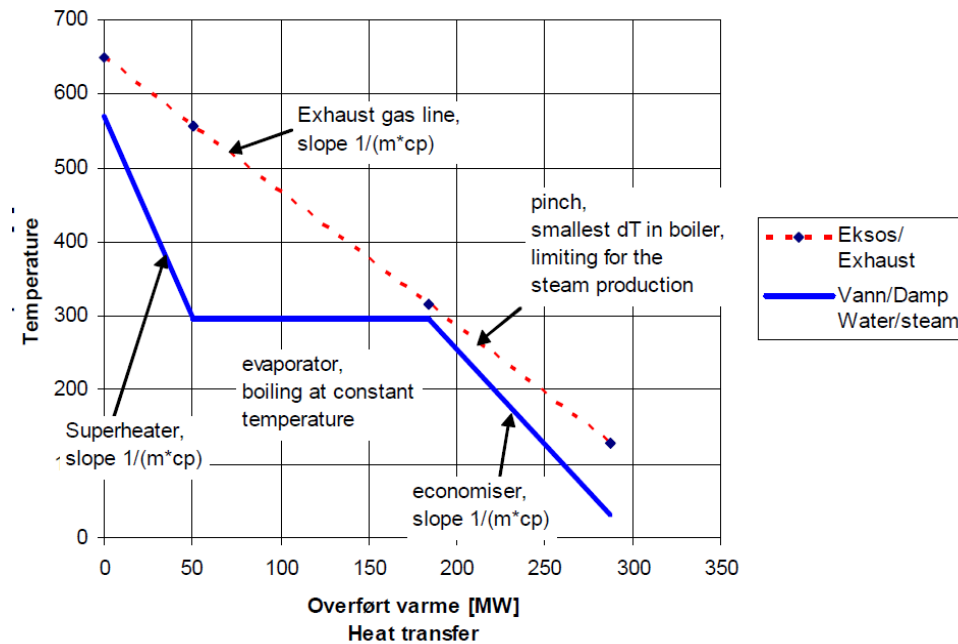


Figure 18 T-Q diagram, for heat transfer in steam generation[10]

In a typical HRSG, the pinch point is located at the end point of the economizer, as can be seen from Figure 18. However, for systems with a fired boiler, the pinch point might be located at the cold end of the economizer. This is due to the large temperature difference between the flue gas and the water. If this is the case, implementation of a BFW preheater is common, as this will enable a greater steam generation.

If performing a heat balance over the evaporator and superheater, the steam production can be expressed as:

$$\dot{m} = \frac{\dot{m}_{flue} c_{p,flue} (T_{1,flue} - T_{3,flue})}{(h_1 - h_3)} \quad (7.3)$$

T_1 is the temperature of the flue gas, at the inlet of the superheater. T_3 is the temperature of the flue gas at the outlet of the evaporator. h_1 and h_3 are the enthalpy of water at the outlet of the superheater and the economizer, respectively.

7.3 Intermediate Heat Carriers

Heat transfer between hot and cold streams can be done either directly or indirectly. If transferred directly, one stream needs to be piped over to the other unit. Depending on the fluid, the piping could be expensive or the pressure drop significant and. In addition direct heat transfer might violate the safety regulations if the fluid is explosive, or if there is risk of freeze-out. If this is the case indirect heating can be done by employing an intermediate Heat Transfer Fluid (HTF). This matter is broadly applied to power plants but there exists only limited research on the accurate use of intermediate heat carriers according to Smith [51].

For cryogenic plants, the use of an intermediate heat carrier reduces the risk of freeze out in the system. The HTFs used in AKSO's system are either MEG/water or Methanol. The properties these HTFs are listed in Table 5.

Table 5 Properties of Methanol and WEG/water[8, 52]

Properties of Methanol	
Freezing point	-97.7 °C
Density, 20°C	791 kg/m ³
Specific heat, 25°C	2.529 kJ/kgK
Properties of MEG/Water	
Freezing point	-56 °C
Density, 25°C	1074 kg/m ³
Specific heat, 25 °C	3.211 kJ/kg

In the preparatory study of the oxy-fuel plant, several other HTFs were evaluated; Tri Ethylene Glycol (TEG), Di Ethylene Glycol (DEG) and Propylene Glycol. Though some of these HTFs are safer than those applied in the system, none of them has lower freezing point than MEG/Water, and are therefore considered inapplicable.

7.4 Heat transfer coefficient

An important parameter in pinch analysis and HX design is the overall heat transfer coefficient, U . For a clean unfinned surface the overall heat transfer coefficient can be expressed as in Eq.(7.4); the overall heat transfer coefficient is defined as the total thermal resistance over an area. Thermal resistance defines the ability for a material or a fluid to resist heat transfer, i.e. a low resistance results in a high U value.

$$U = \frac{1}{R_{tot} \cdot A} \quad (7.4)$$

Heat transfer in heat exchangers is due to both convection and conduction, where the first is heat transfer through a matter while the latter is heat transfer in fluids. When estimating the overall heat transfer coefficient both thermal resistance due to convection and conduction needs to be accounted for. In addition deviation due to fouling, fluid impurities and rust formation is included by adding another thermal resistance; the fouling factor, R_f . This parameter is among other factors, dependent on the operating temperature and the fluid

velocity. If wall resistance is ignored the overall heat transfer coefficient may be expressed as [53]:

$$\frac{1}{U} = \frac{1}{h_c} + \frac{1}{h_h} + R_f \cdot A \quad (7.5)$$

Where $1/h_h$ is the thermal heat resistance for the hot side of the HX and $1/h_c$ is the thermal heat resistances for the cold side of the HX. The heat transfer coefficient, h [$\text{W}/\text{m}^2\text{K}$] depends on conditions in the boundary layer, which again depend on the surface geometry, transport properties and the fluid motion, i.e. laminar or turbulent flow. In addition the h -values will change dynamically through a HX; the change is dependent on pressure, velocity and temperature changes as well as possible phase transitions. Owing to the dependence on numerous factors, the heat transfer coefficient is difficult to determine accurately [53, 54]. For the purpose of this thesis the heat transfer coefficients used are extracted from literature, giving only proposed values for shell and tube HXs. It is important to notice that using tabulated values increase the error of estimation. All values used in this thesis, are extracted from Table 2 “*Typical film heat transfer coefficients for shell-and-tube heat exchangers*” in [55]. These values show that liquids tend to have a significantly higher h value than gases. For the substances in this thesis (NG, water, CO_2 and nitrogen) water has a considerable higher h -value in liquid phase than both LNG and liquid CO_2/N_2 . If LNG is assumed to only contain light hydrocarbons, the proposed h -value lies between $1500\text{-}2000\text{W}/\text{m}^2\text{K}$. The tabulated h -value for a CO_2/N_2 mixture in a gas phase is dependent on the pressure. Table 6 shows typical values for gas² at different pressures.

Table 6 Typical h -values for gas at different pressure [55]

Pressure [kPa]	h [$\text{W}/\text{m}^2\text{K}$]
100-200	80-125
1000	250-400
10 000	500-800

For the use of intermediate heat carrier, the relationship between the film heat transfer coefficient and the contribution of ΔT_i for stream i can be related through Eq.(7.6). Where ΔT_i is the individual temperature contribution for stream i , and C is a constant [56].

$$\Delta T_i = \frac{C}{\sqrt{h_i}} \quad (7.6)$$

² The values given apply to gases like: CO_2 , N_2 , air and light hydrocarbons mixtures.

As can be seen from Eq.(7.6), the temperature difference for stream i , is inversely proportional to the square root of the heat transfer coefficient.

7.5 Area targeting

To optimize the heat integration done in a power plant, the total HX area should be examined, as the cost of a HX increases with increasing area. For a single countercurrent heat exchanger, the area is given by Eq.(7.7).

$$A = \frac{Q}{U \Delta T_{LM}} \quad (7.7)$$

Where Q [kW] is the duty of the heat exchanger U [kW/m²K] is the overall heat transfer coefficient and ΔT_{LM} [K] is the logarithmic mean temperature difference expressed as:

$$\Delta T_{LM} = \frac{\Delta T_H - \Delta T_C}{\ln \frac{\Delta T_H}{\Delta T_C}} \quad (7.8)$$

ΔT_H and ΔT_C are the temperature differences at the hot and cold end of the HX, respectively. In essence the surface area is approximately inversely proportional to the temperature difference. In addition, the capital cost of a system is approximately proportional to surface area, thus there exists a trade-off between CAPEX and energy costs when choosing ΔT_{min} . This is owing to the fact that the utility requirements increase with decreasing ΔT_{min} , while the opposite is true for the relationship between area of a HX and the value of ΔT_{min} [48].

8 Simulation model and methodology

AKSO's concept has been simulated to find possibilities of reducing the power consumption in the system. In this chapter a description of the simulation model is given. The software used for designing the model is presented, and the main specifications for the model are given.

8.1 Simulation software

In this thesis Aspen Hysys Version 7.2, is used as the simulation software. Aspen Hysys is a process design environment, broadly used in the oil and gas industry. In Hysys, rigorous steady-state and dynamic simulation models can be created. For the purpose of this thesis, only steady-state simulation models have been employed. The simulation models are based on flow diagrams provided by AKSO. In addition, an early stage simulation model created by AKSO is used to extract data regarding the distillation column and the accurate fluid package.

8.2 Fluid packages

When predicting the state of gases and liquids at high pressure and low temperature, the ideal gas law is not valid. In Hysys there exists different fluid packages, and choosing the right one is critical to get accurate results. For the NG and the flue gas streams the Soave-Redlich-Kwong (SRK) package is used. The SRK package contains binary interaction parameters for all hydrocarbon-hydrocarbon pairs and is based on Van der Waals' equation of state, Eq.(8.1) This is a generalization of the ideal gas equation. The SRK equation of state is given by Eq.(8.2) [57].

$$p = \frac{\bar{R}T}{\bar{v} - b} - \frac{a}{\bar{v}^2} \quad (8.1)$$

$$p = \frac{RT}{\bar{v} - b} - \frac{a}{\bar{v}(\bar{v} + b)} \quad (8.2)$$

The SRK package would not give accurate results for the water/steam system. For this purpose American Society of Mechanical Engineering (ASME) steam package is employed. This package extracts data from the ASME 1967 steam tables. The limitations of ASME steam are that a pressure below 1035 bar is required, and the temperature is limited to lie between 0 and 816°C [58]. These limitations are acceptable for the purpose of this thesis.

8.2.1 Distillation column in Hysys

The distillation column in Hysys is the most complex unit operation, thus it needs to be specially design to get accurate results. Among others the amount of stages, duty of the reboiler/condenser and pressure drop specifications needs to be set. In addition initial estimates need to be set for the column to converge to solution. This can, among others, be the reflux ratio, the distillate flow or the bottom flow.

In Hysys the Francis Weir equation is used to calculate the liquid fraction leaving a stage[58].

$$L_N = C\rho l_w h^{1.5} \quad (8.3)$$

Where L_N is the liquid flowrate leaving tray N, ρ [kg/m^3] is the density of liquid, l_w is the weir length and h is the height of liquid above weir. As calculation of a distillation column is complex, the formulas used are of great importance. The vapor fraction leaving the tray is calculated by:

$$F_{\text{vap}} = k\sqrt{\Delta P_{\text{friction}}} \quad (8.4)$$

Where F is the flowrate of vapor leaving tray N, k is the conductance and $\Delta P_{\text{friction}}$ is the dry hole pressure drop.

8.3 Process design and methodology

The simulation models are designed as stationary simulations files. The object of the simulations is firstly to evaluate the heat integration in the original system. For this purpose, a model using an oxygen stream with 0.95 mol% oxygen purity (case 1) is used. Thereby the parameters upstream the oxy-burner is changed, and two new simulation models are created; one with 0.90mol% oxygen purity (case 2) and one with 0.97mol% oxygen purity (case 3). These models are used to find the impact on the CO_2 CPU, by changing the oxygen purity. The last simulation model is upgraded; the ASU is integrated and the selected oxygen purity, and heat integration is employed. The process parameters used are based on the plant specification for the proposed regasification plant from AKSO, which will be referred to as the base case in the following. Some specifications were adjusted when needed. The main simulation model is given in Appendix A. The overall assumptions for the simulation models are listed below:

- No heat loss in any components (HXs, distillation column etc.)
- No heat loss in pipelines
- No pressure loss in pipelines
- Polytrophic efficiency of turbines is set to 80 %
- Adiabatic efficiency of compressors is set to 80%
- Polytrophic efficiency of pumps is set to 75%
- Pressure drop in cooler/heater is set to 30 kPa
- Intermediate heat carries are not included in the model
- Complete combustion is assumed in the burner
- All shell and tube heat exchangers works in a counter-current manner

- The duty of the distillation column is expected to be low compared to the other units in the system, and are therefore neglected in the heat balance

8.3.1 Specifications of the LNG stream

The composition of the LNG feed is given in Table 7. The mass flow of LNG in the simulation model, is specified to 44 790 kmol/h in accordance with AKSO's utility flow diagrams.

Table 7 Fuel composition

Component	Chemical symbol	Mole fraction
Methane	CH ₄	0.925
Ethan	C ₂ H ₆	0.055
Propane	C ₃ H ₈	0.010
Nitrogen	N ₂	0.010

The LNG is pumped to 80 bar by two centrifugal pumps, before heated by five heat exchangers, named LNG HX 1 – HX 5. The duties and pressure drop of all HXs are specified. The pressure drop is set to 30 kPa. The duty for each HX is given in the Table 8, including the fuel gas preheater, which preheats the NG routed to the oxy-burner.

Table 8 Duties of LNG heat exchangers

Unit	Duty[MW]
LNG HX 1	4.1
LNG HX 2	2.3
LNG HX 3	28.2
LNG HX 4	63.3
LNG HX 5	59.7
Fuel gas preheater	0.5

After the last LNG HX, a tee is used to split the stream. 1.5 % of the NG is throttled to 250 kPa and heated, before routed to the oxy-fuel burner. The rest of the send-out gas is transported to distributors. To identify which streams should be heat integrated, the heat exchangers are not connected by energy streams in the models. This is done to give a higher degree of freedom.

8.3.2 Specifications of the steam cycle

The steam cycle in the process has two purposes; generate power and produce steam. The water goes in a cycle; after exiting the steam generation and power cycle, it is collected in a drum and sent to condensate treatment. In the simulation model the dehydration is not included, thus the water cycle is simulated as a single train. The mass flow of water in the system is specified to 10 158 kmole/h, and the temperature and pressure prior the BFW pump is specified to 25°C and 150 kPa.

The BFW is pumped to 5470 kPa, to give the accurate pressure upstream the steam boiler (5450 kPa). The water is then preheated against flue gas in a shell and tube HX, where the pressure drop is specified to 20 kPa and the outlet temperature is specified to 155°C. The steam boiler is simulated as a separator and a HX, as there is no accurate unit operator available in Hysys. Steamboiler_1 and steam_boiler_2 are connected by an energy stream, as can be seen in Figure 19. The duty of the steam boiler is specified to 107.2 MW. The shell and tube HX is simulated with weighted HX design to get the accurate T-H profile. In weighted design, the heating curve is broken into intervals. This is applied to all shell and tube heat exchangers in the simulation models.

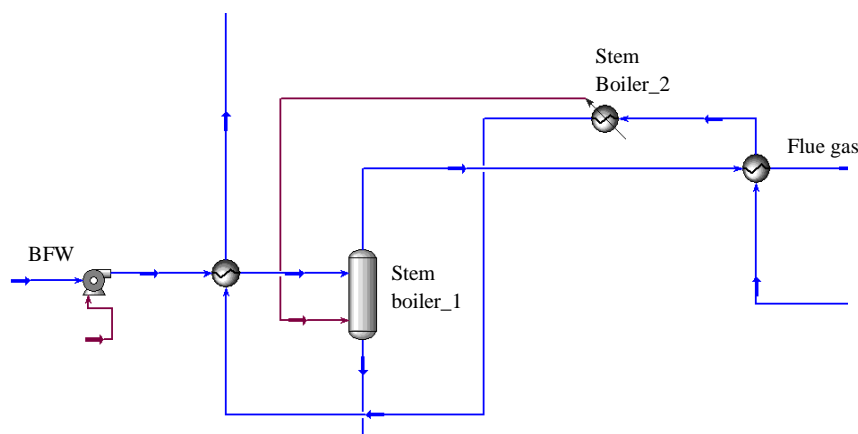


Figure 19 Simulation model of steam boiler

Liquid water exits the bottom of the steam boiler, while steam is drawn-off at the top of the column, where the temperature is specified to 251.9°C. Steam is then superheated against flue gas, where the outlet pressure from the MP superheater is set to 4091 kPa. The liquid water is routed to the collection drum, while the superheated steam is sent to the MP turbine, where the outlet pressure is specified to 500 kPa. LP steam is drawn-off to vaporize LNG (LNG heater 5), and preheat oxygen and fuel prior to the combustion. Approximately 55 % of the steam from the MP turbine is routed to the LP turbine where the outlet pressure is specified to 14 kPa. The steam condensate from the LP turbine is cooled by vaporizing LNG (LNG heater 4) before routed to the collection drum. The oxygen and fuel gas preheater is simulated as one HX, owing to lack of specifications in the flow sheets. In addition the duties

of these heat exchangers are significantly small compared to the other units in the system, hence the simplification is assumed to be applicable.

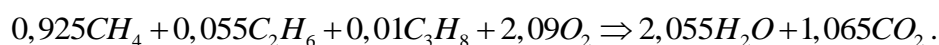
All specified duties and flow rates of the steam cycle are given in Table 9. Only streams of importance are added in the table, for more information see Appendix A.

Table 9 Specifications of steam cycle

Unit	Duty [MW]	Flowrate [kg/s]
BFW pump	361.7	50.80
Steam boiler	107.2	50.80
LNG heater 4	63.3	27.30
LNG heater 5	59.7	21.80
Oxygen/fuel gas preheater	2.0	0.73

8.3.3 Specifications of the reactor

A conversion reactor is used to simulate the oxy-fuel burner. In this type of reactor the reaction-set is specified manually, which limits calculation errors. If neglecting the presence of nitrogen the chemical reaction in the burner can be expressed as;



From the chemical reaction it can be seen that 2.09 kmol/h of oxygen is required to completely combust 1 mole of fuel. To insure complete combustion in the reactor 1mol% excess oxygen is used in the simulation. For a fuel flow rate of 693kmol/h, and an oxygen purity of 95mol% the resulting flow rate of O₂/N₂ is 1450kmol/h. The pressure drop in the reactor is specified to 34 kPa. The O₂/N₂ stream is preheated by steam prior to the combustion; the duty of the heat exchanger is specified to 1.5 MW.

8.3.4 Specifications of the CO₂ recovery process

The aim of the oxy-fuel combustion is to concentrate CO₂ in the flue gas, and thereby capture the CO₂ by cryogenic distillation. The flue gas downstream the burner is compressed by a flue gas fan simulated as a compressor with an after cooler. These unit operators are employed because flue gas fans are not included in Aspen Hysys. The flue gas is then cooled by LNG in the flue gas condenser, before the bulk of water is removed. The flue gas scrubber is simulated as a component splitter, draining out 0.91% of the water amount in the gas. In a stream splitter the split ratio is specified, as well as the overhead pressure. A *set function* is used to set the overhead temperature to resemble the inlet temperature. To control the flame temperature, 73 % of the flue gas is compressed before recycled to the oxy-fuel burner. A *recycle operation* is used downstream the burner, to make Hysys able to calculate the recycle loop explicit. The stream conditions are calculated forward, i.e. the properties of the stream

entering the burner is calculated from the recycle stream exiting the scrubber. The tolerance factor is specified to 0.001. The specifications for units prior to the CO₂ CPU are given in Table 10.

Table 10 Specifications of flue gas stream

Parameter	Unit	Value
Duty of HX steam boiler	[MW]	107.2
Duty of flue gas condenser	[MW]	28.2
Pressure drops MP superheater and BFW heater	[kPa]	10.0
Outlet temperature BFW heater	[°C]	113.0
Flue gas fan – compressor duty	[kW]	6952.0
Flue gas fan – HX exit temperature	[°C]	140.0
Split rate in stream splitter 1, overhead	Mole%	0.0868
Recycle rate	[Kmol/h]	6250.0

The remaining flue gas is then sent to the CO₂ CPU. The flue gas is compressed to 2500 kPa in three stages, with intermediate cooling and water removal. The water is removed in two stream splitters where the pressure drop is specified to 20 kPa. The efficiency and outlet pressure is specified for each compressor stage. To avoid ice formation in the process, the remaining amount of water is removed in the last stream splitter before the gas is cooled to -43°C. The distillation column is simulated with 12 trays, and a partly condenser. The condenser pressure is set to 2450 kPa, while the distillation pressure is specified to 2470 kPa. The specification used to convert the column calculations, is the CO₂ recovery rate, which is specified to 99 %. Table 11 gives the specifications of the CO₂ CPU.

Table 11 Specification of CO₂ CPU

Parameter	Unit	Value
Outlet pressure Compressor 1 (C1)	[kPa]	360
Outlet pressure Compressor 2 (C2)	[kPa]	840
Outlet pressure Compressor 3 (C3)	[kPa]	2500
Duty of LNG heater 1	[kW]	1400
Duty of LNG heater 2	[kW]	900
Duty of LNG heater 3	[kW]	4100

8.4 Results and discussion

In this section the resulting temperatures and duties from the main simulation model (Case 1) are presented and discussed. For further details see Appendix A.

8.4.1 LNG stream

For the base case the inlet temperature of LNG HX 1 was calculated to -160.3°C . This is equivalent with the result from the simulations. The last heat exchanger (LNG HX 5) heats the gas to 3.9°C , which is lower than expected. In AKSO's flow sheets the temperature is calculated to 8.7°C . Getting the accurate outlet temperature would require increasing the duty of LNG HX 5 to 63 MW. However, the low temperature could be caused by the selected fluid package, other program specifications or due to the design of the HX in the base case: The system used a special water bath technology for LNG HXs 4-5. There were not done any changes to gain a higher temperature. In accordance with Hans Kristian Rusten from AKSO, the temperature was decided to be acceptable for the purpose of this thesis. The exit temperatures of the LNG HXs, LNG pumps and the fuel gas preheater are given in Table 12.

Table 12 Exit temperatures of LNG HXs

Unit	$T_{\text{exit}} [^{\circ}\text{C}]$
LNG pump 1	-162.30
LNG pump 2	-160.30
LNG HX 1	-154.60
LNG HX 2	-151.40
LNG HX 3	-114.10
LNG HX 4	-56.80
LNG HX 5	3.92
Fuel gas preheater	26.96

The simulation model shows that the LNG is vaporized and heated transcritical, i.e. above the phase envelope. In subcritical vaporization the fluid evaporates at nearly constant temperature, resulting in a flat T-H profile. In transcritical vaporization a steeper gradient is experienced, as can be seen from Figure 20, which shows the T-H profile of LNG HX 4.

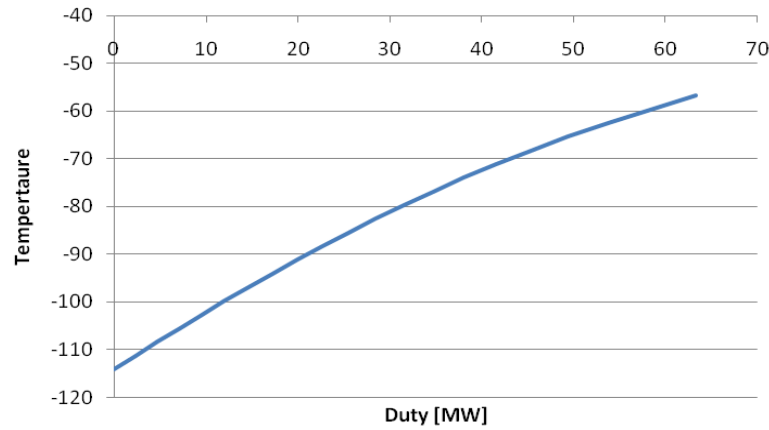


Figure 20 T-H profile of LNG HX 4

8.4.2 Steam cycle

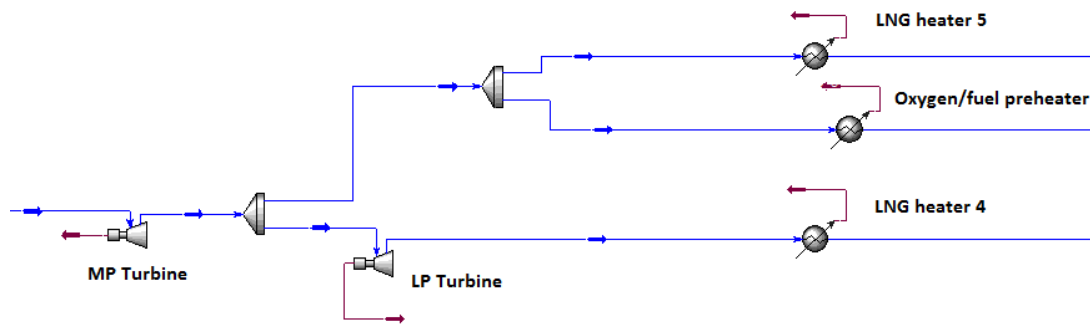
The simulation model shows that water exits the BFW heater as compressed liquid water at 5450 kPa. The steam boiler overhead pressure was calculated to 4107 kPa, giving a vapor molar flow of 9955 kmol/h. This resembles the molar flow calculation in the base case, which is important as the correct amount of steam is required to get the accurate turbine yield. MP steam is then superheated to 398.1°C, against flue gas from the oxy-fuel boiler. The temperature is 2°C lower than expected, which is acceptable. The LP steam used to heat LNG (LNG heater 5) oxygen and fuel gas, is split into two streams; one going to the LNG heater, while the rest is routed to the oxygen/fuel gas preheater. The split rate was adjusted from 98.6 % going to the LNG heater to 97 %, due to freeze out in the oxygen/fuel preheater. With these flow rates the LP steam is condensed and super cooled in both HXs. The vapor fraction of the steam condensate leaving the LP turbine was calculated to 0.8938 and the steam condensate is liquefied and supercooled in LNG heater 4. The exit temperatures of LNG heater 4 and LNG heater 5 are lower than expected. As already mentioned these HXs use a water bath technology. As these HXs are simulated as ordinary heaters this could be the reason for the low temperatures. If the results from the simulation model are correct, the water flow should be increased to gain a higher outlet temperature.

Duties, start temperatures (T_s), target temperatures (T_t), inlet and outlet pressure for each unit is given in Table 13.

Table 13 Output parameters for steam cycle

Unit	T _s [°C]	T _t [°C]	Inlet pressure [kPa]	Outlet pressure [kPa]	Duty [MW]
BFW pump	25.0	25.5	150	5470	361.7
BFW heater	25.5	155.0	5470	5450	27.7
Steam boiler	155.0	251.9	5450	4107	107.2
MP superheater	251.9	396.6	4107	4091	20.3
MP turbine	396.6	174.6	4091	500	20.3
LP Turbine	174.6	52.7	500	14	12.5
LNG heater 4	52.7	5.3	14	13	63.3
LNG heater 5	52.7	15.4	500	470	59.7
O₂/fuel gas	52.7	10.5	500	470	2.0

The pressure drop in the steam boiler is significantly high. However, it matches the pressure drop in the base case, and is therefore considered applicable. The pressure drop in LNG heater 4 was set to 1 kPa. This HX operates under vacuum conditions, and the accurate pressure drop is not given in AKSO's flow sheets. As the selected pressure drop has no impact on the evaluation of the heat integration in the system, it is assumed to be acceptable. A schematic of the power generation and the LP steam consumption is given in Figure 21.

**Figure 21** Power and steam cycle

8.4.3 CO₂ CPU

The reaction balance of the oxy- burner is given in the Table 14. As can be seen from the table the carbon and hydrogen in the fuel is completely converted to CO₂ and water. However,

it is important to notice that this would not be the case in a real combustion, as the flue gas would contain impurities like NO_x and CO as discussed in Chapter 3.

Table 14 Reaction balance for the oxy-burner

Component	Total inflow	Total reaction	Total outflow
Methane	641	641	0
Ethane	38	38	0
Propane	6.9	6.9	0
H ₂ O	118	1424	1542
Oxygen	1557	1450	106.9
Nitrogen	700	0	700
CO ₂	5422	738.1	6160

The composition of the oxygen stream is adjusted from that given in the flowsheets from AKSO. The oxygen stream contained 95mol%, 4mol% N₂ and 1mol% CO₂, originally. In the simulation model the CO₂ content is neglected in accordance with PhD student Fu Chao. For a real process, argon would probably be present in the oxygen stream. In this simulation model however, argon is not included owing to the specifications given in AKSO's flow sheets. The oxygen stream used in this model contains 95mol% oxygen and 5mol% nitrogen.

With the specified recycle rate, O₂/N₂ flow and fuel composition, the composition of the flue gas is as given in Table 15. The flue gas composition obtained in Hysys resembles that of AKSO. The flue gas flow was calculated to 8509 kmol/h.

Table 15 Flue gas composition

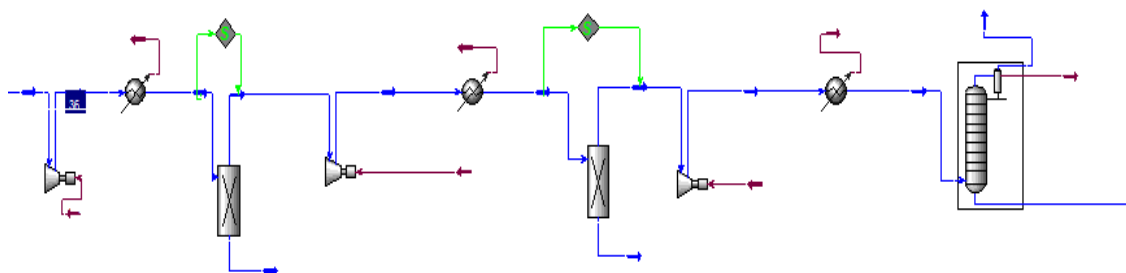
Component	Mole fraction in flue gas	Mole fraction after recycling
H ₂ O	0.180	0.019
Oxygen	0.013	0.015
Nitrogen	0.082	0.099
CO ₂	0.724	0.880

The specified recycle rate of 6250 kmol/h, results in a flame temperature of 1448°C. This result is satisfactory, as the temperature should be below 1450 °C according to AKSO. The duty of the flue gas fan was calculated to 11.5 MW. This result differs from the base case mainly because of the selected unit operators employed. All resulting duties, temperatures and pressures for the CO₂ CPU are given in Table 16.

Table 16 Output parameters for the CO₂ CPU

Unit	T _s [°C]	T _t [°C]	Inlet pressure [kPa]	Outlet pressure [kPa]	Duty [MW]
MP superheater	1448.0	1292.0	101.0	91.0	20.4
Steam Boiler	1292.0	393.8	91.0	81.0	107.2
BFW heater	393.8	113.0	81.0	71.0	27.7
Flue gas fan	113.0	140.0	71.0	130.4	11.5
Flue gas cond.	140.0	18.6	130.4	100.4	28.2
Recycle Comp.	18.6	44.6	100.4	135.0	1.7
Compressor 1	18.6	142.2	100.4	360.0	1.1
HX1	142.2	8.2	360.0	330.0	1.4
Compressor 2	8.2	100.3	310.0	840.0	0.8
HX2	100.3	2.9	840.0	810.0	0.9
Compressor 3	2.9	110.2	790.0	2500.0	0.9
HX3	110.2	-42.0	2500.0	2470.0	4.1

The distillation column was converged with a CO₂ capture rate at 99 %, the weighted error was calculated to 0,000. The duty of the condenser was calculated to 230 kW. The molar flow going to CO₂ storage was calculated to 751.5kmol/h with a CO₂ concentration of 0,972 mol%. A schematic of the CO₂ CPU in Hysys is given in Figure 22.

**Figure 22** CO₂ separation and compression

8.4.4 Power and heat balance

The total heat required in the system is calculated to 315 MW. If neglecting the flue gas fan and the CO₂ heater after the distillation column (as this is an air fan) the cold energy required in the simulation model is calculated to 315.2 MW. The difference is due to the condenser in the distillation column, which is neglected in the heat balance. For more details see Appendix A.

The total power production was calculated to 33 MW. This is 1 MW less than for the base case. The difference may be caused by the selected fluid package, minor temperature or pressure difference or the simulation software used. The power requirements of the different process systems are given in Table 17.

Table 17 Power requirements for different process systems

Process system	Duty[MW]
ASU³	11.30
LNG pumps	5.00
Flue gas recycle fan (simulated as a compressor)	1.67
CO₂ comp. + pumps	3.00
BFW pump	0.40
Flue gas fan	11.45
SUM	32.82

³ The power requirement of the ASU is not simulated; hence the value is extracted from AKSO's base case report.

9 Evaluation of existing heat integration in the system

The evaluation of the existing heat integration in the system is based on the simulation results from Chapter 8. The objective of this chapter is to evaluate the proposed heat integration in the base case and identify possibilities of power reduction in the plant.

9.1 Methodology

A simplified schematic of the heat integration in the base case can be seen in Figure 1. A procedure is established to identify the heat integration in the systems, and thereby evaluate it. Firstly the hot and cold streams are extracted from the simulation model. Only streams of interest to the heat integration are accounted for. The hot and cold streams are drawn separately in a T-Q diagram to evaluate the sequence of the pair matching in the system. For heat exchangers using intermediate heat carriers, the placement of the intermediate HTFs are evaluated, based on individual heat transfer coefficients. The utility consumption is evaluated by using the CC and GCC for the system. The assumptions made in Chapter 8 still apply, in addition the following is assumed:

- Heat losses are not taken into account
- The condenser in the distillation column is not taken into account in the heat balance as the duty is lower than 1MW.
- The flue gas fan HX is not taken into account in the heat integration.

The CC and the GCC are drawn using PRO_PI, which is an add-in to Microsoft Excel, developed by *Industriell Energianalys AB* at *Chalmers Industriteknik* in Sweden. The program draw the curves based on start/target temperatures and duties.

9.2 Data extraction

To be able to evaluate the heat integration in the process, hot and cold streams needs to be identified. The system is divided into three main units; the regasification unit, the steam cycle and the CO₂ CPU. The different stream data are extracted from the main simulation file. A stream is identified as a mass flow with a given pressure, i.e. a new stream is defined whenever the pressure or the flow rate of the stream changes. Exception is made for the steam boiler, see Section 9.2.1.

9.2.1 Steam cycle

The steam cycle are divided into one cold stream and three hot streams. The cold stream is the preheating of BFW and the steam generation. The hot streams are defined as the streams going through LNG heater 5, LNG heater 4 and the oxygen/fuel preheater. In the following the cold stream is named C2 while the hot streams are named H1-H3 as can be seen from Figure 23.

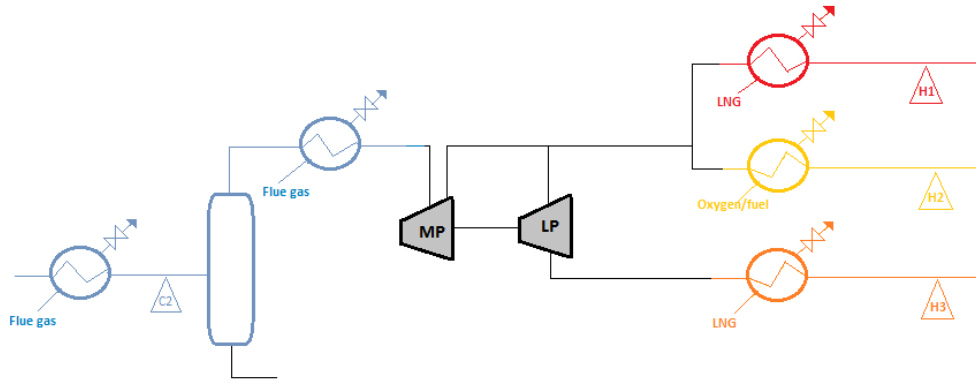


Figure 23 Stream extraction of water cycle

The steam generation and superheating, is separated into three different segments:

1. Preheating in the economizer
2. Boiling of water at constant temperature in the evaporator
3. Superheating of steam, exiting the boiler

As Hysys only provide the overall duty of the steam boiler, the different segments are calculated manually. The total amount of water entering the steam boiler is preheated in the economizer. The duty is calculated by Eq.(9.1).

$$\dot{Q}_{preheat} = \dot{m}_{tot} \cdot (h_{f,T_{sat}} - h_{f,T_{in}}) \quad (9.1)$$

Where \dot{m} is the mass flow in kg/s and h_f is the specific enthalpy of saturated liquid water, and T_{sat} is the saturation temperature. The amount of vapor m_v , is extracted from Hysys. The total duty of the vaporizer is calculated from Eq.(9.2), where h_{fg} is the enthalpy increase during vaporization.

$$\dot{Q}_{Vaporize} = \dot{m}_v \cdot (h_{g,T_{sat}} - h_{f,T_{sat}}) = \dot{m}_v h_{fg,T_{sat}} \quad (9.2)$$

The duty of the superheater is extracted from Hysys. The enthalpy values used to calculate the preheating and vaporization are from steam tables in [15]. A graph showing the temperature as a function of duty is given in Figure 24. The numbers used in the calculation can be found in appendix B.

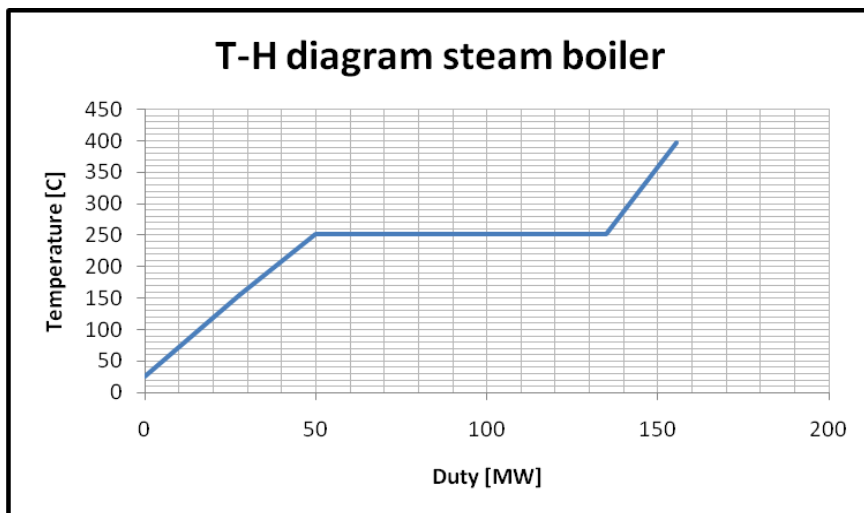


Figure 24 T-H diagram steam boiler

The stream data are given in Table 18. The flow rate of C2 change in the boiler as liquid is drawn-off at the bottom of the vessel. All data is extracted from the simulation model in Hysys, which is equivalent to the information given in Chapter 8.

Table 18 Stream data for water cycle

Stream	Flowrate [kmol/h]	T _{start} [°C]	T _{target} [°C]	Duty [MW]
C2	10160	25.53	398.3	155.4
H1	4361	174.60	16.4	59.7
H2	145	174.60	11.4	2.0
H3	5450	52.58	5.7	63.3

9.2.2 LNG and flue gas streams

The LNG train is identified as one cold stream. The total duty calculated to 157.7 MW. The stream will be referred to as C1 in the following chapters. The flue gas is divided into four different hot streams, where change in mass flow or pressure defines a new stream. The streams are named H₄ – H₈. The stream data for the hot streams is given in Table 19.

Table 19 Stream data of flue gas streams

Stream	T_S [°C]	T_T [°C]	Duty [MW]
H₄	1448.00	113.00	47.9
H₅	135.00	18.61	28.2
H₆	142.20	8.20	1.4
H₇	100.30	2.90	0.9
H₈	110.20	-42.00	4.1
C3	-96.97	25.00	1.5
C4	-44.37	26.96	0.5

Figure 25 shows a simplified schematic of the system, the different colors define the different streams in the system. Cold streams C3-C4 are not given in the figure. These streams include the oxygen and NG streams upstream the burner.

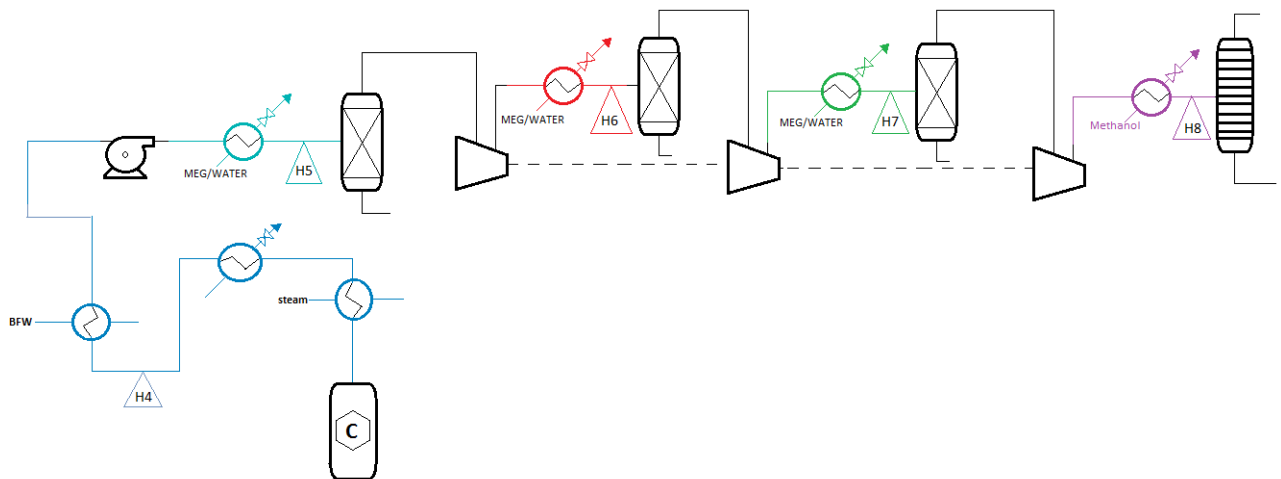


Figure 25 Steam data of the flue gas

9.3 Results and discussion

The objective of the evaluation is to investigate if the heat integration in the base case can be improved. The heat integration is evaluated in terms of sequence of the stream pairing and placement of HTFs. All stream data used are extracted from the previous chapter.

9.3.1 Composite curves for the system

Before evaluating the heat integration in the system, the CC is drawn to visualize the overall temperature-heat content in the system. The steam consumption is not taken into account when drawing the CC, as LP steam is considered an external utility. It can be discussed whether the steam condensate is an external utility. In this thesis cooling of steam condensate is viewed upon as part of the system, and is therefore not considered to be an external utility. The CC for case 1 is given in Figure 26. The input data used to draw the curves can be found in Appendix C.

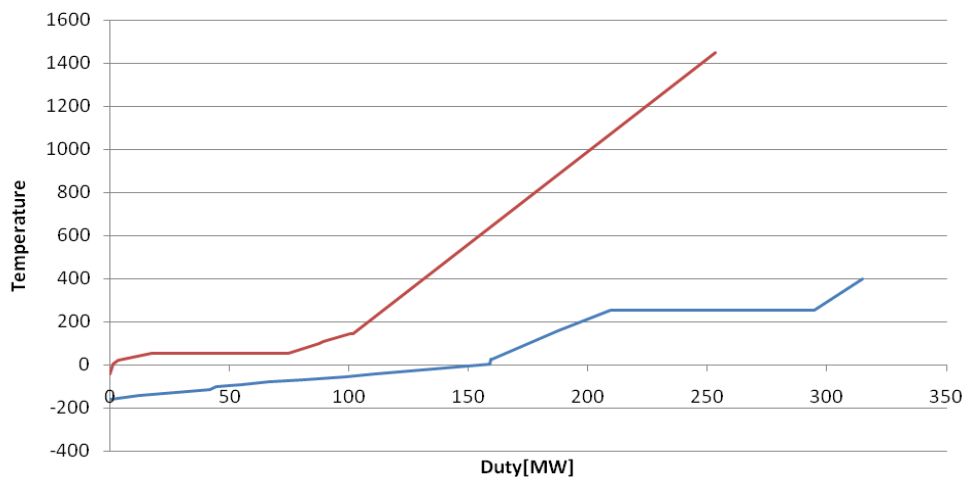


Figure 26 CC for the base case

The composite curve for the system indicates that no external cooling is required, which makes the system a threshold problem, hence shifting the ΔT_{\min} will not reduce the utility requirements. The pinch point in the system is in the cold end of the CC. The cold pinch temperature is calculated to $-160.3\text{ }^{\circ}\text{C}$, and a hot pinch temperature of -43°C resulting in a $\Delta T_{\min} > 110^{\circ}\text{C}$.

9.3.2 Sequence of the streams

The streams extracted from the simulation file, are drawn in a T-Q diagram (Figure 27). As it exist a trade-off between ΔT in and the required heat transfer area, the heat transfer sequence in the plant, should follow logically from temperatures. The logarithmic mean temperature difference is used to select the sequence of the streams.

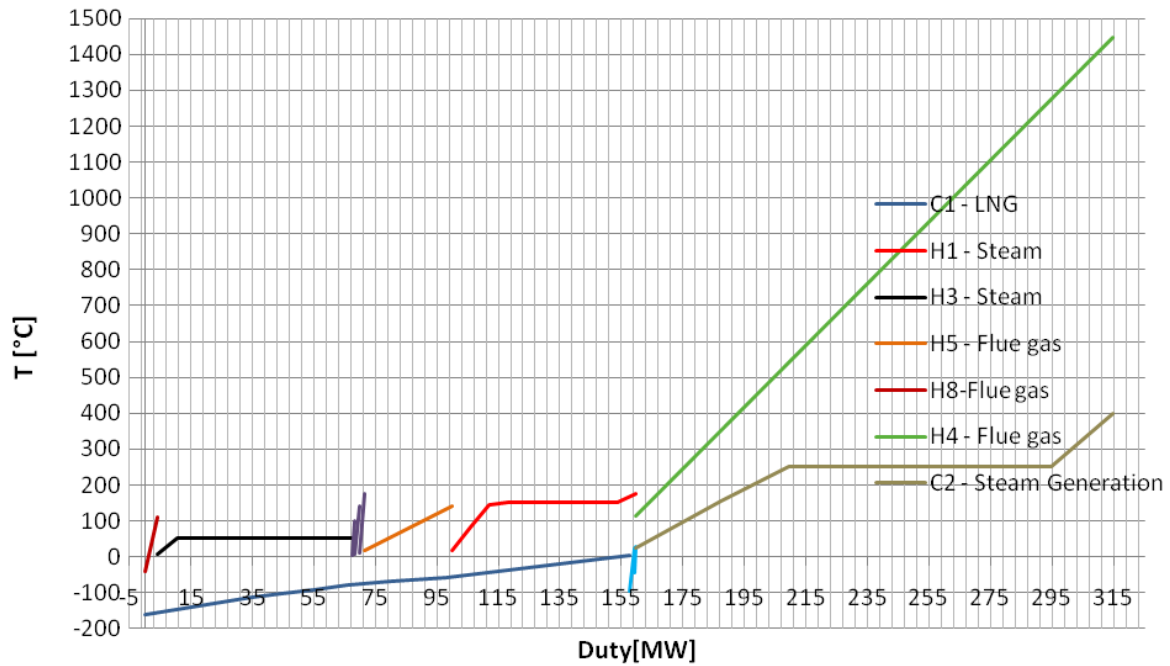


Figure 27 T-Q Diagram for the different streams in the system

The streams in Figure 27 are named as in the previous sections. The lilac streams represent H2 and H6-H7. The light blue streams between C1 and C2, represents C3-C4. As these streams are relatively small they are drawn in a separate diagram, and will be discussed later in this chapter.

In the base case H4 exchange heat with C2. This is the steam generation in the system, and from the T-Q diagram above it can be seen that this pair match is logical from temperatures. But ΔT between the two streams diverges, resulting in a significant approach temperature at the hot end of the superheater. This leads to a poor distribution of driving forces, hence depending on the U-value, the area of the MP superheater will be relatively small compared to the required area of the BFW heater. The UA values were calculated by Hysys to be approximately 19.4 kW/K for the MP superheater and 180 kW/K for the BFW heater. Though the UA value is greater for the BFW, the U-value for a liquid-gas HX exceeds that of a gas-gas HX, as discussed in Chapter 7. The superheater should therefore have a greater ΔT to compensate for the poor U-value. In addition, the amount of steam produced will increase with increasing temperature of the flue gas in the hot end, according to Eq. Feil! Fant ikke referansekilden.. Based on the previous it can be disputed that the HRSG scheme is applicable.

Though the HRSG scheme is applicable from a thermodynamically point of view, it could induce risk of meltdown in the MP superheater, due to the great approach temperature. If this is the case, the system could be rearranged as shown in Figure 28.

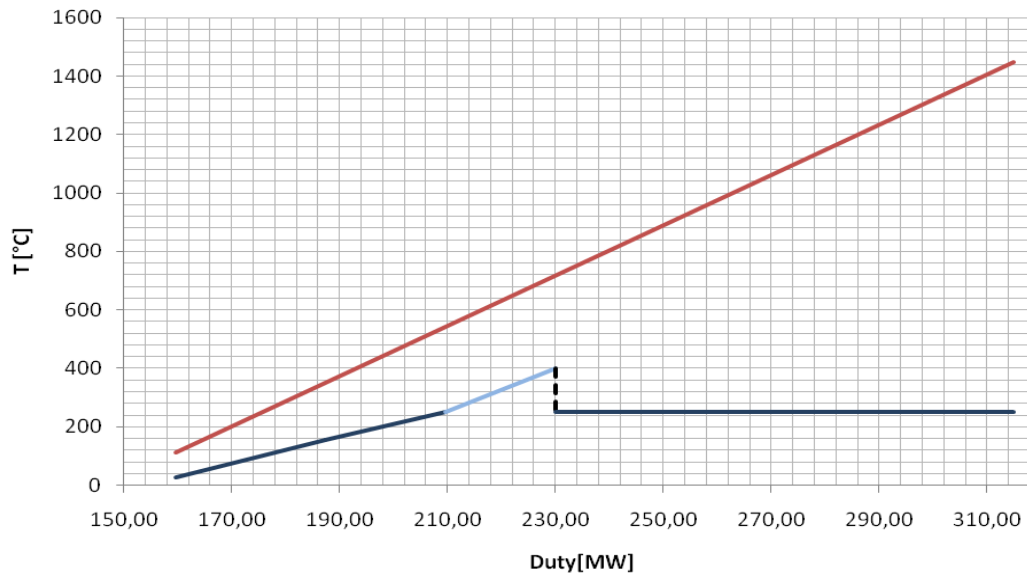


Figure 28 Different boiler scheme

In Figure 28 the superheater is shifted to a lower temperature, while the evaporator is shifted to a higher temperature to reduce risk of meltdown. As the h-value of water is greater than that of steam, the conduction through the material will increase, which will result in less risk of meltdown. However, the area of the MP superheater will increase, as ΔT is reduced. The size of the boiler could however, be reduced as the driving forces are increased in the evaporator. If this scheme will improve the HRSG is dependent on expenses and safety regulations, and will not be further discussed in this thesis.

From Figure 27 it is difficult to evaluate the sequence of H2, H6-H7 and C3-C4 Therefore a separate graph is made, omitting the steam generation. The graph is given in Figure 29.

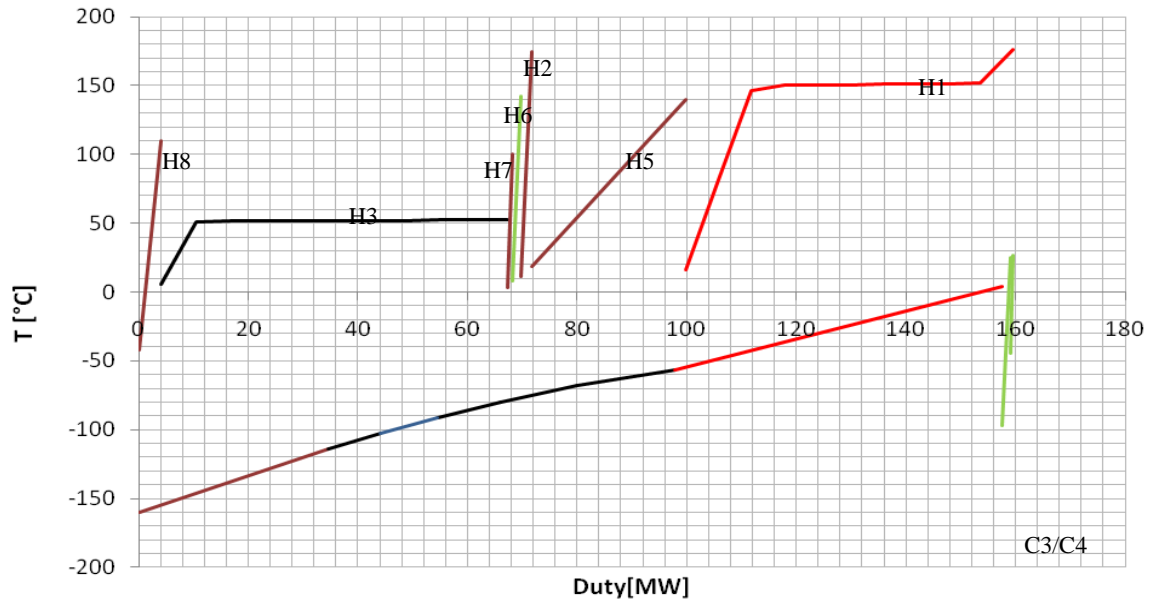


Figure 29 T – Q Diagram omitting H4 and C2

Figure 29 shows the streams drawn logically from LMTD. The colors indicate which hot streams heat exchange with the different temperature intervals for C1, C3 and C4 in the base case (E.g. the hot streams heating LNG from -160.3 to -114 are colored dark red). Though the target temperature for H6-H7 exceeds that of H3 the difference are insignificant making the stream matches acceptable. This is also valid for the other streams in the graph.

Hot stream H1 is LP steam. Reducing the use of LP steam in the system would lead to increased power production. The GCC for the system can be used as a tool to target the required utility level. To minimize the energy cost in the plant the use of expensive utility levels should be minimized. In the base case only LP steam is used in the power and steam plant, while Cooling Water (CW) is used in the ASU. The GCC for case 1 is given in Figure 30. The curve is drawn with a $\Delta T = 30\text{K}$. As can be seen from the graph only a low level utility is required in the system. The required amount of utility is calculated to 61.7 MW. The input data used to calculate to GCC is given in Appendix C.

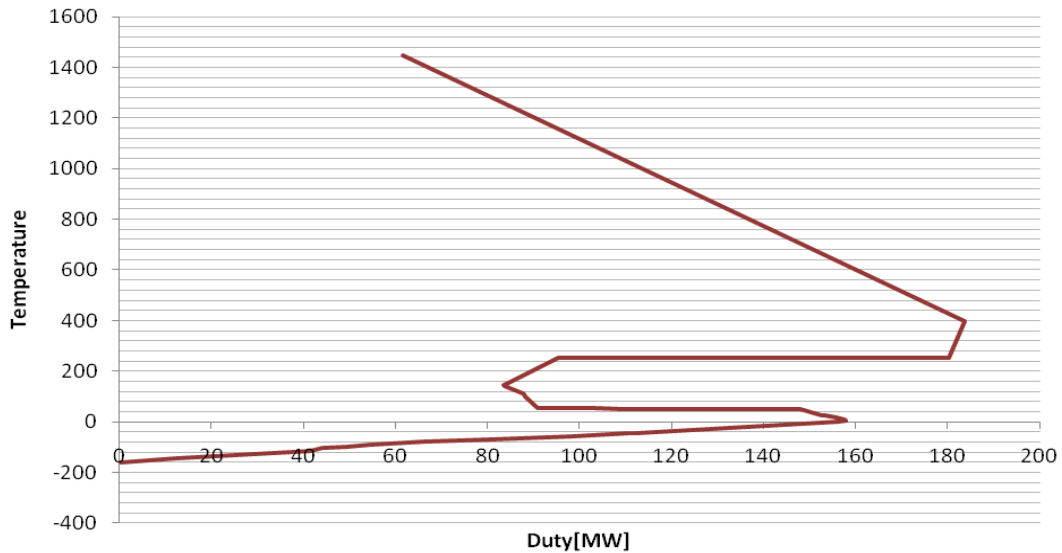


Figure 30 GCC for the base case

From a thermodynamic point of view CW could be used instead of steam. However, this would require significant amounts of water to prevent freeze-out in the system, thus this would require implementation of a vast water system. The water needs to be purified and chlorinated, which would make the system more climate sensitive and less environmental friendly. Another possible solution is to lower the LP steam production and increase the duty of the steam condenser, which would result in increased power production in the LP turbine. In the main simulation model the molar flow of LP steam is set to 4506 kmol/h, and the power production in the LP steam turbine is calculated to 12.52 MW. If reducing the LP production to 3704 kmol/h and the duty of LNG heater 5 with 10 MW, the power production in the LP steam turbine is increased with 1.35 MW. However, the outlet temperature of LNG heater 4 is reduced to approximately 1°C, which increase the risk of freeze-out in the system.

9.4 Placement of HTFs

For stream H5 – H8 HTFs either MEG/water or Methanol are used as heat transfer fluids. The placement of the HTFs is important to the heat exchanger design, as explained in Chapter 7. To determine the accurate temperature level for the intermediate heat carrier, according to Eq.(7.6), an estimated h -value for the different streams is required. For LNG an average value is used; 1750 W/m²K. For the hot streams H5-H6, the h -value is dependent on the pressure of the streams. The h -values chosen are average values of tabulated h -values for gas, given in Chapter 7.4. Table 20 gives the chosen values.

Table 20 Chosen h-values for the hot streams in the system

Stream	Chosen h [W/m ² K]
H5	103
H6	103
H7	325
H8	325

As the film transfer coefficient on the hot side of all HXs, using HTFs are much lower than that of LNG; the chosen individual ΔT_i should be higher than that of the cold stream. If two streams (i and j) should experience the same heat transfer area the following should apply:

$$\sqrt{h_i} \cdot \Delta T_i = \sqrt{h_j} \cdot \Delta T_j \tag{9.3}$$

This equation is derived from Eq.(7.6), where ΔT is inversely proportional to the **square root** of the h-value. It is important to notice that increasing the magnitude of the h-value by 100 will only decrease ΔT by 10. In the following the placement of the HTF in the different HXs will be discussed.

9.4.1 Placement of HTF in LNG HX 1

In the first LNG HX Methanol is employed as the HTF.. The heat carrier extracts and emits heat at the same temperature level, as can be seen from Figure 31. LNG is heated to approximately -155°C, by cooling flue gas prior to the distillation column (LNG heater 3).

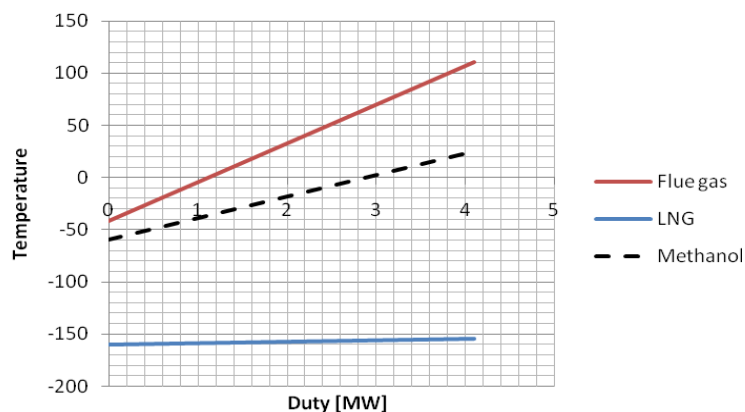


Figure 31 Placement of HTF in LNG HX 1

Figure 31 shows that the HTF is placed closest to the hot stream. The h-value of the hot stream is estimated to 325 W/m²K, while the h-value for LNG is estimated to be 1750 W/m²K. The square root of these h-values is 18 and 42, respectively. This means that the temperature approach between the hot stream and the HTF should be twice that of the LNG and the HTF, (Eq.(9.3)). As can be seen from Figure 31, this is not valid for. As already discussed the HTF

should approach the LNG from a thermodynamic point of view. However, it is important to avoid freeze-out in the system. The cold temperature of Methanol in the system is -60°C , while the freezing point of Methanol is -97.7°C according to Table 5.

9.4.2 Placement of HTF in LNG HX 2 and LNG HX3

In LNG HX 2 WEG/water is used. The HTF firstly heats the LNG, before it is split into two streams, one going LNG heater 1 and one going to LNG heater 2, as can be seen from Figure 32. In LNG HX3 the same HTF is applied and placement of the HTF coincides with that of LNG HX 2, hence only the placement of the HTF in LNG HX 2 is discussed.

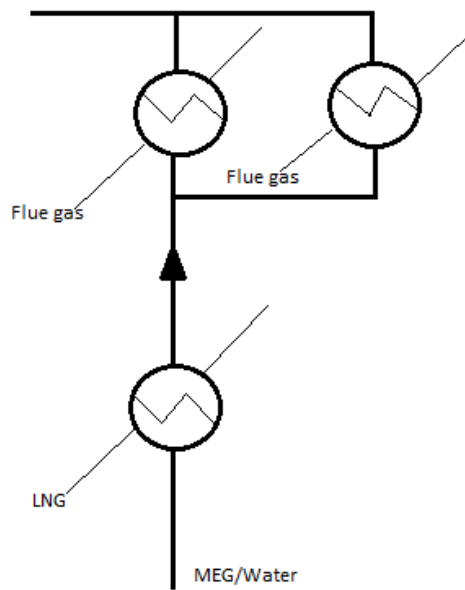


Figure 32 MEG/Water cycle

Figure 33 shows the placement of the HTF. The HTF emits heat at 25°C and extracts heat at -30°C . After heating the LNG, 60 % of the HTF is routed to LNG heater 1. From the graph to the left it can be seen that the HFT is placed close to the hot fluid. The same is valid for LNG heater 2. As already discussed, the HTF should be place closest to the fluid possessing the greater h-value, in this case the LNG. However, safety needs to be taken into consideration. For all HXs using HTFs, AKSO has chosen to place the HFT at least 25°C above its freezing point. This is done to prevent freeze-out in the system. As the freezing point of MEG/Water is -56°C , the HTF cannot be shifted closer to the LNG. However, it could be beneficial to choose another HTF. If using Methanol instead, the HTF could be shifted closer to the LNG as can be seen in the graph at the right. This would increase the temperature difference in LNG heaters 1-2. However, it is important to notice that the selection of HTFs is dependent on several factors. The density is higher for MEG/Water then for Methanol; hence the pipe diameter can be reduced if employing MEG/Water as the HTF. In addition, the heat capacity is greater for MEG/Water compared to Methanol. I.e. a smaller ΔT is experienced using MEG/Water if the duty is held constant. In addition, the expenses of using Methanol instead

of MEG/Water should be considered. As economical data is not given in this thesis, this will not be further discussed.

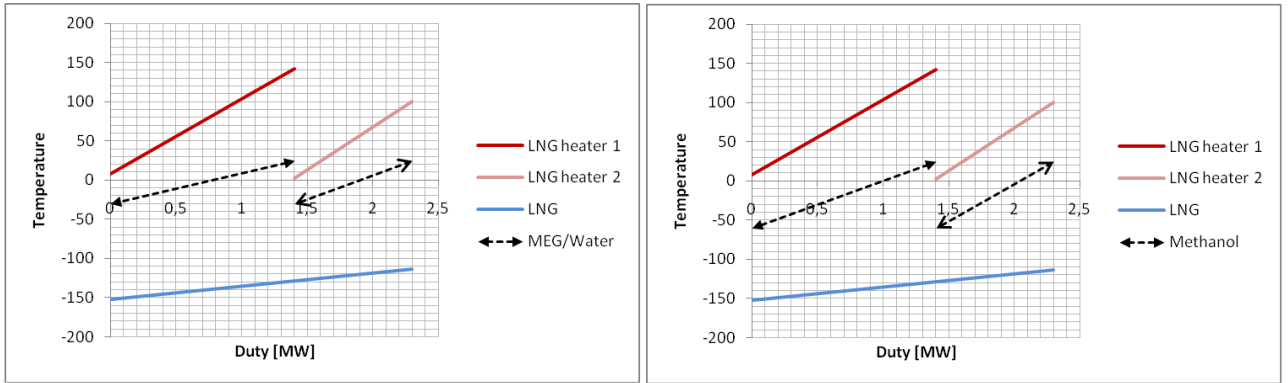


Figure 33 Left: WEG/Water as HTF Right: Methanol as HTF

10 Different oxygen purities

Different oxygen purities were tested to find the impact on the CO₂ CPU. Three different purity levels were evaluated; 90, 95 and 97 mol%. For the main simulation model the molar flow of O₂/N₂ were set to 1540 kmol/h. When simulating the process with different oxygen purity, the molar flow rate of O₂/N₂ was adjusted to maintain 1 mole% excess oxygen in the feed. The molar flow is calculated from the flow rate in case 1:

$$\dot{n}_{97} \cdot x_{97} = \dot{n}_{95} \cdot x_{95} = \dot{n}_{90} \cdot x_{90} \quad (10.1)$$

Where \dot{n} is the molar flow of O₂/N₂, and x is the molar fraction of oxygen.

To give a complete evaluation the simulation model needs to be specially designed for each case, to simplify the problem some variables are kept constant in the different cases;

- All duties of heater/coolers in the purification unit are held constant, e.g. temperatures are expected to change with oxygen purity.
- The recycle rate is held constant.
- The distillation column is converged to give the same CO₂ recovery rate for the different cases, as a specified recovery rate is required for transportation and storage of CO₂. The CO₂ recovery rate is defined as the fraction of CO₂ captured from the formed CO₂ in the combustion.
- The duty of the flue gas fan is not taken into account when comparing the different cases, owing to the fact that a different operator is used in the simulations.
- In addition the ASU is not simulated; hence, only the power consumption of the CO₂ CPU is calculated for the different cases. Though the ASU is not simulated, the trade-off between power savings in the CO₂ CPU and the ASU is discussed.

With the previous assumptions the different cases are evaluated in terms of:

1. Compression work in the CO₂ purification unit
2. Duty of distillation column
3. Overall power consumption

10.1 Case studies

Three different case studies were investigated. For case 1 the oxygen purity is specified to 95 mol%. The results from this case study resemble those given in Chapter 8. For case 2 the oxygen purity is increased to 0.97 mol%, giving a molar flow of 1508 kmol/h from

Eq. Feil! Fant ikke referansekilden. For case 3 the oxygen purity is decreased to 0.90 mol%. The flow of N_2/O_2 is specified to 1626 kmol/h.

10.2 Result and discussion

10.2.1 Flue gas composition

As discussed in Chapter 5, the composition of the flue gas is dependent on the oxygen purity, as the fraction of CO_2 will increase with increasing oxygen purity. The molar fraction in the flue gas after the burner, and to the CO_2 CPU for the different oxygen purities are given in Table 21.

Table 21 Molar fraction of CO_2 in flue gas for different oxygen purities

Parameter	Unit	90	95	97
Molar flow of flue gas	[kmol/h]	8595	8509	8477
Molar fraction of CO_2 in flue gas	[mole%]	0.6579	0.7239	0.7521
Molar flow to CPU	[kmol/h]	938.3	850.9	818.4
Molar fraction of CPU	[mole%]	0.7866	0.8675	0.9019

As expected, the molar fraction of CO_2 increases with oxygen purity. However, the water amount in the flue gas remains somewhat constant. In an incomplete combustion the water content would vary with the oxygen purity, due to changes in recycle rate and characteristics of combustion. The amount of oxygen is also nearly constant for the different oxygen purities. In an incomplete combustion, the NO_x and CO production would change with oxygen purity, resulting in changed oxygen content in the flue gas. As the NO_x production depends on the mole fraction of nitrogen in the feed, the NO_x production will increase with decreasing oxygen purity. This means that the local emission of NO_x will be reduced with increased oxygen purity.

Changing the oxygen purity will also affect the HRSG. When assuming constant recycle rate, the molar flow of flue gas increases. As discussed in Chapter 7 the amount of steam produced is dependent on the flue gas flow (Eq. Feil! Fant ikke referansekilden.). In addition, the steam production is dependent on the C_p value of the flue gas. The results from the simulation show that the C_p value is reduced with decreasing oxygen purity. However, the product of the mass flow and the C_p value increases with decreasing oxygen purity. Hence, more steam will be produced if the oxygen purity is reduced.

10.2.2 Compressor work of the CO₂ CPU and the ASU

As discussed in Chapter 3.2, the compression work is dependent on the composition and flow rate of flue gas to the CO₂ CPU. The overall compression work of the CO₂ CPU is given in Figure 34. The recycle compressor work depends on the recycle rate, as the recycle rate is assumed constant the variations in compressor work are insignificant and are therefore not included.

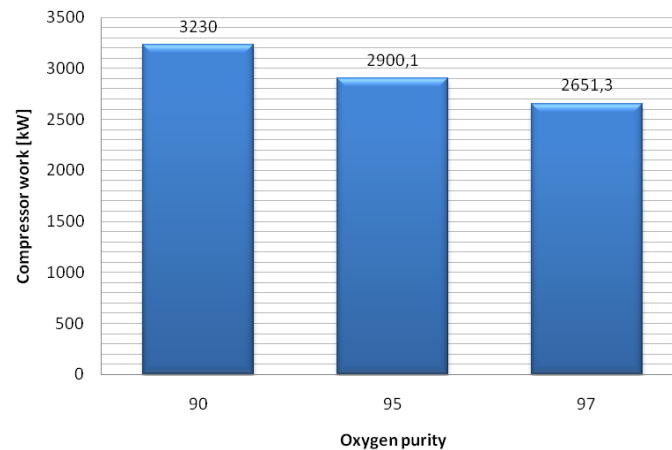


Figure 34 Compressor work of CO₂ CPU

As expected the power consumption decreases with increasing oxygen purity. The reasons are as follows:

- The molar flow to the CPU decreases with oxygen purities, resulting in lower power consumption. For case 3 the molar flow to the CO₂ CPU is calculated to 938kmol/h, while for case 2, the molar flow was reduced to 818kmol/h.
- The inlet temperature of the compressors decreases with increased oxygen purity. For compressor 2 the inlet temperature falls from 8.2 °C to 3.7°C when changing the oxygen purity from 95mole% to 97mole%.
- From Table 21 it can be seen that the molar fraction of CO₂ in the flue gas, increases sufficiently with increasing oxygen purity. As a result, the molecular weight of the flue gas increases, leading to lower specific compressor work. The specific compression work for the different oxygen purities are given in

Table 22.

- The k-value decreases with oxygen purity, hence the power consumption will decrease.

Table 22 Specific compressor work in CO₂ CPU

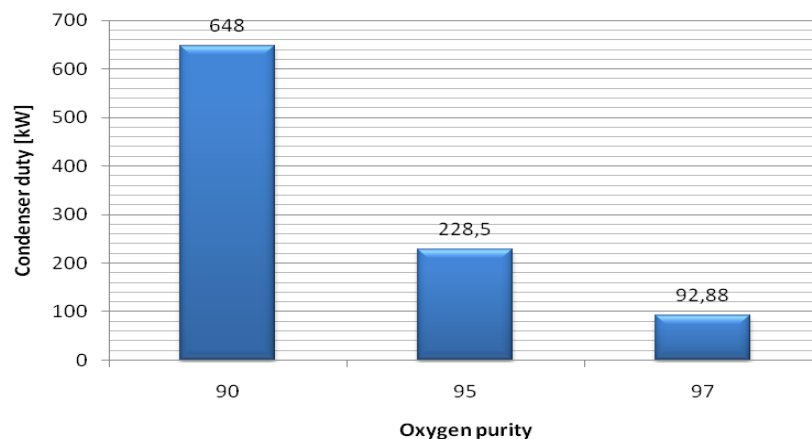
	90	95	97
Specific work in CO₂ CPU [kJ/kmol flue gas]	3.48	3.30	3.28

There exist a trade-off between the power consumption in the CO₂ CPU and the ASU. If the oxygen purity is decreased, the compressor work of the CO₂ CPU is increased by 10%. However, the opposite is true for the ASU; the power consumption will be reduced. As the ASU accounts for 33% of the overall power consumption in the plant, the impact on the ASU is of greater concern than the impact on the CO₂ CPU.

If the oxygen purity is increased to 97mol%, the savings in compressor work in the CO₂ CPU is 10%. This is a relatively insignificant change compared to the increased power requirement of the ASU for purities greater than 95mol%. The oxygen flow required from the ASU will be reduced for high oxygen purities, hence only relatively minor changes in compressor work is expected. However, the energy of separation will increase, resulting in increased OPEX and CAPEX. This is further discussed in the following section.

10.2.3 Energy of separation in the CO₂ CPU and the ASU

As already discussed, the change in the CO₂ CPU compressor work with oxygen purity, is only minor. However, the changes in condenser duty in the N₂/CO₂ distillation column are significant. The duty of the condenser for the different oxygen purities are given in Figure 35.

**Figure 35** Condenser duty for different oxygen purities

The bar chart shows that the duty of the condenser increases with 86% when the oxygen purity is reduced from 97mol% to 90mol%. The reason for the increased duty is the rise in vapor leaving each tray, resulting in a higher molar flow to the condenser. For Case 3 above 300kmol/h of vapor leaves the first separation stage, compared to 70kmol/h for Case 2. In addition, the calculation shows that the inlet temperature of the condenser is reduced with

decreasing oxygen purity. The results from Hysys show that the temperature is -95°C for the case 3, compared to -80°C for case 2.

Though the condenser duty of the CO_2/N_2 distillation is reduced with increasing oxygen purity, the duty is below 1MW for all the different cases. The savings in condenser duty is therefore considered insignificant compared to the changes in the ASU. The energy of separation in the ASU will increase sufficiently if the purity is increased above 95mol%. The separation will change from oxygen-nitrogen to oxygen-argon, which requires more energy, and implementation of a supplementary distillation column. If the oxygen purity is reduced there will be some savings in the ASU. However reducing the oxygen purity will increase the size of the operation equipment. For AKSO's concept the equipment size of the ASU is of great concern, as the system is planned to be located off-shore.

11 Possibilities of integrating the ASU

As already mentioned the ASU accounts for a significant amount of the overall power consumption in the base case. If the ASU is integrated with the power plant the overall power consumption of the unit will be reduced. In this chapter the possibilities of integrating the ASU will be discussed.

11.1 Methodology

Integrating the ASU could decrease the external utility requirements in the plant. If the composite curve is shifted to the right, cold energy from the LNG could be utilized in the ASU. The CC shifted to the right is shown in Figure 36.

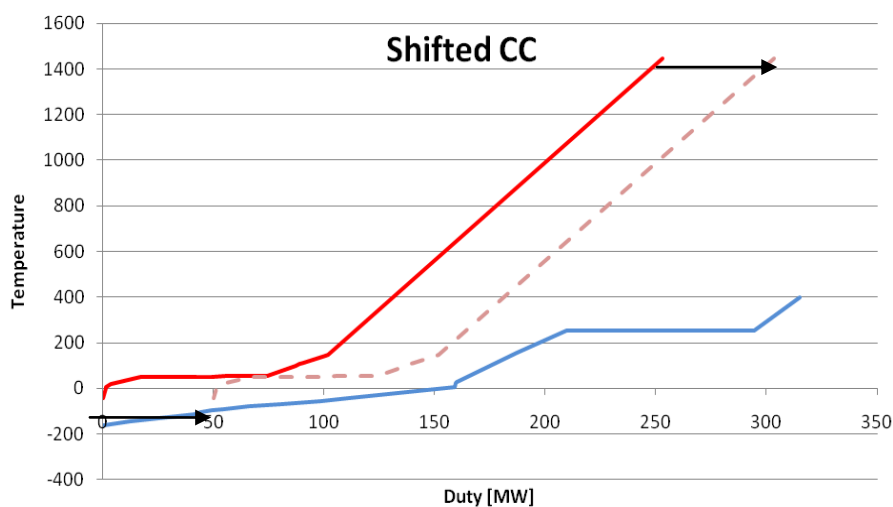


Figure 36 Shifted CC

The unbroken red line indicates the original hot CC, while the dotted line indicates the shifted CC. When shifting the curve to the right the temperature approach get closer. The system is no longer a threshold system; hence shifting the curves will reduce the utility consumption.

To evaluate the possibility of integrating the ASU two simulation models are created. In the first model, the ASU is integrated with the regasification train. Data used are collected from the main simulation model (Case 1). The second model represents a conventional ASU. This model is created to gain a standard of reference. The following simplifications apply:

- Only the equipment upstream the cold box are simulated (for both models), hence the impact on the cold box will not be discussed.
- To simplify the problem the air compressors are assumed to be the only power consuming unit in the ASU.

11.1.1 Simulation models

For the integrated ASU the simulation model is created as it follows; the purification unit is simulated as a component splitter removing the water and CO₂ content in the air. The air is then routed to a compressor with pre-cooling and after-cooling, where cryogenic LNG is heat exchanged against the air. In a conventional ASU, air is compressed in three stages to 4.4 bar with intercooling, and enters the cold box at approximately 30°C. If integrating the ASU with the LNG regasification unit, only one compression stage is required according to PhD student Fu Chao. The molar flow of ambient air is specified to 7897 kmol/h. The composition of the ambient air, fed to the component splitter, is given in Table 23. The ambient air enters the ASU at 100 kPa and 27°C.

Table 23 Composition of the air prior to the purification

Component	Mole fraction
H ₂ O	0.031
Oxygen	0.203
Nitrogen	0.757
CO ₂	0.009

In the precooler the air is cooled to -60°C. If the air is cooled prior to the compression, the power consumption decreases, as explained in Section 3.2.1. The adiabatic efficiency of the compressors is specified to 75 %. After the compression the air is cooled to 27°C by LNG. Cooling the air further would result in surplus cold energy in the cold box. The simulation model of the integrated ASU is shown in Figure 37.

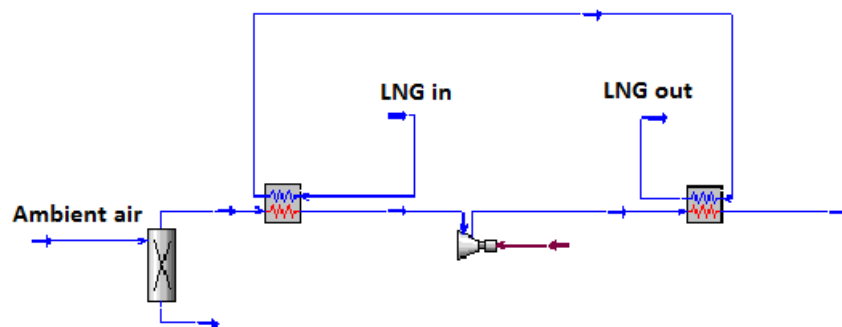


Figure 37 Integrated ASU

To be able to compare the integrated ASU solution with the original system, a three stage compressor with intercooling is simulated in Hysys. The air is assumed to be dried and purified prior to the compression. In the base case the air is split into two portions after the second compressor. It is assumed in this simulation model, that the total amount of air is

compressed in a three stage compressor. The simulation model of the conventional ASU is given in Figure 38.

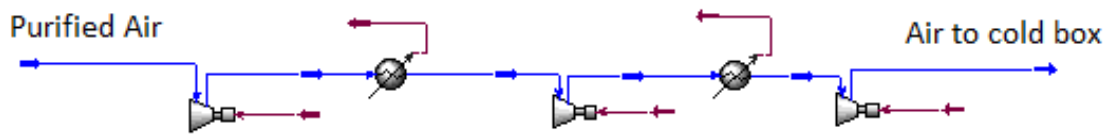


Figure 38 Conventional ASU

11.2 Results and discussion

The component splitter separates out the water and CO₂ content in the ambient air, the overhead molar flow is calculated to 7581 kmol/h. In the first LNG heater the air is cooled to -60°C by heating LNG to -152.1°C, as can be seen in Table 24. The air is then compressed in a one-stage compressor. The outlet temperature of the compressor is calculated to 134.1 °C.

Table 24 Properties of HXs prior and after the air compressor

Unit	$T_{h,inlet}$ [°C]	$T_{h,outlet}$ [°C]	$T_{c,inlet}$ [°C]	$T_{c,outlet}$ [°C]	Duty [MW]
Pre-cooler	27	-60	-160.3	-152.1	5.30
After-cooler	134.1	27	-152.1	-144.4	5.90
SUM					11.2

Table 24 shows that the overall duty of the HXs is calculated to 11.2 MW. This means that 11.2 MW of cold energy from the LNG regasification train is utilized in the ASU; hence the utility consumption in the power plant can be reduced by the same amount. The compressor work of the air compressor was calculated to 11.38 MW. The result from the simulation model of the original system, gives a compressor duty of 13.3 MW. Thus, integrating the ASU will result in 1.92 MW saving in compression work.

In Figure 39 the CC of the base case is shown to the left, while the CC when integrating the ASU is shown to the right. As can be seen from the graphs the change in pinch point is relatively small, and the temperature approach of the two graphs is only slightly reduced. Hence, the increase in heat transfer area will not be significant if implementing this system configuration.

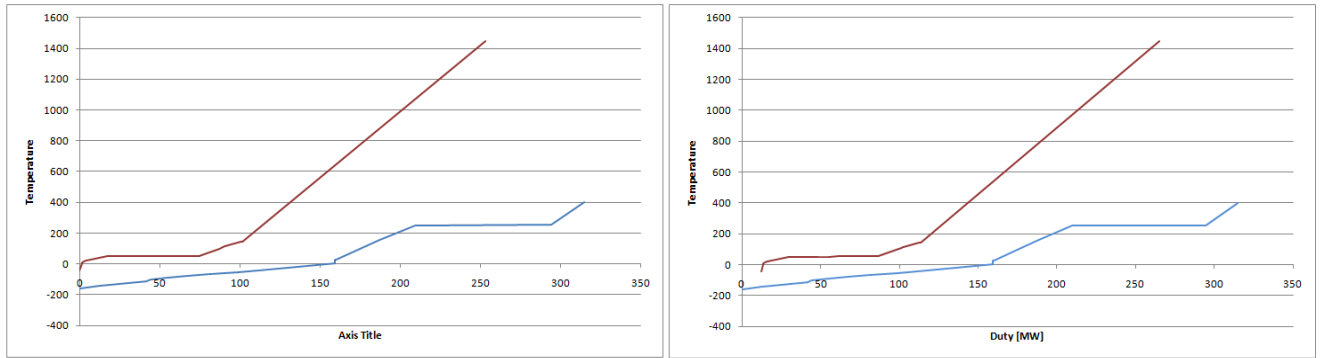


Figure 39 Left: CC of base case. Right: CC when integrating the ASU.

The main issue if the ASU is heat integrated with the regasification train is regulation of the ASU. From the simulation model it was found that if reducing the LNG load with 50%, temperature cross will occur in the aftercooler. In addition, the outlet temperature of air will be greater than 100°C. As the regulation of an ASU is found difficult, supplementary heaters/coolers could be implemented to be able to run the unit during part load operations. If the outlet temperature of LNG from the aftercooler is set, the case would be as stated above. Hence, a supplementary air cooler is required. If instead the temperature of air is set, the outlet temperature of LNG would decrease to -129°C. Hence, the utility requirements would increase. A supplementary heater could be installed, and more LP steam produced when required.

12 Proposed system

A proposed solution with heat integration between the CO₂ CPU, the ASU, the regasification train and the steam and power unit will be presented in this chapter. In addition, the possibility of using membranes for air separation in AKSO's system is discussed.

12.1 Chosen parameters and assumptions

12.1.1 Selected oxygen purity

As discussed in Chapter 10, decreasing the oxygen purity will decrease the required energy of separation in the ASU. However, the investments cost is likely to increase, as the size of the ASU will increase. If the oxygen purity is increased to 97mol%, the power consumption of the CO₂ CPU will decrease, but both capital and operational costs of the ASU will increase sufficiently. As this is the main energy consuming unit in the facility, it is likely that increasing the oxygen purity would be unprofitable. The selected oxygen purity is therefore set to 95mol% in the proposed system configuration.

12.1.2 Selected heat integration scheme

As stated in Chapter 9 the sequence of the pair-matching is found acceptable. It is chosen to heat integrate the ASU as the integration leads to lower power demand in the unit. The integration scheme given in Chapter 11 will be implemented.

12.2 Proposed system configuration

The integration between the ASU and the regasification train can be seen in Figure 40. If the LNG should be directly heat integrated with the ambient air, this will require pipes with a significant diameter due to the high density of LNG. Therefore it could be profitable to use indirect heating to reduce the investment cost. This is not further evaluated in this thesis.

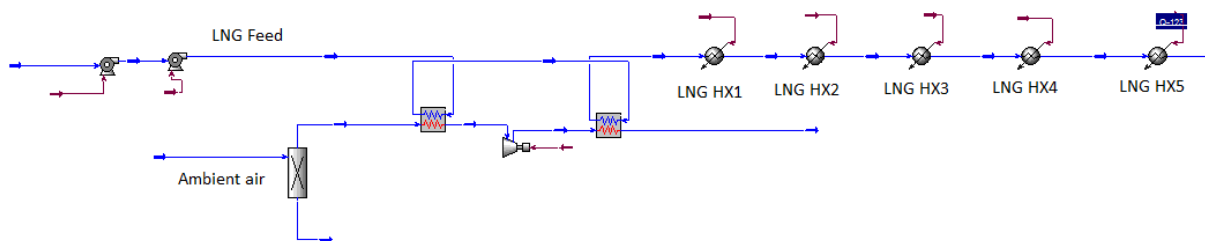


Figure 40 Integration of the ASU

For the new system configuration the CC is shifted to the right, thus LNG heaters 1-5 are shifted to a higher temperature. The streams follows logical from temperature as can be seen

in Figure 42, where the dotted line indicates the ASU. The steam generation will not be affected by the integration of the ASU.

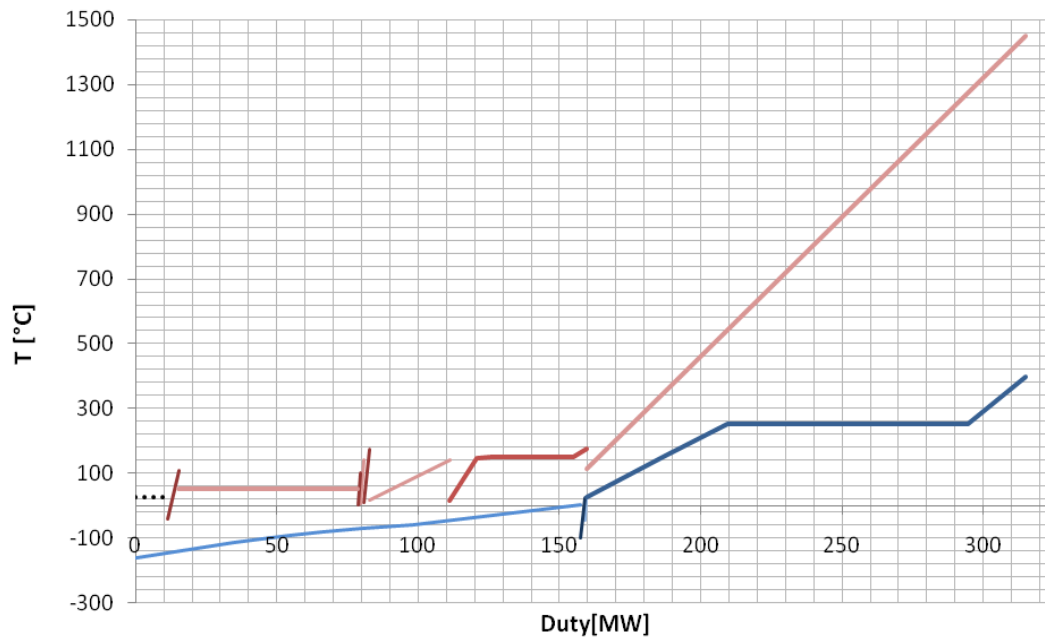


Figure 41 T-Q Diagram system with integrated ASU

The gains of implementing the proposed solution are as follows (compared to case 1):

1. The LP consumption is reduced to 3684 kmol/h
2. The duty of LNG heater 5 is reduced to 48.5 MW
3. No supercooling is experienced in LNG heater 4, as can be seen in Figure 42. Thus, there is less risk of freeze-out in the system. In addition a greater temperature approach between the steam condensate and the LNG is detected. This results in decreased heat transfer area.
4. The power production in the LP turbine is increased to 14.41 MW.
5. The LNG will be shifted closer to the HTFs employed in LNG HX 1-3. This will lead to greater driving forces in these HXs.

The disadvantages of implementing the new system configuration are:

1. The system configuration is more complex as the ASU is integrated with the power and steam plant. A greater regulation system is required, and oxygen buffer tanks will be necessary.
2. The ΔT in the different HXs will be reduced, which will affect the required heat transfer area.

3. The capital expenses of the system might increase, due to the heat exchange between the LNG train and the ASU.

12.3 Possibility of using ITMs for oxygen production

If reducing the power consumption in the system further, implementation of membranes could be an option. As stated in Chapter 6 ITMs have the greatest potential of large-scale production of high purity oxygen. As the MIECs do not require an electric circuit, these membranes would be the best solution for an off-shore facility. In the following a proposition of a system configuration with membranes is given. As MIECs are capable of producing oxygen with 99% purity, this would lead to energy savings in the CO₂ CPU. To evaluate the savings, the main simulation model is simulated for 99mol% oxygen purity. The results are given in Chapter 12.5.

12.4 Possible configuration of the system

As the oxygen flux through the membrane is proportional to $\ln(p_1/p_2)$, a vacuum condition is required on the permeate side or the air can be compressed to a high pressure prior to the membranes. Both solutions will cause supplementary compressor work in the system, thus the best system configuration should be based on an economical analysis.

The ideal membrane structure is dependent on several factors, as discussed in Chapter 6. For AKSO's system a production rate greater than 1000 tons/day is required. The most promising perovskite, of those given in Table 4 is **Ba_{0.5}Sr_{0.5}Co_{0.8}Fe_{0.2}O_{3-δ}**, as this membrane has a relatively high flux (compared to other perovskites) and thickness. These membranes are 1.8 mm thick, and the oxygen flux is approximately $1.563 \cdot 10^{-6}$ mol/s·cm². This means that one of these membranes can produce $1.013 \cdot 10^{-6}$ kmol/h oxygen. I.e. more than $1 \cdot 10^9$ membranes in stacks are required to produce the amount of oxygen needed in AKSO's system.

If employing membranes for air separation, a similar system configuration as that given in Section 6.3.2 should be implemented. The air can be heated firstly by the nitrogen from the air separation. Thereby a hot utility is required to heat the air to at least 800°C. This could be done by burning part of the send-out gas in a supplementary burner. However, this would lead to increased CAPEX and emissions. Another solution could be to utilize the flue gas from the oxy-burner to heat the air prior to the separation, though this would decrease the steam production in the HRSG.

If the technology develops as suggested by Ted Foster, implementing membranes for air separation in AKSO's system could be an economical option. As stated in Chapter 6 the cost is intended to be 30 % lower than for an ASU configuration. In addition all ITMs produce oxygen with greater than 99mol% purity, hence the implementation of membranes would decrease the power consumption in the CO₂ CPU. This will be discussed in the next section.

12.5 Impact on the CO₂ CPU

To evaluate the savings, the main simulation model was tested for 99mol% oxygen purity. The O₂/N₂ molar flow was specified to 1478 kmol/h. The recycle rate is held constant at 6250 kmol/h. The CO₂ capture rate was adjusted to 0.9999. The results are given in the Table 25:

Table 25 Impact on the CO₂ CPU

Parameter	Unit	Value
CO ₂ fraction in flue gas	[mol%]	0.78
CO ₂ fraction flue gas to CO ₂ CPU	[mol%]	0.94
Molar flow to CO ₂ CPU	[kmol/h]	790
Compressor work CO ₂ CPU	kW	2500
Condenser duty	kW	16

The condenser work of the N₂/CO₂ is significantly decreased when the oxygen purity is increased to 99 mol%. In addition the molar flow of CO₂ to the purification unit is decreased; hence the CAPEX and OPEX of the unit are decreased, due to the reduction in equipment size. The savings in the CO₂ CPU are dependent on the selected utility used to heat air. If a combustor is used, the flue gas from the burner should be purified. This would increase the molar flow to the CO₂ CPU, and decrease the CO₂ fraction.

If implementation of membranes does not lead to increased CO₂ production, the CO₂ CPU scheme could be changed to reduce both energy cost and CAPEX. As the CO₂ fraction in the flue gas to the CO₂ CPU is nearly 95mol%, the *no purification scheme* could be a more economical solution. In this scheme no distillation column is required. This will result in lower investment and operation costs.

13 Conclusion and further work

13.1 Conclusion

Simulation models were created in **Aspen Hysys** to investigate the heat integration in the system, validate the feasibility of integrating an ASU and to find the impact on the CO₂ CPU when changing the oxygen purity.

The **heat integration** in AKSO's system was found acceptable. The sequence of the pair-matching of the streams was logical from temperature. However, it could be beneficial to change the HTF in LNG heaters 2-3 to a HTF with a lower freezing point (e.g. Methanol).

The system was tested for three different **oxygen purities**; 90, 95 and 97mol%, where 95mol% is the oxygen purity employed in the base case. If reducing the purity the compressor work of the CO₂ CPU is increased by 10%, while the opposite is true if the purity is increased to 97mol%. The duty of the condenser in the N₂/CO₂ distillation column is increased by 65% if the purity is reduced to 90mol%. A literature review states that the energy of separation on the ASU will increase sufficiently for purities above 95mol%. If the oxygen purity is reduced however, only a minor reduction in separation energy is experienced. In addition, the equipment size of the ASU will increase for purities below 95mol%. Base on the previous, and owing to the fact that the ASU accounts for 33% of the overall power consumption in the plant, **the oxygen purity should not be changed.**

Integrating the ASU with the power plant was found to be technically possible at full load. However, it may be technical issues regarding regulation of the ASU when running the plant at part load. If integrating the ASU the power consumption in the air compressors are reduced with 14%. In addition, 18 % reduction in LP steam consumption is experienced. This results in a greater turbine yield; approximately 2 MW increased power production. As the equipment size, the OPEX and the energy cost the ASU is decreased if integrated with the power plant, this is considered an adequate solution if it is found possible to regulate the unit during part load operation.

If **using membranes for air separation**, MIECs with a perovskite structure should be employed. The most promising structure found was **Ba_{0.5}Sr_{0.5}Co_{0.8}Fe_{0.2}O_{3-δ}**. Today 1·10⁹ such membranes are required to produce enough oxygen. Hence, the technology needs to be further evolved before it is feasible.

13.2 Further work

Implementation of **membrane technology** should be simulated in a model where the ITM is integrated with the oxy-fuel plant. Special care should be addressed to the heating of the air prior to the ITM. In addition, an **economical analysis** of the implementation should be carried out.

An **economical evaluation** on employing Methanol instead of MEG/Water as the HTF, in LNG heaters 2-3 should be investigated. In addition the **thermodynamic benefits** of changing the HTF should be investigated.

A complete **simulation model of the ASU** should be created in Aspen Hysys, to find the accurate changes in power demand when changing the oxygen purity.

A study on possibilities of regulating an integrated ASU should be carried out. This includes finding the impact on the cold box when the feed load changes.

List of References

1. Buhre, B.J.P., et al., *Oxy-fuel combustion technology for coal-fired power generation*. Progress in Energy and Combustion Science, 2005. **31**(4): p. 283-307.
2. Amann, J.M., M. Kanniche, and C. Bouallou, *Natural gas combined cycle power plant modified into an O₂/CO₂ cycle for CO₂ capture*. Energy conversion and management, 2009. **50**(3): p. 510-521.
3. Metz, B., *IPCC special report on carbon dioxide capture and storage*. 2005: Cambridge University Press.
4. EIA. *International Energy Outlook 2010*. 2010; Available from: http://www.eia.doe.gov/oiarf/ieo/nat_gas.html.
5. Mario Ditaranto, Øyvind Langørgen, and L. Aksetøy, *Oxy-Fuel Burners for a Zero Emission LNG Regasification Plant*. 2010.
6. Yang, C. and Z. Huang, *Lower emission LNG vaporization*. LNG journal, 2004: p. 24.
7. Yang, C.C. *Possible LNG Receiving Terminal Air Emission sources and Mitigation Procedures*. in Zeus LNG Conferance. 2006. Houston: Foster Wheeler.
8. AkerSolution, *Zero Emission Power Production for LNG Regasification*. 2010
9. Ministry of Petroleum and Energy. *Carbon dioxide capture and storage*. 2010; Available from: <http://www.regjeringen.no/en/dep/oed/Subject/carbon-capture-and-storage/capture-transport-and-storage-of-co2.html?id=443518>.
10. Bolland, O., *Power generation: CO₂ Capture and Storage*. 2010.
11. Krammer, G., *Introduction to Combustion - Formation and Depletion of Air Pollutants*. 2008.
12. McCauley, K., et al., *Commercialization of oxy-coal combustion: Applying results of a large 30MWth pilot project*. Energy Procedia, 2009. **1**(1): p. 439-446.
13. Metz, B., *Capture of CO₂*, in *IPCC special report on carbon dioxide capture and storage*. 2005, Cambridge University Press.
14. *European Technology Platform for Zero Emission Fossil Fuel Power Plants* 2007.
15. Michael J. Moran and H.N. Shapiro, *Fundamentals of Engineering Thermodynamics*. Fifth ed. 2006: John Wiley & Sons.
16. Øverlie, J.M., *Strømningsmaskiner, Bind 3*. 1992: Tapir.
17. Romeo, L.M., et al., *Optimization of intercooling compression in CO₂ capture systems*. Applied Thermal Engineering, 2009. **29**(8-9): p. 1744-1751.
18. Arora, R.C., *Refrigeration and Air Conditioning*. 2010: PHI.
19. Darde, A., et al., *Air separation and flue gas compression and purification units for oxy-coal combustion systems*. Energy Procedia, 2009. **1**(1): p. 527-534.
20. ya Nsakala, N., et al., *Oxygen-fired circulating fluidized bed boilers for greenhouse gas emissions control and other applications*. 2004.
21. Wall, T.F., *Combustion processes for carbon capture*. Proceedings of the Combustion Institute, 2007. **31**(1): p. 31-47.
22. Bensakhria, A. and M. Leturia, *Natural gas oxy-combustion with flue gas recycling for CO₂ capture*. CHEMICAL ENGINEERING, 2010. **21**: p. 637-642.
23. Ochs, T., et al., *Results of initial operation of the Jupiter Oxygen Corporation oxy-fuel 15 MWth burner test facility*. Energy Procedia, 2009. **1**(1): p. 511-518.
24. Smith, R., *Choice of Separator for Heterogeneous Mixtures*, in *Chemical Process Design and Integration*. 2005, John Wiley and Son.
25. Kister, H.Z. and Knovel, *Distillation design*. 1992: McGraw-Hill New York.
26. Nakaiwa, M., et al., *Evaluation of an energy supply system with air separation*. Energy conversion and management, 1996. **37**(3): p. 295-301.

27. Smith, A. and J. Klosek, *A review of air separation technologies and their integration with energy conversion processes*. Fuel Processing Technology, 2001. **70**(2): p. 115-134.
28. Richard Dubettier, et al., *Air Separation Unit: Flexibility & Energy Storage*, in *2nd Oxyfuel Combustion Conference*, Air Liquide Engineering: France.
29. Nicklas Simonsson, Marie Anheden, and R. Dubettier, *Development Opportunities for Future Large Scale Lignite Oxyfuel Power Plants*, in *2nd Oxyfuel Combustion Conference*: France.
30. Wilkinson, M.B., et al. *CO₂ capture via oxyfuel firing: optimisation of a retrofit design concept for a refinery power station boiler*. 2001: Citeseer.
31. Hägg, M.-B., *Handbook of Membrane Separations: Chemical, Pharmaceutical and Biotechnological Applications*. 2006: NTNU.
32. Lichtenthaler, R.N. *Forschung*. Available from: <http://www.uni-heidelberg.de/institute/fak12/PC/lichtenthaler/Forschung-RNL.html>.
33. Burggraaf, A. and L. Cot, *Fundamentals of inorganic membrane science and technology*. 1996: Elsevier Science Ltd.
34. Bouwmeester HJM, B.A., *Dense ceramic membranes for oxygen separation*, in *Fundamentals of Inorganic Membrane Science and technology* 1996.
35. Dyer, P., et al., *Ion transport membrane technology for oxygen separation and syngas production*. Solid State Ionics, 2000. **134**(1-2): p. 21-33.
36. Bose, A. and E. Corporation, *Inorganic membranes for energy and fuel applications*. 2007: Springer New York.
37. Geankoplis, C.J., *Transport processes and separation process principles (includes unit operations)*. Fourth ed. 2003: Prentice Hall Press Upper Saddle River, NJ, USA.
38. Sunarso, J., et al., *Mixed ionic-electronic conducting (MIEC) ceramic-based membranes for oxygen separation*. Journal of Membrane Science, 2008. **320**(1-2): p. 13-41.
39. Hashim, S., A. Mohamed, and S. Bhatia, *Current status of ceramic-based membranes for oxygen separation from air*. Advances in Colloid and Interface Science, 2010.
40. Li, K., *Ceramic Membranes for Separation and Reaction 2007*: John Wiley & Sons.
41. Sammells, A. and M. Mundschau, *Nonporous inorganic membranes: for chemical processing*. 2006: Vch Verlagsgesellschaft Mbh.
42. Shao, Z., et al., *Investigation of the permeation behavior and stability of a Ba_{0.5}Sr_{0.5}Co_{0.8}Fe_{0.2}O_{3-δ} oxygen membrane*. Journal of Membrane Science, 2000. **172**(1-2): p. 177-188.
43. Teraoka, Y., T. Nobunaga, and N. Yamazoe, *Effect of cation substitution on the oxygen semipermeability of perovskite-type oxides*. Chemistry Letters, 1988. **17**(3): p. 503-506.
44. Wang, H., et al., *A cobalt-free oxygen-permeable membrane based on the perovskite-type oxide Ba_{0.5}Sr_{0.5}Zn_{0.2}Fe_{0.8}O₃*. Adv. Mater, 2005. **17**(14): p. 1785–8.
45. Ted Foster, et al., *Enabling Clean Energy Production from Coal: ITM Oxygen Development Update*, in *International Pittsburgh Coal Conference*. 2009, Air products and Chemicals.
46. Ciferno, J., *Pulverized Coal Oxycombustion Power Plants*. Final Report, August, 2007.
47. Zhang, N. and N. Lior, *Proposal and Analysis of a Novel Zero CO Emission Cycle With Liquid Natural Gas Cryogenic Exergy Utilization*. Journal of Engineering for Gas Turbines and Power, 2006. **128**: p. 81.
48. Kemp, I.C., *Pinch analysis and process integration: a user guide on process integration for the efficient use of energy*. 2007: Butterworth-Heinemann.
49. Process Design Center. *Energy pinch technology*. 2009 [cited 2010 01.12]; Available from: <http://www2.lse.ac.uk/library/services/training/endnote/Quick%20Tip%20citing%20webpages.aspx>.
50. Al-Sobhi, S., H. Alfadala, and M. El-Halwagi. *Simulation and Energy Integration of a Liquefied Natural Gas (LNG) Plant*. 2009.
51. Smith, R., *A quick one*, T. Gundersen, Editor. 2011.

52. GETINER ENGINEERING CORPORATION. *Physical Properties of Methanol: CH₃OH*. Available from: <http://www.cetinerengineering.com/Properties.htm>.
53. Frank P. Incropera, D.P.D., Theodore L. Bergman, Adrienne S. Lavine, *Fundamentals of heat and mass transfer*. sixth ed. 2007: John Wiley & Sons.
54. Kemp, I.C., *Pinch Analysis and Process Integration*. second edition ed. 2007: Elsevier Ltd. .
55. Bell, K.J., *Introduction to heat exchanger design*, in *Heat exchanger design handbook*. 1983, Hemisphere Publishing Corporation.
56. Rev, E. and Z. Fonyo, *Diverse pinch concept for heat exchange network synthesis: the case of different heat transfer conditions*. *Chemical engineering science*, 1991. **46**(7): p. 1623-1634.
57. Hamid, A. and M. Kamaruddin, *HYSYS: an introduction to chemical engineering simulation for UTM Degree++ program*. 2007.
58. Aspen Tech, *HYSYS 2004.2 Operations Guide*. 2005.

Appendices

Appendix A: Simulation model

Appendix B: Interpolation in steam tables

Appendix C: Input/output data from PRO-PI

Appendix D: Results – different oxygen purities

Appendix E: Mail from Ted Foster, *Air Products*

Appendix A

A.1 Simulation model

Figure A.1 shows the main simulation model created in Aspen Hysys. The properties of LNG/NG are found in Table A.1. The properties of the steam cycle are found in Table A.2. The properties of the flue gas are found in Table A.3. The duty of the heater/coolers is given in Table A.4. Table A.5 gives the power consumption/production in the different units.

Table A.1 Stream data LNG train

Stream Nr	F1	F2	F3	F4	F5	F6	F7	F8	F9
Temperature	-160,3	-154,6	-151,4	-114,14	-56,82	3,9	3,9	-44,37	26,96
Pressure	80	79,7	79,4	79,1	78,8	78,5	78,5	2,5	2
Molar flow	$4,48 \cdot 10^4$	$4,48 \cdot 10^4$	$4,48 \cdot 10^4$	$4,48 \cdot 10^4$	$4,48 \cdot 10^4$	$4,48 \cdot 10^4$	693	693	693
Mol% (CH ₄)	0,925	0,925	0,925	0,925	0,925	0,925	0,925	0,925	0,925
Mol% (C ₂ H ₆)	0,055	0,055	0,055	0,055	0,055	0,055	0,055	0,055	0,055
Mol% (C ₃ H ₈)	0,01	0,01	0,01	0,01	0,01	0,01	0,01	0,01	0,01
Mol% (N ₂)	0,01	0,01	0,01	0,01	0,01	0,01	0,01	0,01	0,01

Table A.2 Stream data steam cycle

Stream Nr	S1	S2	S3	S4	S5	S6	S7	S8	S9
Temperature	25	25,53	155	251,9	398,3	176,5	176,5	176,5	16,29
Pressure	1,5	54,70	54,50	41,07	40,91	5,0	5,0	5,0	4,7
Molar flow	$1,02 \cdot 10^4$	$1,02 \cdot 10^4$	$1,02 \cdot 10^4$	9956	9956	9956	4506	4361	4361
Mol% (H ₂ O)	1	1	1	1	1	1	1	1	1
Stream Nr	S10	S11	S12	S13	S14				
Temperature	176,5	11,42	176,5	52,58	5,7				
Pressure	5,0	4,7	5,0	0,14	0,13				
Molar flow	145	145	5450	5450	5450				
Mol% (H ₂ O)	1	1	1	1	1				

Table A.3 Stream data flue gas

Stream Nr	X1	X2	X3	X4	X5	X6	X7	X8	X9
Temperature	-96,97	25	1448	1292	393,8	113	187,6	140	18,61
Pressure	1,8	1,5	1,01	0,91	0,81	0,71	1,4	1,3	1,0
Molar flow	1540	1540	8509	8509	8509	8509	8509	8509	7101
Mol% (H2O)	0	0	0,18121	0,18121	0,18121	0,18121	0,18121	0,18121	0,01884
Mol% (O2)	0,95	0,95	0,01256	0,01256	0,01256	0,01256	0,01256	0,01256	0,01505
Mol% (N2)	0,05	0,05	0,08231	0,08231	0,08231	0,08231	0,08231	0,08231	0,09864
Mol% (CO2)	0	0	0,7239	0,7239	0,7239	0,7239	0,7239	0,7239	0,86746
Stream Nr	X10	X11	X12	X13	X14	X15	X16	X17	X18
Temperature	18,61	142,2	8,3	8,3	100,3	2,9	2,9	110,2	-42
Pressure	1,0	3,6	3,3	3,1	8,4	8,1	7,9	25	24,7
Molar flow	851	851	851	851	851	851	851	851	851
Mol% (H2O)	0,0188	0,01884	0,01884	0,00191	0,00191	0,0019	0	0	0
Mol% (O2)	0,0150	0,01505	0,01505	0,01531	0,01531	0,01531	0,01534	0,01534	0,01534
Mol% (N2)	0,0986	0,09864	0,09864	0,10034	0,10034	0,10034	0,10053	0,10053	0,10053
Mol% (CO2)	0,8674	0,86746	0,86746	0,88242	0,88242	0,88242	0,88412	0,88412	0,88412
Stream Nr	X19	X20	X21	X22	X23				
Temperature	-42	-31,2	10	18,61	44,6				
Pressure	24,7	220	219,7	1,0	1,35				
Molar flow	751,6	751,6	751,6	6250	6250				
Molar (H2O)	0	0	0	0,01884	0,01884				
Mol% (O2)	0,0059	0,00597	0,00597	0,01505	0,01505				
Mol% (N2)	0,0218	0,02181	0,02181	0,09864	0,09864				
Mol% (CO2)	0,9722	0,97220	0,97220	0,86746	0,86746				

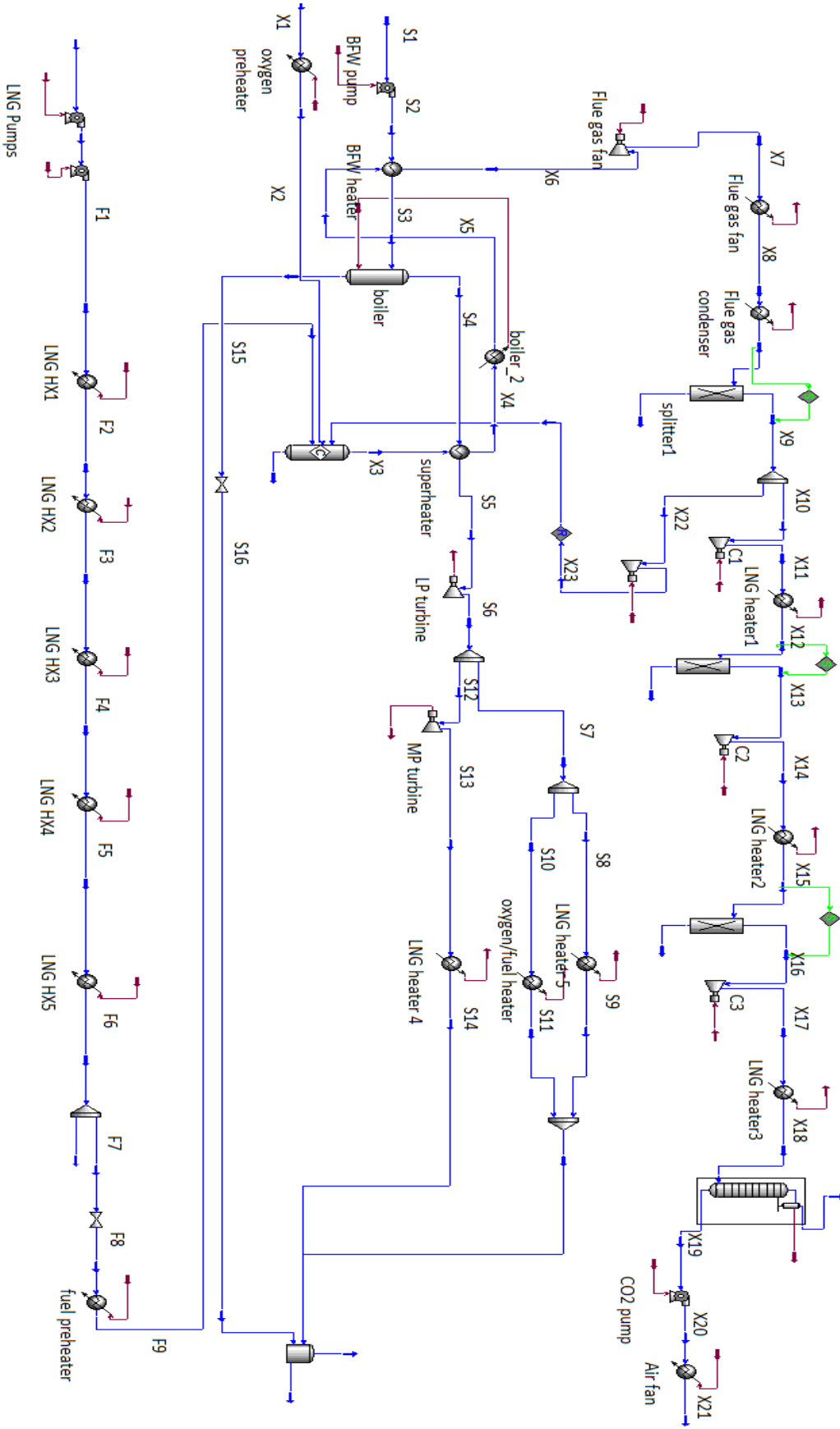


Table A.4 Duty of heater/coolers

Unit	LNG HX1	LNG HX2	LNG HX3	LNG HX4	LNG HX5
Duty[MW]	4,1	2,3	28,2	63,3	59,7
Unit	BFW heater	Boiler	Boiler_2	Superheater	O ₂ /fuel preheater
Duty[MW]	27,7	107,2	107,2	20,4	2
Unit	LNG heater1	LNG heater 2	LNG heater 3	LNG heater 4	LNG heater 5
Duty[MW]	1,4	0,9	4,1	63,3	59,7
Unit	Oxygen preheater	Fuel gas preheater	Flue gas cond.	Condenser	
Duty[MW]	1,5	0,5	28,2	0,228	

Table A.5 Power production/consumption

Unit	LNG pumps	BFW pump	CO2 pump	LP turbine	MP turbine	Flue gas fan Comp.
Duty [MW]	5,0	0,36	0,2	12,52	20,26	6,95
Unit	C1	C2	C3	Air Fan	Recycle comp	Flue gas fan cooler
Duty[MW]	1,12	0,8	0,9	0,75	1,67	4,5

Appendix B

B.1 Interpolation to find accurate properties of water

The enthalpy profile of the steam boiler is found by manual calculations. Table 1 gives the mass flows used in the calculations; all values are extracted from Hysys. Table B.1 shows the interpolation done to find the enthalpy value of the compressed liquid entering the steam boiler. Table Three shows the values found by interpolation for the saturated water.

Table B.1 Mass flows of water used in the calculations

Parameter	mass flows from HYSYS	
Total water amount	10158	kmol/h
Vapor leaving boiler	9955	kmol/h
Liquid leaving boiler	203	kmol/h
Molecular weight	18,02	kg/kmol
Total mass flow	183047,2	kg/h
Total vapor flow	179389,1	kg/h

Table B.2 Interpolation compressed liquid water

Compressed liquid - interpolation	
Temperature prior to boiler [°C]:	155
Pressure prior to boiler [bar]:	54,5
h-value @ 50 bar, 155°C:	657,0625
h-value @ 75 bar, 155°C:	658,56875
h-value at 54,5 bar, 155°C:	657,33362

Table B.3 Interpolation saturated water

Saturated water - Interpolation	
Saturated Temperature:	251,9
h_{fg}	1705,9
h_f	1094,7

Appendix C

C: Input data to PRO PI

PRO-PI draws the CC and GCC based on temperatures and duties of the different streams. The input data is given in Table C.1

Table C.1 Input data to PRO PI

T start [°C]	T target [°C]	Duty [MW]	Type
25,53	155	27,7	Cold
155	251,9	22,24	Cold
251,90	252	85,01	Cold
252,00	398,1	20,42	Cold
-160,3	-114,1	34,6	Cold
-144,1	-102,63	9,544	Cold
-102,632	-91,18	10,32	Cold
-91,1795	-79,727	11,597	Cold
-79,7274	-68,275	13,88	Cold
-68,2753	-56,823	17,9	Cold
-56,8232	3,921	59,7	Cold
-44,37	26,96	0,5	Cold
-96,97	25	1,5	Cold
1448	113	155,35	Hot
145	18,62	28,2	Hot
141,6	7,7	1,4	Hot
106,8	-43,1	4,1	Hot
99,96	2,24	0,9	Hot
52,58	52,43	6,33	Hot
52,43	52,28	6,33	Hot
52,28	52,13	6,33	Hot
52,13	51,98	6,33	Hot
51,98	51,83	6,33	Hot
51,83	51,7	6,33	Hot
51,7	51,5	6,33	Hot
51,5	51,37	6,32	Hot
51,37	51,22	6,34	Hot
51,22	7,75	6,33	Hot

C2: Output data from PRO PI

The two tables below show the output data from PRO PI.

Table C.2 Output data for CC

Cold CC		Hot CC	
Duty[MW]	T[°C]	Duty[MW]	T[°C]
0	-160,3	253,25	1448
12,13246	-144,1	101,6237	145
41,5046	-114,1	100,4694	141,6
44,144	-102,632	90,4606	113
49,2461	-96,97	89,01233	106,8
54,53521	-91,1795	87,22747	99,96
66,27305	-79,7274	74,42759	52,58
80,29388	-68,2753	68,05707	52,43
98,33472	-56,8232	61,68655	52,28
110,727	-44,37	55,31602	52,13
159,1203	3,921	48,9455	51,98
159,5273	25	42,57498	51,83
159,531	25,53	36,20986	51,7
159,8469	26,96	29,82583	51,5
187,241	155	23,47071	51,37
209,481	251,9	17,09019	51,22
294,491	252	3,536043	18,62
314,911	398,1	1,442103	7,75
		1,439752	7,7
		1,240126	2,24
		0	-43,1

Table C.3 Output data GCC

Duty[MW]	T[°C]
61,661	1448
183,8348	398,1
180,416	252
95,41762	251,9
84,45358	155
83,47776	145
83,90465	141,6
87,79453	113
87,91632	106,8
88,23776	99,96
90,90073	52,58
97,23916	52,43
103,5776	52,28
109,916	52,13
116,2545	51,98
122,5929	51,83
128,9302	51,7
135,2714	51,5
141,5987	51,37
147,9472	51,22
152,8434	26,96
153,1219	25,53
153,3386	25
155,868	18,62
157,7521	7,75
157,7535	7,7
157,8187	3,921
156,1956	2,24
111,9997	-43,1
110,727	-44,37
98,33472	-56,8232
80,29388	-68,2753
66,27305	-79,7274
54,53521	-91,1795
49,2461	-96,97
44,144	-102,632
41,5046	-114,1
12,13246	-144,1
0	-160,3

Appendix D

D1: Simulation results – different oxygen purities. All results are extracted from Hysys.

Mole percent oxygen :	90	95	97
Molar fraction flue gas			
Component	Molar fraction	Molar fraction	Molar fraction
Water	0,1792	0,1812	0,1820
Oxygen	0,0118	0,0126	0,0128
Nitrogen	0,1511	0,0823	0,0532
CO2	0,6579	0,7239	0,7521
Mole fraction flue gas to CO2 CPU			
Component	Mole fraction	Mole fraction	Mole fraction
Water	0,0186	0,0188	0,0189
Oxygen	0,0141	0,0151	0,0154
Nitrogen	0,1807	0,0986	0,0638
CO2	0,7866	0,8675	0,9019
Molar flow			
Stream	Flow[kmol/h]	Flow[kmol/h]	Flow[kmol/h]
Oxygen flow	1626	1540	1508
Flue gas flow	8595	8509	8477
Flue gas flow to CO2 CPU	938,3	850	818,3
CO2 flow to CO2 CPU	738,0852255	850,9	738,0205929
CO2-rich stream from dist.	749,2	751,6	754
CO2 flow separated from dist.	730,7128524	730,7174598	730,7310869
Compressor	Work[kW]	Work[kW]	Work[kW]
Compressor work			
C1	1239	1122	1078
C2	914	796	751,2
C3	1077	982,1	822,1
Recycle compressor	1686	1674	1668
Total compressor work	4916	4574,1	4319,3
Total compressor work CPU	3230	2900,1	2651,3
Work distillation	648	228,5	92,88

Appendix E

E-mail received 18th November 2010

Hi,

Air Products is in the development scale-up stages of the ITM Oxygen technology. We are currently procuring equipment for a 100 tpd pilot plant Intermediate Scale Test Unit that will start up the end of 2011. Due to some recently announced funding from the U.S. Department of Energy we will be able to fabricate enough ceramic membranes to produce more than 1000 tpd Oxygen in 2014. The next scale up is planned to be a 2000 tpd oxygen test facility to start up in 2015.

Regards Ted

E.P. Ted Foster

Director, Business Development

Air Products and Chemicals, Inc.

7201 Hamilton Boulevard

Allentown, PA 18195-1501, USA